THEORY OF THREE-LEVEL AND MULTILEVEL-ANHARMONIC-OSCILLATOR LASER TRANSITIONS

by

Farzaneh Najmabadi

A Dissertation Submitted to the Faculty of the

COMMITTEE ON OPTICAL SCIENCES

In Partial Fulfillment of the Requirements
For the Degree of

DOCTOR OF PHILOSOPHY

In the Graduate College

THE UNIVERSITY OF ARIZONA

1 9 7 4

THE UNIVERSITY OF ARIZONA

GRADUATE COLLEGE

I hereby recommend that this dissertation prepared under my direction by Farzaneh Najmabadi

entitled THEORY OF THREE-LEVEL AND MULTILEVEL-ANHARMONIC-OSCILLATOR LASER TRANSITIONS

be accepted as fulfilling the dissertation requirement of the degree of DOCTOR OF PHILOSOPHY

Murray Sargent III — March 26, 1974
Dissertation Director — Date

After inspection of the final copy of the dissertation, the following members of the Final Examination Committee concur in its approval and recommend its acceptance:*

Richard L. Shoemaker	3/26/74
Frederic A. Hopf	3/26/74
John D. McCullen	3/27/74
Hassan Mahmoud	3/29/74

*This approval and acceptance is contingent on the candidate's adequate performance and defense of this dissertation at the final oral examination. The inclusion of this sheet bound into the library copy of the dissertation is evidence of satisfactory performance at the final examination.

STATEMENT BY AUTHOR

This dissertation has been submitted in partial fulfillment of requirements for an advanced degree at The University of Arizona and is deposited in the University Library to be made available to borrowers under rules of the Library.

Brief quotations from this dissertation are allowable without special permission, provided that accurate acknowledgment of source is made. Requests for permission for extended quotation from or reproduction of this manuscript in whole or in part may be granted by the head of the major department or the Dean of the Graduate College when in his judgment the proposed use of the material is in the interests of scholarship. In all other instances, however, permission must be obtained from the author.

SIGNED: Farzaneh Najmabadi

ACKNOWLEDGMENTS

In doing this research I am in large part indebted to my advisors Dr. Murray Sargent, III, and Dr. Frederick A. Hopf. It was due to their continuous encouragement and stimulating discussions that this research was brought up to this state of the art.

I would also like to thank the other members of my committee, Dr. Richard L. Shoemaker, Dr. John D. McCullen, and Dr. Hormoz M. Mahmoud. My special thanks goes to the other members of the Quantum Optics group, Dr. Marlan O. Scully and Dr. Stephen F. Jacobs and the rest of the faculty of the Optical Sciences Center for what I learned from them during my stay at the Center.

Mr. Bradley T. Frazier was also of great help to me in doing the computer part of my work.

I would also like to express my sincere gratitude to Dr. Robert H. Noble, now with the Institute Nacional Astrofisica Optica y Electronica, Apartado Postal 216, Puebla, Puebla Mexico, and Dr. Aden B. Meinel who encouraged me to transfer to this school four years ago, and to Dr. Peter A. Franken and Dr. Jack D. Gaskill for their encouragment.

TABLE OF CONTENTS

TABLE OF CONTENTS--Continued

LIST OF ILLUSTRATIONS

LIST OF ILLUSTRATIONS--Continued

LIST OF ILLUSTRATIONS--Continued

LIST OF TABLES

ABSTRACT

In Part I of this dissertation the theory of Lamb is extended to treat the three level cascade and competitive transitions in both homogeneously and inhomogeneously broadened laser media. The electromagnetic field is treated as a classical superposition of two modes, one for each transition. The atoms obey the laws of quantum mechanics, and the atom-field interaction energy is expanded in the electric-dipole approximation. Equations determining the amplitudes and frequencies of the modes are found with the use of the self consistency requirement that the electric field assumed to induce the polarization of the medium equals the field sustained by the resulting polarization. These equations are solved to third order in the perturbation energy. Graphs of intensities and coupling constants of steady-state intensities are obtained. Stability conditions for various physical solutions are discussed. The mutual aid of the two modes in the cascade case is contrasted with the competition occurring in the competitive configuration. In fact in the inhomogeneously broadened cascade case peaks are observed in the center of the Lamb dips, and this interesting phenomena is solely due to the coherence terms which are ignored in all previous papers on this subject.

Part II treats a multilevel anharmonic cascade laser which can be applied to diatomic systems. P-branch transitions are considered from one of the many rotational levels with a quantum vibrational number v to another rotational level of the set with quantum number v-1. The formulation is along the lines of Part I. A set of rate equations is written for the three-level case to get an estimate of the error of the third-order theory versus the exact theory. It turns out that the third-order cascade theory is more accurate for the intensities (and pumping rates) considered than the corresponding competitive case. The intensity plots of the third-order theory and the exact case versus the relative excitation of one mode are obtained for a range of fixed values of decay rates of the levels.

PART I

THEORY OF THREE-LEVEL LASER TRANSITIONS IN HOMOGENEOUS AND INHOMOGENEOUS BROADENED MEDIA; PERTURBATION SOLUTION

CHAPTER 1

INTRODUCTION TO THREE-LEVEL SYSTEMS

In 1957 a theory was proposed by Javan [1] for a three-level maser oscillator. By introducing a high intensity saturating field between two levels, he showed that an induced emission of power at a lower frequency corresponding to a transition between an intermediate energy level and one or the other of the two levels can occur. From 1961 to 1964 when Lamb's [2] paper appeared and proved to be the best theory for laser transitions, several papers were published on the subject. In 1963 and 1964 the detection of two- and three-step laser cascades were reported in a series of papers. A list of these papers is given in Haken, Der Agobian, and Pauthier's [3] paper of 1965, where they have treated a solid-state, two-step cascade laser using the second quantization formalism. However, the semiclassical Lamb [2] theory can be extended to most any case of interest, and the quantum mechanical treatment, which would be very complicated for multilevel cases, is not necessary. The problem of laser-induced line narrowing on two coupled transitions has been studied by Feld and Javan [4] for the case of laser transitions detuned from the center of its atomic gain profile and later for a

high-intensity gas laser by Feldman and Feld [5, 6]. Feld and Javan [4] by scanning the gain profile with a weak, monochromatic probe field collinear with the laser field, found two sharp resonances at frequencies symmetric about the line center. One of the peaks was considerably narrower and one broader, and both were much narrower than the Doppler width of the laser field, and they named this effect "laser-induced line-narrowing." Further references to the literature are also given in these papers. The theory of a three-level gas laser amplifier has been treated by Hänsch and Toschek [7]. They also treat the problem semi-classically, using the rotating wave approximation. A good review and list of references of the work to date is also given in that paper. In the first part of this research we follow the theory of Lamb [2] to treat the problem of both homogeneous and collision broadened (gas) three-level laser media. We treat two configurations known as cascade and competitive which are shown in Figure 1(a) and 1(b).

As in the Lamb [2] theory, each mode is assumed to be a plane wave with sinusoidal z dependence[1]

$$U_n(z) = \sin K_n z \qquad (1)$$

---

1. The running wave case $U_n(z) = \exp(ik_n z)$ is a simple case of this analysis.

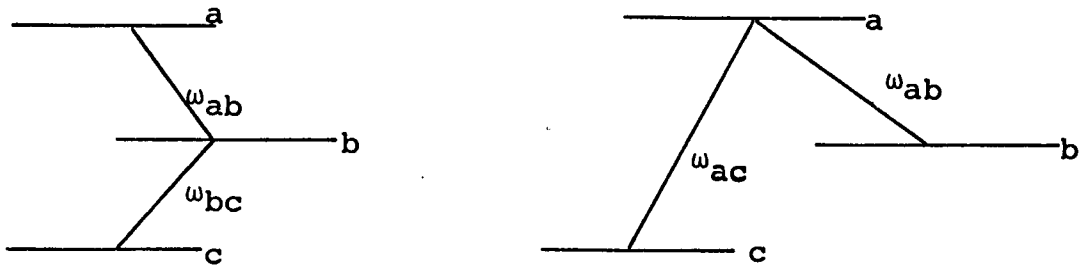

(a) Cascade case in which transitions between a and b levels and between b and c levels are allowed.

(b) Competitive case with allowed transitions between a and b levels and between a and c levels.

Figure 1. The two cases of the three-level transitions.

for which the cavity frequency

$$\Omega_n \equiv K_n c = \frac{n\pi c}{L}, \tag{2}$$

Here L is the length of the cavity, c is the speed of light and n is a large integer on the order of 10^6. In general the electric field is expanded as

$$E(z,t) = \frac{1}{2} \sum_n E_n(t)\exp[-i(\nu_n t + \phi_n)]U_n(z) + c.c., \tag{3}$$

where amplitude $E_n(t)$ and phase ϕ_n vary little in an optical frequency period. The corresponding induced polarization has the Fourier expansion

$$P(z,t) = \frac{1}{2} \sum_n P_n(t)\ \exp[-i(\nu_n t + \phi_n)]U_n(z) + c.c., \tag{4}$$

where the complex amplitude $P_n(t)$ is slowly varying in time. The electromagnetic field in the cavity satisfies Maxwell's equations. We demand that the field be self-consistent; that is, that the field inducing polarization is equal to the resulting field from Maxwell's equations (we work in M.K.S. units). Figure 2 shows the idea clearly [8].

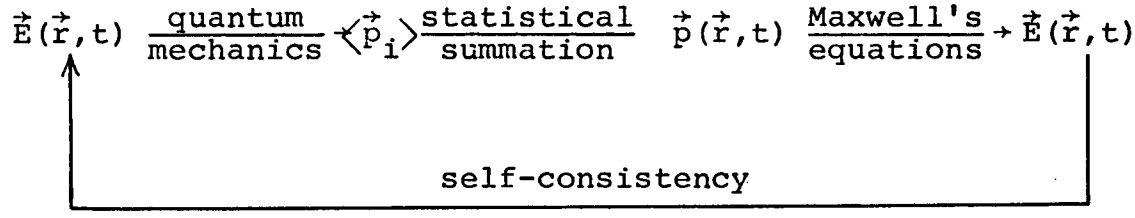

Figure 2. Self-consistency condition demanding that electric field in the cavity inducing the macroscopic polarization equals the field sustained by the polarization.

Combining Eqs. (3) and (4) with Maxwell's equations we get the self-consistency equations [8].

$$\dot{E}_n = -\frac{1}{2}(\nu_n/Q_n)E_n - \frac{1}{2}(\nu_n/\varepsilon_o)\,\mathrm{Im}(P_n), \tag{5}$$

$$\nu_n + \dot{\phi}_n = \Omega_n - \frac{1}{2}(\nu_n/\varepsilon_o)E_n^{-1}\,\mathrm{Re}(P_n), \tag{6}$$

where ε_o is the dielectric constant of the medium and Q_n is the quality factor of the cavity for mode n.

We calculate the polarizations P_n from quantum mechanics using a (3 x 3) population matrix whose elements are derived from probability amplitudes of atomic wave

functions. The rate equation approximation often used in laser theory here yields nine linear equations for the population matrix elements which are not readily solved by analytical techniques. Two elements represent coherence between levels of a forbidden transition (e.g., levels a and c in cascade case). This coherence results from two interactions of the electric field and is referred to as an electric-quadrupole term. It introduces additional terms in the equations of motion. Hence the perturbation method is followed, and in general terms like ρ_{ac} (population matrix component) in the cascade case are nonzero in second (and higher) order. Computer analysis of two mode operation of both homogeneously broadened and gas laser is done in each case. Plots of mode intensities and the coupling constant are obtained. The latter reveals that the coupling is quite weak, i.e., the modes saturate themselves considerably more than one another and hence oscillate almost independently. Moreover, in the cascade case the terms coupling the modes result in mutual aid rather than the usual competition, and interestingly enough this effect results in a small peak in the center of the Lamp dip in gas medium.

In Chapter 2, general equations of motion for the population matrix for both media are derived and the relationship between matrix components and the polarizations P_n are given. In Chapter 3 the equations for the cascade and the competitive cases respectively for homogeneously

broadened media are solved in detail. In Chapter 4 the amplitude and frequency determining equations for both cases are given. The general discussion of this section applies to both homogeneous and gaseous media. The table of coefficients in the equations for homogeneous cases are included in this section. Chapter 5 is along the lines of Chapter 3 in gas media, and it also includes the table of coefficients for these cases and the so-called perturbation tree diagrams. In Chapter 6 steady state numerical solutions are discussed.

CHAPTER 2

POLARIZATION OF THE HOMOGENEOUSLY BROADENED AND THE DOPPLER BROADENED MEDIA

We represent the atom-field interaction by the electric dipole perturbation energy

$$V = -e\vec{r} \cdot \vec{E}. \tag{7}$$

In the rotating wave approximation for cascade case, this energy has matrix elements

$$V_{ab} = -\frac{1}{2}\wp_{ab}E_2(t)\exp[-i(\nu_2 t + \phi_2)]U_2(z) \tag{8}$$

$$V_{bc} = -\frac{1}{2}\wp_{bc}E_1(t)\exp[-i(\nu_1 t + \phi_1)]U_1(z), \tag{9}$$

where $\wp_{ab}(\wp_{bc})$ is the electric-dipole matrix element between the a and b (b and c) levels. For the competitive case $V_{ac} = V_{bc}$ with $b \to a$. In general the equation of motion for the population matrix is given by

$$\dot{\rho} = \lambda - \frac{i}{\hbar}[\mathcal{H},\rho] - \frac{1}{2}[\Gamma\rho + \rho\Gamma], \tag{10}$$

where $\mathcal{H}$ is the total Hamiltonian of the system, $\Gamma_{ij} = \gamma_i\delta_{ij}$ for which γ_i is the decay rate of the level i, and $\lambda_{ij} = \lambda_i\delta_{ij}$ where λ_i is the pump rate to the level i (assumed to vary little in an atomic lifetime). Along the lines for a two-level medium [8], we obtain the component equations of

motion for the population matrix for each case. In cascade case V_{ac} is zero so that

$$\dot{\rho}_{ab} = -(i\omega_{ab}+\gamma_{ab})\rho_{ab} + \frac{i}{\hbar} V_{ab}(\rho_{aa}-\rho_{bb}) + \frac{i}{\hbar} V_{cb}\rho_{ac}, \quad (11)$$

$$\dot{\rho}_{bc} = -(i\omega_{bc}+\gamma_{bc})\rho_{bc} + \frac{i}{\hbar} V_{bc}(\rho_{bb}-\rho_{cc}) - \frac{i}{\hbar} V_{ba}\rho_{ac}, \quad (12)$$

$$\dot{\rho}_{ac} = -(i\omega_{ac}+\gamma_{ac})\rho_{ac} - \frac{i}{\hbar} (V_{ab}\rho_{bc}-\rho_{ab}V_{bc}), \quad (13)$$

$$\dot{\rho}_{aa} = \lambda_a - \gamma_a\rho_{aa} - [\frac{i}{\hbar} V_{ab}\rho_{ba} + c.c.], \quad (14)$$

$$\dot{\rho}_{bb} = \lambda_b - \lambda_b\rho_{bb} + [\frac{i}{\hbar} V_{ab}\rho_{ba} + c.c.] - [\frac{i}{\hbar} V_{bc}\rho_{cb} + c.c.], \quad (15)$$

$$\dot{\rho}_{cc} = \lambda_c - \gamma_c\rho_{cc} + [\frac{i}{\hbar} V_{bc}\rho_{cb} + c.c.], \quad (16)$$

where the frequencies ω_{ab}, ω_{bc}, and ω_{ac} are given in Figure 1. To account approximately for collision effects, i.e., the dephasing time due to collisions, we include an additional γ_{ab}^{phase}, etc., in our definition of γ_{ab} in component equations defined by

$$\gamma_{ab} = \frac{1}{2}(\gamma_a+\gamma_b) + \gamma_{ab}^{phase}, \quad (17)$$

i.e., there is additional broadening due to collisions. For the competitive case V_{bc} is zero and the equations are

$$\dot{\rho}_{ab} = -(i\omega_{ab}+\gamma_{ab})\rho_{ab} + \frac{i}{\hbar} V_{ab}(\rho_{aa}-\rho_{bb}) - \frac{i}{\hbar} V_{ac}\rho_{cb} \quad (18)$$

$$\dot{\rho}_{ac} = -(i\omega_{ac}+\gamma_{ac})\rho_{ac} + \frac{i}{\hbar} V_{ac}(\rho_{aa}-\rho_{cc}) - \frac{i}{\hbar} V_{ab}\rho_{bc} \tag{19}$$

$$\dot{\rho}_{bc} = -(i\omega_{bc}+\gamma_{bc})\rho_{bc} - \frac{i}{\hbar} (V_{ba}\rho_{ac}-\rho_{ba}V_{ac}) \tag{20}$$

$$\dot{\rho}_{aa} = \lambda_a - \gamma_a\rho_{aa} - [\frac{i}{\hbar} V_{ab}\rho_{ba}+c.c.] - [\frac{i}{\hbar} V_{ac}\rho_{ca}+c.c.] \tag{21}$$

$$\dot{\rho}_{bb} = \lambda_b - \gamma_b\rho_{bb} + [\frac{i}{\hbar} V_{ab}\rho_{ba}+c.c.] \tag{22}$$

$$\dot{\rho}_{cc} = \lambda_c - \gamma_c\rho_{cc} + [\frac{i}{\hbar} V_{ac}\rho_{ca}+c.c.]. \tag{23}$$

The matrix is called a population matrix because $\rho_{\alpha\alpha}(z,t)$ is the population of the αth level at time t and point z. Among the off-diagonal elements, ρ_{ac} in cascade case (ρ_{bc} in competitive case) in particular represents the coherence due to two electric-dipole interactions and is like a quadratic term. We might mention that the other off-diagonal terms like ρ_{cb} are given by taking the complex conjugate of say ρ_{bc} as an example. In terms of the population matrix components the complex polarization of (4) for the ab transition is given by

$$P_2(t) = 2 \exp[i(\nu_2 t+\phi_2)] \frac{\wp_{ab}}{\mathcal{N}_2} \int_0^L dz\, U_2^*(z)\rho_{ab}(z,t), \tag{24}$$

where $\mathcal{N}$ is the normalization constant

$$\mathcal{N}_2 = \int_0^L |U_2(z)|^2 dz. \tag{25}$$

Similarly (for the cascade case)

$$P_1(t) = 2 \exp[i(\nu_1 t+\phi_1)] \frac{\wp_{bc}}{\hbar_1} \int_0^L dz\ U_1^*(z)\rho_{bc}(z,t). \qquad (26)$$

Hence we see that the off-diagonal elements ρ_{ab} and ρ_{bc} lead to polarization of the medium. P_1 for the competitive case is given by Eq. (26) with b → a.

In a gas medium atoms move through the standing-wave electric field, seeing Doppler shifted frequencies and an amplitude modulated field. Each atom sees two frequencies, one Doppler upshifted and the other down-shifted, and hence the steady-state solution to the amplitude equations shows a Lamb dip. If v is the component of velocity along the laser (z) axis, the velocity distribution is

$$W(v) = (\sqrt{\pi}u)^{-1} \exp[-(v/u)^2], \qquad (27)$$

where u is the most probable speed of the atom. Hence, in forming the macroscopic polarization $P(z,t)$, one must include integrals over the velocity distribution and excitation positions as well as those over states and times of excitation. We assume collisions do not take place within the lifetime of an atom. The excitation position z_o and the interaction position z' with corresponding times t_o and t' are related by

$$z' = z_o + v\ (t'-t_o). \qquad (28)$$

Specifically, the macroscopic polarization, say, for the ab transition is given by

$$P_2(z,t) = \wp_{ab} \int_{-\infty}^{\infty} dv \sum_{\alpha} \int_{-\infty}^{t} dt_o \int_{0}^{L} dz_o \lambda_\alpha (z_o,t_o,v)$$

$$\times \rho_{ab} (\alpha,z_o,t_o,v,t)\delta(z-z_o-vt+vt_o) + c.c., \qquad (29)$$

where $\lambda_\alpha (z_o,t_o,v)$ is the pump rate to the eigenstate $|\alpha\rangle$ at time t_o, position z_o and with $\dot{z}$ component of velocity v. In other words in terms of the dipole moment it can be written as

$$P_2(z,t) = \wp_{ab} \int_{-\infty}^{\infty} dv \, \rho_{ab} (z,v,t) + c.c., \qquad (30)$$

which essentially leads to the integral over velocity of the equation (24) [and similarly (26)], but with velocity dependent population matrix components, where it is now given by

$$\rho_{ab}(z,v,t) = \sum_{\alpha} \int_{-\infty}^{t} dt_o \int_{0}^{L} dz_o \, \lambda_\alpha (z_o,t_o,v)$$

$$\times \rho_{ab} (\alpha,z_o,t_o,v,t)\delta(z-z_o-vt+vt_o). \qquad (31)$$

Taking the time derivative of (31), one finds that the population matrix $\rho(z,v,t)$ obeys the same equations as in the homogeneous case [9]. In summary the equations of motion are (11)-(16) for the cascade case and (18)-(23) for

the competitive case and the complex polarization, say, for the ab transition is given by

$$P_2(t) = 2\wp_{ab} \exp[(i\nu_2 t+\phi_2)] \int_0^\infty dv \left(\frac{1}{N_2}\right) \int_0^L dz\ U_2^*(z)\rho_{ab}(z,v,t). \tag{32}$$

CHAPTER 3

INTEGRATION OF THE EQUATIONS OF MOTION

Homogeneous Cascade Case

Following the perturbation method, we solve equations of motion up to third order in the electric field interaction and find the complex polarization (24) and (26). This is used in Eqs. (5) and (6) to obtain amplitude and frequency determining equations. The off-diagonal elements are given by the following formal integrals of (11)-(13)

$$\rho_{ab} = \frac{i}{\hbar} \int_{-\infty}^{t} dt' \exp[-(i\omega_{ab}+\gamma_{ab})(t-t')]\{V_{ab}(z,t')(\rho_{aa}-\rho_{bb}) + V_{cb}\rho_{ac}\} \tag{33}$$

$$\rho_{bc} = \frac{i}{\hbar} \int_{-\infty}^{t} dt' \exp[-(i\omega_{bc}+\gamma_{bc})(t-t')]\{V_{bc}(\rho_{bb}-\rho_{cc}) - V_{ba}\rho_{ac}\} \tag{34}$$

$$\rho_{ac} = \frac{i}{\hbar} \int_{-\infty}^{t} dt' \exp[-(i\omega_{ac}+\gamma_{ac})(t-t')]\{V_{bc}\rho_{ab}-V_{ab}\rho_{bc}\} \tag{35}$$

In zeroth order (no perturbation), off-diagonal elements are zero while the diagonal elements (populations of levels) are given by

$$\rho_{\alpha\alpha}^{(0)} = \lambda_\alpha/\gamma_\alpha, \qquad \alpha = a,b,c \tag{36}$$

and (unsaturated) population differences are given by

$$N_{ab}(z,t) = \rho_{aa}^{(0)} - \rho_{bb}^{(0)} = (\lambda_a/\gamma_a) - (\lambda_b/\gamma_b), \tag{37}$$

$$N_{bc}(z,t) = \rho_{bb}^{(0)} - \rho_{cc}^{(0)} = (\lambda_b/\gamma_b) - (\lambda_c/\gamma_c). \tag{38}$$

Now we iterate the calculation to third order with the assumption that the amplitudes E_n and phases ϕ_n of the electric field (3) vary sufficiently little in atomic lifetimes to be factored outside the time integrations. Using the zeroth-order differences (37) and (38) in integrals (33)-(35), we find the first-order contributions

$$\rho_{ab}^{(1)} = -\frac{1}{2}(\wp_{ab}/\hbar)N_{ab}(z,t)E_2U_2\exp[-i(\nu_2 t+\phi_2)] \left[\frac{(\omega_{ab}-\nu_2)+i\gamma_{ab}}{(\omega_{ab}-\nu_2)^2+\gamma_{ab}^2}\right], \tag{39}$$

$$\rho_{bc}^{(1)} = -\frac{1}{2}(\wp_{bc}/\hbar)N_{bc}(z,t)E_1U_1\exp[-i(\nu_1 t+\phi_1)] \left[\frac{(\omega_{bc}-\nu_1)+i\gamma_{bc}}{(\omega_{bc}-\nu_1)^2+\gamma_{bc}^2}\right], \tag{40}$$

$$\rho_{ac}^{(1)} = 0. \tag{41}$$

The diagonal elements have vanishing contributions in first order, because excitation to a superposition of levels is assumed not to occur. Substituting (39)-(41) into the

equations of motion (11)-(16) we get (accurate to second order)

$$\dot{\rho}_{aa} \approx \lambda_a - \gamma_a \rho_{aa} - \{\tfrac{1}{2}(\wp_{ab}/\hbar)^2 (N_{ab}/\gamma_{ab}) E_2^2 |U_2|^2 \cdot L_{ab}(\omega_{ab}-\nu_2)\}, \tag{42}$$

where $L_{ab}(\omega_{ab}-\nu_2)$ is the Lorentzian function defined to be

$$L_{ab}(\omega_{ab}-\nu_2) = \frac{\gamma_{ab}^2}{(\omega_{ab}-\nu_2)^2+\gamma_{ab}^2} \tag{42a}$$

We denote the term in the curly braces of (42) by $N_{ab}R_{ab}$ (R_{ab} has the form of a rate constant), that is,

$$R_{ab} \equiv \tfrac{1}{2} (\wp_{ab}/\hbar)^2 (1/\gamma_{ab}) E_2^2 |U_2|^2 L_{ab}(\omega_{ab}-\nu_2). \tag{43}$$

Then the second order contributions for the populations are

$$\rho_{aa}^{(2)} = -N_{ab}R_{ab}/\gamma_a, \tag{44}$$

$$\rho_{bb}^{(2)} = (N_{ab}R_{ab}/\gamma_b) - (N_{bc}R_{bc}/\gamma_b), \tag{45}$$

$$\rho_{cc}^{(2)} = N_{bc}R_{bc}/\gamma_c. \tag{46}$$

The electric dipole elements ρ_{ab} and ρ_{bc} have vanishing contributions in second order, but the "electric quadrupole" term ρ_{ac} is given by

$$\rho_{ac}^{(2)} = \tfrac{1}{4} (\wp_{ab}\wp_{bc}/\hbar^2) E_1 U_1 E_2 U_2 \exp[-i(\nu_1 t+\nu_2 t+\phi_1+\phi_2)]$$

$$\times [N_{bc}\mathcal{D}_{bc}(\omega_{bc}-\nu_1) - N_{ab}\mathcal{D}_{ab}(\omega_{ab}-\nu_2)]\mathcal{D}_{ac}(\omega_{ac}-\nu_1-\nu_2). \tag{47}$$

Here the complex denominator

$$\mathcal{D}_x(\omega_x-\nu_n) = [\gamma_x+i(\omega_x-\nu_n)]^{-1}. \tag{48}$$

To go to third order, we form from (44)-(46) the population difference terms

$$\rho_{aa}^{(2)} - \rho_{bb}^{(2)} = -(1/\gamma_a+1/\gamma_b)N_{ab}R_{ab}+N_{bc}R_{bc}/\gamma_b, \tag{49}$$

$$\rho_{bb}^{(2)} - \rho_{cc}^{(2)} = N_{ab}R_{ab}/\gamma_b - (1/\gamma_b+1/\gamma_c)N_{bc}R_{bc}. \tag{50}$$

The third order contributions to the populations and electric quadrupole are zero. Inserting (47), (49), and (50) into the formal integrals (33) and (34), we find the polarization elements

$$\begin{aligned}\rho_{ab}^{(3)} = {} & \tfrac{1}{2}\, i\, \exp[-i(\nu_2 t+\phi_2)]\mathcal{D}_{ab}(\omega_{ab}-\nu_2)(\wp_{ab}/\hbar)E_2U_2 \\ & \times \{(1/\gamma_a+1/\gamma_b)N_{ab}R_{ab}-N_{bc}R_{bc}/\gamma_b - \tfrac{1}{4}(\wp_{bc}/\hbar)^2E_1^2|U_1|^2 \\ & \times \mathcal{D}_{ac}(\omega_{ac}-\nu_1-\nu_2)\,[N_{bc}\mathcal{D}_{bc}(\omega_{bc}-\nu_1)-N_{ab}\mathcal{D}_{ab}(\omega_{ab}-\nu_2)]\},\end{aligned} \tag{51}$$

and

$$\begin{aligned}\rho_{bc}^{(3)} = {} & \tfrac{1}{2}\, i\, \exp[-i(\nu_1 t+\phi_1)]\mathcal{D}_{bc}(\omega_{bc}-\nu_1)(\wp_{bc}/\hbar)E_1U_1 \\ & \times \{(1/\gamma_b+1/\gamma_c)N_{bc}R_{bc} - N_{ab}R_{ab}/\gamma_b + \tfrac{1}{4}(\wp_{ab}/\hbar)^2 \\ & \times E_2^2|U_2|^2\mathcal{D}_{ac}(\omega_{ac}-\nu_1-\nu_2)[N_{bc}\mathcal{D}_{bc}(\omega_{bc}-\nu_1) \\ & - N_{ab}\mathcal{D}_{ab}(\omega_{ab}-\nu_2)]\}.\end{aligned} \tag{52}$$

Using (24) we get for first order polarization

$$P_2^{(1)}(t) = -(\wp_{ab}^2/\hbar)\bar{N}_{ab}E_2 \frac{(\omega_{ab}-\nu_2)+i\gamma_{ab}}{[(\omega_{ab}-\nu_2)^2+\gamma_{ab}^2]} \tag{53}$$

where

$$\bar{N}_{ab} = \frac{1}{\mathcal{N}_2}\int_0^L |U_2(z)|^2 N_{ab}(z,t)dz, \tag{54}$$

and for $U(z) = \sin kz$, it reduces to

$$\bar{N}_{ab} = (1/L)\int_0^L N_{ab}(z,t)dz. \tag{55}$$

Similarly for $P_1^{(1)}(t)$ we get

$$P_1^{(1)}(t) = -(\wp_{bc}^2/\hbar)\bar{N}_{bc}E_1 \frac{(\omega_{bc}-\nu_1)+i\gamma_{bc}}{[(\omega_{bc}-\nu_1)^2+\gamma_{bc}^2]}. \tag{56}$$

The third order contributions contain integrals of the form

$$\frac{1}{\mathcal{N}_2}\int_0^L |U_2(z)|^4 N_{ab}(z,t)dz,$$

and

$$\frac{1}{\mathcal{N}_2}\int_0^L |U_1(z)|^2 |U_2(z)|^2 N_{ab}(z,t)dz.$$

For sinusoidal mode functions (1) we have

$$|U_2(z)|^4 = \frac{3}{8} - \cos 2k_2z + (1/8)\cos 4k_2z,$$

and

$$|U_1(z)|^2|U_2(z)|^2 = (\tfrac{1}{4})\{1-\cos 2k_1z-\cos 2k_2z$$

$$+ (\tfrac{1}{2})\{\cos[2(k_1+k_2)z] + \cos[2(k_1-k_2)z]\}\}.$$

The cosine functions vary rapidly as functions of z and vanish in the spatial integration. Hence we get

$$P_2^{(3)}(t) = \tfrac{1}{4}i\mathcal{D}_{ab}(\omega_{ab}-\nu_2)(\wp_{ab}^2/\hbar)E_2\{\tfrac{3}{2}(\wp_{ab}/\hbar)^2(\bar{N}_{ab}/\gamma_{ab})E_2^2$$

$$x\ (1/\gamma_a+1/\gamma_b)L_{ab}(\omega_{ab}-\nu_2)-(1/\gamma_b)(\wp_{bc}/\hbar)^2E_1^2(\bar{N}_{bc}/\gamma_{bc})$$

$$x\ L_{bc}(\omega_{bc}-\nu_1) - \tfrac{1}{2}(\wp_{bc}/\hbar)^2E_1^2\ \mathcal{D}_{ac}(\omega_{ac}-\nu_1-\nu_2)$$

$$x\ [\bar{N}_{bc}\mathcal{D}_{bc}(\omega_{bc}-\nu_1)-\bar{N}_{ab}\mathcal{D}_{ab}(\omega_{ab}-\nu_2)]\}, \qquad (57)$$

and

$$P_1^{(3)}(t) = \tfrac{1}{4}i\mathcal{D}_{bc}(\omega_{bc}-\nu_1)(\wp_{bc}^2/\hbar)E_1\{\tfrac{3}{2}(\wp_{bc}/\hbar)^2(\bar{N}_{bc}/\gamma_{bc})E_1^2$$

$$x\ (1/\gamma_b+1/\gamma_c)L_{bc}(\omega_{bc}-\nu_1)-(1/\gamma_n)(\wp_{ab}/\hbar)^2E_2^2$$

$$x\ (\bar{N}_{ab}/\gamma_{ab})L_{ab}(\omega_{ab}-\nu_2) + \tfrac{1}{2}(\wp_{ab}/\hbar)^2E_2^2\mathcal{D}_{ac}(\omega_{ac}-\nu_1-\nu_2)$$

$$x\ [\bar{N}_{bc}\mathcal{D}_{bc}(\omega_{bc}-\nu_1)-\bar{N}_{ab}\mathcal{D}_{ab}(\omega_{ab}-\nu_2)]\}. \qquad (58)$$

The total polarization up to third order is given approximately by the sum of $P^{(1)}(t)$ and $P^{(3)}(t)$. Thus combining the polarization contributions (53) and (57) or (56) and (58) with the self-consistency Eqs. (5) and (6), we can find

equations that determine the field amplitudes and frequencies. We do this in Chapter 4 after carrying out calculations for the competitive case paralleling those given here.

Homogeneous Competitive Case

In this section, we integrate the population matrix equations of motion (18)-(23) for the competitive transition (Figure 1b) along the lines given in the previous section for the cascade case. The off-diagonal elements are given by the formal integrals

$$\rho_{ab} = \frac{i}{\hbar} \int_{-\infty}^{t} dt' \exp[-(i\omega_{ab}+\gamma_{ab})(t-t')]\{V_{ab}(z,t')(\rho_{aa}-\rho_{bb}) - V_{ac}\rho_{cb}\}, \tag{59}$$

$$\rho_{bc} = \frac{i}{\hbar} \int_{-\infty}^{t} dt' \exp[-(i\omega_{bc}+\gamma_{bc})(t-t')](V_{ac}\rho_{ba}-V_{ba}\rho_{ac}), \tag{60}$$

$$\rho_{ac} = \rho_{ab} \text{ with } b \leftrightarrow c. \tag{61}$$

The only nonzero components to first order are now $\rho_{ab}^{(1)}$ and $\rho_{ac}^{(1)}$ for which $\rho_{ab}^{(1)}$ is identical with (39) and $\rho_{ac}^{(1)} = \rho_{ab}^{(1)}$ with $b \leftrightarrow c$ and $1 \leftrightarrow 2$. The second order contributions for the populations are given by

$$\rho_{aa}^{(2)} = -(N_{ab}R_{ab}/\gamma_a) - (N_{ac}R_{ac}/\gamma_a), \tag{62}$$

$$\rho_{bb}^{(2)} = N_{ab}R_{ab}/\gamma_b, \tag{63}$$

$$\rho_{cc}^{(2)} = N_{ac}R_{ac}/\gamma_c. \tag{64}$$

Here R_{ac} is associated with the mode 1 (and ν_1), corresponding to R_{bc} in cascade case.

The "electric quadrupole" term $\rho_{bc}^{(2)}$ is given by

$$\rho_{bc}^{(2)} = \tfrac{1}{4}(\wp_{ab}\wp_{bc}/\hbar^2)E_1U_1^*E_2U_2 \exp[i\{(\nu_2-\nu_1)t+\phi_2-\phi_1\}]$$

$$\times [N_{ac}\mathcal{D}_{ac}(\omega_{ac}-\nu_1)+N_{ab}\mathcal{D}_{ab}(\nu_2-\omega_{ab})]\mathcal{D}_{bc}(\omega_{bc}+\nu_2-\nu_1). \tag{65}$$

The population differences in second order are

$$\rho_{aa}^{(2)} - \rho_{bb}^{(2)} = -(N_{ab}R_{ab}+N_{ac}R_{ac})/\gamma_a - N_{ab}R_{ab}/\gamma_b, \tag{66}$$

$$\rho_{aa}^{(2)} - \rho_{cc}^{(2)} = -(N_{ab}R_{ab}+N_{ac}R_{ac})/\gamma_a - N_{ac}R_{ac}/\gamma_c. \tag{67}$$

Again the third order population differences and quadrupole vanish and the "polarization" density matrix components acquire the contributions

$$\rho_{ab}^{(3)} = \tfrac{1}{2}\, i \exp[-i(\nu_2 t+\phi_2)]\mathcal{D}_{ab}(\omega_{ab}-\nu_2)(\wp_{ab}/\hbar)E_2U_2$$

$$\times \{(1/\gamma_a+1/\gamma_b)N_{ab}R_{ab} + N_{ac}R_{ac}/\gamma_a + \tfrac{1}{4}(\wp_{ac}/\hbar)^2E_1^2|U_1|^2$$

$$\times \mathcal{D}_{bc}^*(\omega_{bc}+\nu_2-\nu_1)[N_{ab}\mathcal{D}_{ab}(\omega_{ab}-\nu_2) + N_{ac}\mathcal{D}_{ac}(\nu_1-\omega_{ac})]\}, \tag{68}$$

and

$$\rho_{ac}^{(3)} = \rho_{ab}^{(3)} \text{ with } b \leftrightarrow c \text{ and } 1 \leftrightarrow 2.$$

Again first order polarization $P_2^{(1)}(t)$ is identical with (53) and $P_1^{(1)}(t)$ with (56) with $b \leftrightarrow a$. The third order results are (for standing waves)

$$P_2^{(3)}(t) = \frac{1}{4} i \mathcal{D}_{ab}(\omega_{ab}-\nu_2)(\wp_{ab}^2/\hbar)E_2\{\frac{3}{2}(\wp_{ab}/\hbar)^2(\bar{N}_{ab}/\gamma_{ab}) E_2^2$$

$$x (1/\gamma_a+1/\gamma_b) L_{ab}(\omega_{ab}-\nu_2) + (1/\gamma_a)(\wp_{ac}/\hbar)^2 E_1^2$$

$$x (\bar{N}_{ac}/\gamma_{ac}) L_{ac}(\omega_{ac}-\nu_1) + \frac{1}{2}(\wp_{ac}/\hbar)^2 E_1^2$$

$$x \mathcal{D}_{bc}(\nu_1-\nu_2-\omega_{bc})[\bar{N}_{ab}\mathcal{D}_{ab}(\omega_{ab}-\nu_2) + \bar{N}_{ac}\mathcal{D}_{ac}(\nu_1-\omega_{ac})]\} \quad (69)$$

and $P_1^{(3)}(t) = P_2^{(3)}(t)$ with $b \leftrightarrow c$ and $1 \leftrightarrow 2$.

CHAPTER 4

AMPLITUDE-FREQUENCY DETERMINING EQUATIONS-- FORMAL STEADY STATE SOLUTIONS

Now that we have complex polarizations up to third order for each case, we can solve for the amplitude and frequency determining equations. Using the self-consistency equations (5) and (6), we find

$$\dot{E}_1 = E_1 \ (\alpha_1 - \beta_1 E_1^2 - \theta_{12} E_2^2), \tag{70}$$

$$\dot{E}_2 = E_2 \ (\alpha_2 - \beta_2 E_2^2 - \theta_{21} E_1^2), \tag{71}$$

and the frequency determining equations

$$\nu_1 + \dot{\phi}_1 = \Omega_1 + \sigma_1 - \rho_1 E_1^2 - \tau_{12} E_2^2, \tag{72}$$

$$\nu_2 + \dot{\phi}_2 = \Omega_2 + \sigma_2 - \rho_2 E_2^2 - \tau_{21} E_1^2. \tag{73}$$

The coefficients for the homogeneous cases are given in Table 1. In the cascade case the θ's and τ's have opposite signs to the usual two-mode transitions and our competitive case. In essence the two transitions help each other to lase rather than compete. This can be seen from a physical point of view in that mode 2 (the upper transition) populates the middle laser level which is the upper level for mode 1, that is, mode 2 increases the population inversion

Table 1. Summary of coefficients appearing in the amplitude and frequency determining Eqs. (70)-(73).

Coefficient	Physical Interpretation
$\alpha_2 = -\frac{1}{2}\frac{\nu_2}{Q_2} + F_{ab}^{(1)} L_{ab}(\omega_{ab}-\nu_2)$	linear net gain
$\beta_2 = L_{ab}^{\ 2}\ (\omega_{ab}-\nu_2)\ F_{ab}^{(3)}$	self-saturation
$F_{ab}^{(1)} = \frac{1}{2}\nu_2 [\frac{\wp_{ab}^2}{\hbar\varepsilon_o\gamma_{ab}}] \bar{N}_{ab}$	first order factor
$F_{ab}^{(3)} = \frac{3}{2}(\frac{\wp_{ab}}{2\hbar})^2 \frac{1}{\gamma_{ab}} F_{ab}^{(1)} (\frac{1}{\gamma_a}+\frac{1}{\gamma_b})$	third order factor
$\sigma_2 = [\frac{\omega_{ab}-\nu_2}{\gamma_{ab}}] L_{ab}(\omega_{ab}-\nu_2)\ F_{ab}^{(1)}$	linear mode pulling
$\rho_2 = \frac{\omega_{ab}-\nu_2}{\gamma_{ab}} L_{ab}^{\ 2}(\omega_{ab}-\nu_2)\ F_{ab}^{(3)}$	self-pushing
$\upsilon_{2222} = i\gamma_{ab}F_{ab}^{(3)}\mathcal{D}_{ab}(\omega_{ab}-\nu_2)L_{ab}(\omega_{ab}-\nu_2)$	complex self-saturation
$\upsilon_{2211} = -\frac{i}{4}\frac{F_{bc}^{(1)}}{\gamma_b}(\frac{\wp_{ab}}{\hbar})^2 \mathcal{D}_{ab}(\omega_{ab}-\nu_2)$ $\times L_{bc}(\omega_{bc}-\nu_1)$	complex cross-saturation hole burning part (cascade)

Table 1.--Continued Summary of coefficients appearing in the amplitude and frequency determining Eqs. (70)-(73).

Coefficient	Physical Interpretation
$\upsilon_{2112} = -\frac{i}{8}\mathcal{D}_{ab}(\omega_{ab}-\nu_2)\mathcal{D}_{ac}(\omega_{ac}-\nu_1-\nu_2)$ $\times\left[\left(\frac{\wp_{ab}}{\hbar}\right)^2 F_{bc}^{(1)}\gamma_{bc}\mathcal{D}_{bc}(\omega_{bc}-\nu_1)\right.$ $\left.-\left(\frac{\wp_{bc}}{\hbar}\right)^2 F_{ab}^{(1)}\gamma_{ab}\mathcal{D}_{ab}(\omega_{ab}-\nu_2)\right]$	complex cross-saturation quadrupole part (cascade)
$\upsilon_{2211} = \frac{i}{4}\frac{F_{ac}^{(1)}}{\gamma_a}(\wp_{ab}/\hbar)^2\mathcal{D}_{ab}(\omega_{ab}-\nu_2)$ $L_{ac}(\omega_{ac}-\nu_1)$	complex cross-saturation hole burning part (competitive)
$\upsilon_{2112} = \frac{i}{8}\mathcal{D}_{ab}(\omega_{ab}-\nu_2)\mathcal{D}_{bc}(\nu_1-\nu_2-\omega_{bc})$ $\times\left[(\wp_{ab}/\hbar)^2 F_{ac}^{(1)}\gamma_{ac}\mathcal{D}_{ac}(\nu_1-\omega_{ac})\right.$ $\left.+(\wp_{ac}/\hbar)^2 F_{ab}^{(1)}\gamma_{ab}\mathcal{D}_{ab}(\omega_{ab}-\nu_2)\right]$	complex cross-saturation quadrupole part (competitive)
$\theta_{nm} = \mathrm{Im}(\upsilon_{nnmm} + \upsilon_{nmmn})$	cross-saturation

Table 1.--Continued Summary of coefficients appearing in the amplitude and frequency determining Eqs. (70)-(73).

Coefficient	Physical Interpretation
$\tau_{nm} = \text{Re}\ (\upsilon_{nnmm} + \upsilon_{nmmn})$	cross-pushing

n = 2 refers to ab transition and n = 1 to other transition. The corresponding coefficients for n = 1 mode are given by the values above with $2 \leftrightarrow 1$ and $ab \leftrightarrow bc, \gamma_a \leftrightarrow \gamma_c$ for cascade, and $ab \leftrightarrow ac$, $\gamma_b \leftrightarrow \gamma_c$ for competitive. The $\alpha, \beta, F^{(1)}, F^{(3)}, \sigma, \rho$, and υ_{2222} coefficients are same for both cases and υ_{2211} and υ_{2112} are given separately. Terms here are defined as follows: the frequency ν_n, (3); Q_n the cavity factor (Q) for mode n; ω_{ab} (Figure 1); $\wp_{ab}$ is the electric dipole element of transition (8); L_{ab} is the Lorentzian (42a): ε_o is the permittivity of free space; γ_a, γ_b, and γ_c are the decay constants of the levels a, b, and c and γ_{ab} is the decay constant of the polarization induced between levels a and b (24); $\bar{N}_{ab}$ is the population inversion (54).

for mode 1. Similarly mode 1 depopulates the lower level for mode 2 increasing the latter's inversion.

The analysis of steady-state operation is considerably simplified through the use of the intensities $I_n = E_n^2$. Multiplying (70) and (71) by $2E_1$ and $2E_2$ respectively, we find the equations of motion

$$\dot{I}_1 = 2I_1 \ (\alpha_1 - \beta_1 I_1 - \theta_{12} I_2) \tag{74}$$

$$\dot{I}_2 = 2I_2 \ (\alpha_2 - \beta_2 I_2 - \theta_{21} I_1). \tag{75}$$

Stationary solutions occur when $\dot{I}_1 = \dot{I}_2 = 0$. Physical solutions of interest are those for which intensities are non-negative and stable. Conditions for stability are discussed in detail in Appendix A and are summarized in Table 2. In this table the coupling constant

$$C = \theta_{12}\theta_{21}/(\beta_1\beta_2) \tag{76}$$

expresses the degree to which the modes are coupled. $C < 1$ defines weak coupling, $C = 1$ neutral coupling, and $C > 1$ strong coupling. It is convenient to express the coefficients in terms of the relative excitation defined by

$$m = \bar{N}/\bar{N}_T, \tag{77}$$

where $\bar{N}_T$ is the value of the population inversion $\bar{N}$ at threshold (given by $\alpha = 0$ for central tuning). Then the constant $F_{ab}^{(1)}$ is given by

$$F_{ab}^{(1)} = \frac{1}{2} \ (\nu_2/Q_2) m_2. \tag{78}$$

Table 2. Stable, physical solutions ($I_1, I_2 \geq 0$)

I_1	I_2	Conditions for Stability
0	0	$\alpha_1 < 0$, $\alpha_2 < 0$
α_1/β_1	0	$\alpha_1 > 0$, $\alpha_2' < 0$
0	α_2/β_2	$\alpha_1' < 0$, $\alpha_2 > 0$
$\frac{\alpha_1'/\beta_1}{1 - C}$	$\frac{\alpha_2'/\beta_2}{1 - C}$	general solutions
or		
I_1	$(\alpha_1 - \beta_1 I_1)/\theta_{12}$	
$C < 1$ for all the above cases		
α_1/β_1	0	Competitive
		$C > 1$ (θ's > 0)
0	α_2/β_2	and α_1' and $\alpha_2' > 0$

No stable solution for Cascade case when $C > 1$.

The "effective" net gain α_n' is defined by $\alpha_n' = \alpha_n - \theta_{nm}\, \alpha_m/\beta_m$ with $n \neq m$, and is the linear net gain of mode n in the presence of mode m oscillating with intensity α_m/β_m. The coupling constant $C = \theta_{12}\theta_{21}/(\beta_1\beta_2)$.

CHAPTER 5

INTEGRATION OF THE EQUATIONS OF MOTION FOR THE DOPPLER-BROADENED MEDIA

Cascade Case

As mentioned in Chapter 2, gas laser atoms moving with appreciable z components of velocity v through the electric field see two Doppler shifted frequencies which may differ by more than the atomic decay constants. This can result in pulsations in population differences varying appreciably in atomic decay times. Nevertheless, Stenholm and Lamb [10] have shown that the rate equation approximation, that is, neglect of these pulsations is quite accurate for single mode operation. Because the present problem has three atomic levels, we use perturbation theory which can be generalized for the multimode case (see Part II). Here we must particularly consider the implicit time dependence in the normal mode function $\sin(K_n z)$ and the v dependence in the population matrix components. The iteration procedure of the perturbation method is essentially the same as in the homogeneous case, while the algebra is simpler if the time integrations are performed after the third order formal integrals for the off-diagonal population matrix components are derived. It is also more convenient to choose the time differences like

$$\tau' = t - t', \tag{79}$$

as the variables of integrations. The formal integrals for the off-diagonal elements are given by (33)-(35), with the v dependences included, e.g.,

$$\rho_{ab}(z,v,t) = i\hbar^{-1} \int_0^\infty d\tau' \exp[-(i\omega_{ab}+\gamma_{ab})\tau'][V_{ab}(z',t') \times [\rho_{aa}(z',v,t') - \rho_{bb}(z',v,t')] + V_{cb}(z',t')\rho_{ac}(z',v,t')]. \tag{80}$$

The zeroth-order (unsaturated) population differences are assumed to have the same Maxwellian velocity dependences like

$$N_{ab}(z,v,t) = \rho_{aa}^{(0)} - \rho_{bb}^{(0)} = \lambda_a(z,v,t)\gamma_a^{-1} - \lambda_b(z,v,t)\gamma_b^{-1} = W(v)\, N_{ab}(z,t) = W(v)[\Lambda_a(z,t)\gamma_a^{-1} - \Lambda_b(z,t)\gamma_b^{-1}]. \tag{81}$$

Thus at a fixed excitation level, the zeroth-order population difference is a constant in time, and can be factored outside of the integral (80). Hence the first order off-diagonal terms are given by

$$\rho_{ab}^{(1)}(z,v,t) = i\hbar^{-1} N_{ab}(z,v,t) \int_0^\infty d\tau' \exp[-(i\omega_{ab}+\gamma_{ab})\tau'] \times V_{ab}(z',t'), \tag{82}$$

$$\rho_{bc}^{(1)}(z,v,t) = i\hbar^{-1} N_{bc}(z,v,t) \int_0^\infty d\tau' \exp[-(i\omega_{bc}+\gamma_{bc})\tau']$$

$$x\ V_{bc}(z',t'), \tag{83}$$

and

$$\rho_{ac}^{(1)}(z,v,t) = 0. \tag{84}$$

The second order contributions to the population matrix components are given by

$$\rho_{aa}^{(2)}(z,v,t) = -i\hbar^{-1} \int_0^\infty d\tau'\ e^{-\gamma_a\tau'} V_{ab}(z',t')\rho_{ba}^{(1)}(z',v,t')$$

$$+ c.c. = -\hbar^{-2} N_{ab} \int_0^\infty d\tau' \int_0^\infty d\tau''\ e^{-\gamma_a\tau'} V_{ab}(z',t')V_{ba}(z'',t'')$$

$$x \exp[(i\omega_{ab}-\gamma_{ab})\tau''] + c.c., \tag{85}$$

$$\rho_{bb}^{(2)}(z,v,t) = i\hbar^{-1} \int_0^\infty d\tau'\ e^{-\gamma_b\tau'} [V_{ab}(z',t')\rho_{ba}^{(1)}(z',v,t')$$

$$- V_{bc}(z',t')\rho_{cb}^{(1)}(z',v't') + c.c.]$$

$$= h^{-2} N_{ab} \int_0^\infty d\tau' \int_0^\infty d\tau''\ e^{-\gamma_b\tau'} V_{ab}(z',t')V_{ba}(z'',t'')$$

$$x \exp[(i\omega_{ab}-\gamma_{ab})\tau''] + c.c. - \hbar^{-2} N_{bc} \int_0^\infty d\tau' \int_0^\infty d\tau''\ e^{-\gamma_b\tau'}$$

$$x\ V_{bc}(z',t')V_{cb}(z'',t'')\ x \exp[(i\omega_{bc}-\gamma_{bc})\tau''] + c.c., \tag{86}$$

$$\rho_{cc}^{(2)}(t) = \hbar^{-2} N_{bc} \int_0^\infty d\tau' \int_0^\infty d\tau'' \, e^{-\gamma_c \tau'} V_{bc}(z',t') V_{cb}(z'',t'')$$

$$\times \exp[(i\omega_{bc}-\gamma_{bc})\tau''] + c.c. \qquad (87)$$

Similarly the electric quadrupole term is given by

$$\rho_{ac}^{(2)}(t) = -\hbar^{-2} \int_0^\infty d\tau' \exp[-(i\omega_{ac}+\gamma_{ac})\tau'] \{ N_{ab} \int_0^\infty d\tau''$$

$$\times \exp[-(i\omega_{ab}+\gamma_{ab})\tau''] V_{bc}(z',t') V_{ab}(z'',t'')$$

$$- N_{bc} \int_0^\infty d\tau'' \exp[-(i\omega_{bc}+\gamma_{bc})\tau''] V_{ab}(z',t') V_{bc}(z'',t'') \}. \qquad (88)$$

Hence the second order population differences are given by

$$\rho_{aa}^{(2)}(t) - \rho_{bb}^{(2)}(t) = -\hbar^{-2} N_{ab} \int_0^\infty d\tau' \int_0^\infty d\tau'' \, (e^{-\gamma_a \tau'}$$

$$+ e^{-\gamma_b \tau'}) V_{ab}(z',t') V_{ba}(z'',t'') \exp[(i\omega_{ab}-\gamma_{ab})\tau'']$$

$$+ \hbar^{-2} N_{bc} \int_0^\infty d\tau' e^{-\gamma_b \tau'} \int_0^\infty d\tau'' V_{bc}(z',t') V_{cb}(z'',t'')$$

$$\times \exp[(i\omega_{bc}-\gamma_{bc})\tau''] + c.c., \qquad (89)$$

$$\rho_{bb}^{(2)}(t) - \rho_{cc}^{(2)}(t) = \hbar^{-2} N_{ab} \int_0^\infty d\tau' \int_0^\infty d\tau'' e^{-\gamma_b \tau'} V_{ab}(z',t')$$

$$x\ V_{ba}(z'',t'')\exp[(i\omega_{ab}-\gamma_{ab})\tau''] - \hbar^{-2} N_{bc} \int_0^\infty d\tau'$$

$$x \int_0^\infty d\tau''(e^{-\gamma_b \tau'} + e^{-\gamma_c \tau''})\ V_{bc}(z',t')V_{cb}(z'',t'')$$

$$x\ \exp[(i\omega_{bc}-\gamma_{bc})\tau''] + c.c. \qquad (90)$$

Substituting (88), (89), and (90) into the formal integrals (33) and (34), we get the third order contributions to ρ_{ab} and ρ_{bc}

$$\rho_{ab}^{(3)}(t) = -i\hbar^{-3} \int_0^\infty d\tau' \exp[-(i\omega_{ab}+\gamma_{ab})\tau'] \{N_{ab} V_{ab}(z',t') \int_0^\infty d\tau''$$

$$x \int_0^\infty d\tau''' (e^{-\gamma_a \tau''} + e^{-\gamma_b \tau''})[V_{ab}(z'',t'')V_{ba}(z''',t''')$$

$$x\ \exp[(i\omega_{ab}-\gamma_{ab})\tau'''] + c.c.] - N_{bc} V_{ab}(z',t')$$

$$x \int_0^\infty d\tau'' \int_0^\infty d\tau''' e^{-\gamma_b \tau''} [V_{bc}(z'',t'')V_{cb}(z''',t''')$$

$$x\ \exp[(i\omega_{bc}-\gamma_{bc})\tau'''] + c.c.] + V_{cb}(z',t') \int_0^\infty d\tau''$$

$$x\ \exp[-(i\omega_{ac}+\gamma_{ac})\tau''][N_{ab} \int_0^\infty d\tau''' \exp[-(i\omega_{ab}+\gamma_{ab})\tau''']$$

$$x\ V_{bc}(z",t")V_{ab}(z"',t"') - N_{bc}\int_0^\infty d\tau"'$$

$$x\ \exp[-(i\omega_{bc}+\gamma_{bc})\tau"']V_{ab}(z",t")V_{bc}(z"',t"')]\}, \qquad (91)$$

$$\rho_{bc}^{(3)}(t) = i\hbar^{-3}\int_0^\infty d\tau'\exp[-(i\omega_{bc}+\gamma_{bc})\tau']\{V_{bc}(z',t')$$

$$x\ N_{ab}\int_0^\infty d\tau"\int_0^\infty d\tau"'e^{-\gamma_b\tau"}[V_{ab}(z",t")V_{ba}(z"',t"')$$

$$x\ \exp[(i\omega_{ab}-\gamma_{ab})\tau"'] + c.c.] - V_{bc}(z',t')N_{bc}\int_0^\infty d\tau"$$

$$x\int_0^\infty d\tau"'(e^{-\gamma_b\tau"}+e^{-\gamma_c\tau"})[V_{bc}(z",t")V_{cb}(z"',t"')$$

$$x\ \exp[(i\omega_{bc}-\gamma_{bc})\tau"'] + c.c.] + V_{ba}(z',t')\int_0^\infty d\tau"$$

$$x\ \exp[-(i\omega_{ac}+\gamma_{ac})\tau"]\{N_{ab}\int_0^\infty d\tau"'\exp[-(i\omega_{ab}+\gamma_{ab})\tau"']$$

$$x\ V_{bc}(z",t")V_{ab}(z"',t"') - N_{bc}\int_0^\infty d\tau"'\exp[-(i\omega_{bc}+\gamma_{bc})\tau"']$$

$$x\ V_{ab}(z",t")V_{bc}(z"',t"')\}\}. \qquad (92)$$

Then we find the complex polarizations up the the third order. The first order contributions to ρ_{ab} and ρ_{bc} are

$$\rho_{ab}^{(1)}(t) = -(1/4)i(\wp_{ab}/\hbar)\ E_2 \exp[-i(\nu_2 t+\phi_2)]$$

$$x\ U_2(z) N_{ab}[\mathcal{D}(\omega_{ab}-\nu_2+K_2 v) + \mathcal{D}(\omega_{ab}-\nu_2-K_2 v)], \tag{93}$$

$$\rho_{bc}^{(1)}(t) = -(1/4)i(\wp_{bc}/\hbar) E_1 \exp[-i(\nu_1 t+\phi_1)]$$

$$x\ U_1(z) N_{bc}[\mathcal{D}(\omega_{bc}-\nu_1+K_1 v) + \mathcal{D}(\omega_{bc}-\nu_1-K_1 v)], \tag{94}$$

which yield (since $W(v) = W(-v)$)

$$P_2^{(1)}(t) = -i(\wp_{ab}^2/\hbar)\ E_2\ \bar{N}_{ab} \int_0^\infty dv\ W(v)\ \mathcal{D}(\omega_{ab}-\nu_2+Kv)$$

$$= -\wp_{ab}^2\ (Ku\hbar)^{-1} E_2 \bar{N}_{ab}\ Z[\gamma_{ab}+i(\omega_{ab}-\nu_2)], \tag{95}$$

and

$$P_1^{(1)}(t) = -\wp_{bc}^2\ (Ku\hbar)^{-1} E_1 \bar{N}_{bc} Z[\gamma_{bc}+i(\omega_{bc}-\nu_1)], \tag{96}$$

where the plasma dispersion function $Z(\upsilon)$ is given by

$$Z(\upsilon) = (iK/\sqrt{\pi}) \int_{-\infty}^{\infty} dv\ \exp[-(v/u)^2](\upsilon+iKv)^{-1}, \tag{97}$$

and $\bar{N}_{ab}$ by (54) or equivalently by (55) for the sinusoidal eigenfunction. In third order we find

$$P_2^{(3)} = (1/4)i\wp_{ab}^4 \hbar^{-3}E_2^3(1/\mathcal{N}_2)\int_0^L dz\, N_{ab}(z)\, U_2^*(z)\int_{-\infty}^{\infty} dv$$

$$\times W(v)\int_0^\infty d\tau'\int_0^\infty d\tau''\int_0^\infty d\tau'''\exp[-(i\omega_{ab}-i\nu_2+\gamma_{ab})\tau']$$

$$\times (e^{-\gamma_a\tau''}+e^{-\gamma_b\tau''})U_2(z-v\tau')\{\exp[-(i\omega_{ab}-i\nu_2+\gamma_{ab})\tau''']$$

$$\times U_2^*(z-v\tau'-v\tau'')U_2(z-v\tau'-v\tau''-v\tau''') + c.c.\}$$

$$- (1/4)i\wp_{ab}^2\wp_{bc}^2\hbar^{-3}E_2E_1^2(1/\mathcal{N}_2)\int_0^L dz N_{bc}(z)U_2^*(z)\int_{-\infty}^{\infty} dv$$

$$\times W(v)\int_0^\infty d\tau'\int_0^\infty d\tau''\int_0^\infty d\tau'''\exp[-(i\omega_{ab}-i\nu_2+\gamma_{ab})\tau']e^{-\gamma_b\tau''}$$

$$\times U_2(z-v\tau')\{\exp[-(i\omega_{bc}-i\nu_1+\gamma_{bc})\tau''']U_1^*(z-v\tau'-v\tau'')$$

$$\times U_1(z-v\tau'-v\tau''-v\tau''') + c.c.\} + (i/4)\wp_{ab}^2\wp_{bc}^2\hbar^{-3}E_2E_1^2(1/\mathcal{N}_2)$$

$$\times \int_0^L dz\, U_2^*(z)\int_{-\infty}^{\infty} dv\, W(v)\int_0^\infty d\tau'\int_0^\infty d\tau''\int_0^\infty d\tau'''\exp[-(i\omega_{ab}$$

$$-i\nu_2+\gamma_{ab})\tau']\exp[-i(\omega_{ac}-\nu_2-\nu_1)\tau''-\gamma_{ac}\tau'']U_1^*(z-v\tau')\{N_{ab}(z)$$

$$\times \exp[-i(\omega_{ab}-\nu_2)\tau'''-\gamma_{ab}\tau'''']U_1(z-v\tau'-v\tau'')U_2(z-v\tau'-v\tau''-v\tau''')$$

$$- \text{same with } ab \leftrightarrow bc \text{ and } 1 \leftrightarrow 2\}. \qquad (98)$$

The product of four U's in the third term with use of trigonometric formulas and neglect of odd functions in v and

rapidly varying terms in z (like cos $(2K_1 z)$ which vanish after integrations over v and z) becomes

$$(1/8)\{\cos[2(K_1-K_2)z]\cos[Kv(\tau"'-\tau')] + \cos[Kv(\tau"'+\tau')] + \cos[Kv(\tau"'+2\tau"+\tau')]\}. \quad (99)$$

Similarly the last term in (98) contains the terms

$$(1/8)\{\cos[Kv(\tau"'-\tau')] + \cos[2(K_2-K_1)z]\cos[Kv(\tau"'+\tau')] + \cos[Kv(\tau"'+2\tau"+\tau')]\}. \quad (100)$$

In both (99) and (100) still the rapidly varying terms in z like $\cos[2(K_2-K_1)z]$ have zero contributions to the polarizations. The negligible terms are crossed out. Similarly the third order $P_1^{(3)}$ is given by

$$P_1^{(3)} = (i/4)\wp_{bc}^4\hbar^{-3}E_1^3(1/\mathcal{N}_1)\int_0^L dz\, N_{bc}(z)U_1^*(z)\int_{-\infty}^{\infty} dv$$

$$\times W(v)\int_0^\infty d\tau'\int_0^\infty d\tau"\int_0^\infty d\tau"'\exp[-(i\omega_{bc}-i\nu_1+\gamma_{bc})\tau']$$

$$\times (e^{-\gamma_b\tau"}+e^{-\gamma_c\tau"})U_1(z-v\tau')\{\exp[-(i\omega_{bc}-i\nu_1+\gamma_{bc})\tau"']$$

$$\times U_1^*(z-v\tau'-v\tau")U_1(z-v\tau'-v\tau"-v\tau"') + c.c.\} - (i/4)$$

$$\times \wp_{ab}^2\wp_{bc}^2\hbar^{-3}E_1E_2^2(1/\mathcal{N}_1)\int_0^L dzN_{ab}(z)U_1^*(z)\int_{-\infty}^{\infty} dvW(v)\int_0^\infty d\tau'$$

$$\times \int_0^\infty d\tau"\int_0^\infty d\tau"'\exp[-(i\omega_{bc}-i\nu_1+\gamma_{bc})\tau']e^{-\gamma_b\tau"}U_1(z-v\tau')$$

$$x \{\exp[-(i\omega_{ab}-i\nu_2+\gamma_{ab})\tau"']U_2^*(z-v\tau'-v\tau")U_2(z-v\tau'-v\tau"-v\tau"')$$

$$+ \text{c.c.}\} - (i/4)\wp_{ab}^2\wp_{bc}^2\hbar^{-3}E_1E_2^2(1/\mathcal{N}_1)\int_0^L dzU_1^*(z)\int_{-\infty}^{\infty} dv$$

$$x\, W(v)\int_0^\infty d\tau'\int_0^\infty d\tau"\int_0^\infty d\tau"'\, \exp[-(i\omega_{bc}-i\nu_1+\gamma_{bc})\tau']$$

$$x \exp[-i(\omega_{ac}-\nu_2-\nu_1)\tau"-\gamma_{ac}\tau"]U_1^*(z-v\tau')\{N_{ab}(z)$$

$$x \exp[-(i\omega_{ab}-i\nu_2+\gamma_{ab})\tau"']U_1(z-v\tau'-v\tau")U_2(z-v\tau'-v\tau"-v\tau"')$$

$$- \text{same with ab} \leftrightarrow \text{bc and 1} \leftrightarrow 2\ , \tag{101}$$

With the third and last product of U's as

$$(1/8)\{\cos[Kv(\tau"'-\tau')] + \cos[2(K_1-K_2)z]\cos[Kv(\tau"'+\tau')]$$

$$+ \cos[Kv(\tau"'+2\tau"+\tau')]\}, \tag{102}$$

$$(1/8)\{\cos[Kv(\tau"'-\tau')] + \cos[2(K_2-K_1)z]\cos[Kv(\tau"'+\tau')]$$

$$+ \cos[Kv(\tau"'+2\tau"+\tau')]\}. \tag{103}$$

In general the third order polarizations can be written as

$$P_n^{(3)}(t) = \frac{1}{16}(\hbar^3 Ku)^{-1}\wp_n^2 E_n[\wp_n^2 E_n^2 \sum_{\ell=1}^{4}\sum_{w=1}^{3} T_{\ell w}$$

$$+ \wp_m^2 E_m^2 \sum_{\ell=5}^{8}\sum_{w=1}^{3} T_{\ell w}],\ m\neq n \tag{104}$$

where each $\wp$ is the electric dipole moment of the corresponding mode, and the third-order integrals $T_{\ell w}$ are given by

$$T_{\ell w} = iN_{\ell w} K\sqrt{\pi} \int_{-\infty}^{\infty} dv \exp[-(v/u)^2] \int_0^{\infty} d\tau' \int_0^{\infty} d\tau'' \int_0^{\infty} d\tau'''$$

$$x \exp\{-[(\upsilon_{\ell 1}+ic_{w1}Kv)\tau' + (\upsilon_{\ell 2}+ic_{w2}Kv)\tau''$$

$$+ (\upsilon_{\ell 3}+ic_{w3}Kv)\tau''']\}. \qquad (105)$$

The excitation parameters $N_{\ell w}$ for the ab transition are defined in Table 3(a) and the complex frequencies $\upsilon_{\ell k}$ are given in Table 4(a). The corresponding parameters for the bc transition are given in Tables 3(b) and 4(b). For large Doppler broadening (Ku >> atomic decay rates and beat frequencies) which we refer to as the "strong Doppler limit," the third-order integrals reduce to (O'Bryan and Sargent [11])

$$T_{\ell 1} \cong 2i\sqrt{\pi}\, N_{\ell 1}[\upsilon_{\ell 2}(\upsilon_{\ell 1}+\upsilon_{\ell 3})]^{-1}, \quad T_{\ell 2} \cong T_{\ell 3} \cong 0. \qquad (106)$$

The third-order saturation coefficients are then given by

$$\upsilon_{nnnn} = \frac{1}{32}\, \nu(\hbar^3 Ku\varepsilon_o)^{-1}\, \wp_n^2\wp_n^2 \sum_{\ell=1}^{4} \sum_{w=1}^{3} T_{\ell w} \qquad (107)$$

and

$$\upsilon_{nnmm} \text{ or } \upsilon_{nmmn} = \frac{1}{32}\, \nu(\hbar^3 Ku\varepsilon_o)^{-1}\, \wp_n^2\wp_m^2 \sum_{\ell=5}^{8} \sum_{w=1}^{3} T_{\ell w}$$

$$\text{for } n \neq m. \qquad (108)$$

Table 3. Definitions of the parameters $N_{\ell w}$ of Eq. (105) for the ab and bc transitions of the gas, cascade case

$N_{\ell w}$	w = 1	2	3
(a):			
ℓ = 1,2,3,4	$\bar{N}_{ab}$	$\bar{N}_{ab}$	$\bar{N}_{ab}$
5,6	$-\bar{N}_{bc}$	$-\bar{N}_{bc}$	0
7	0	$\bar{N}_{ab}$	$\bar{N}_{ab}$
8	$-\bar{N}_{bc}$	0	$-\bar{N}_{bc}$
(b):			
ℓ = 1,2,3,4	$\bar{N}_{bc}$	$\bar{N}_{bc}$	$\bar{N}_{bc}$
5,6	$-\bar{N}_{ab}$	$-\bar{N}_{ab}$	0
7	$-\bar{N}_{ab}$	0	$-\bar{N}_{ab}$
8	0	$\bar{N}_{bc}$	$\bar{N}_{bc}$

$\bar{N}$'s are defined in general by Eq. (55). The c_{wk}'s are defined by the matrix

$$c = \begin{pmatrix} -1 & 0 & 1 \\ 1 & 0 & 1 \\ 1 & 2 & 1 \end{pmatrix}.$$

Table 4. Definitions of the complex frequencies $\upsilon_{\ell k}$ appearing in the third-order integrals (105), for the ab and bc transitions, respectively, of the gas cascade case.

$\upsilon_{\ell k}$	k = 2	k = 3
(a):		
ℓ = 1	γ_a	$\gamma_{ab} + i(\omega_{ab}-\nu_2)$
2	γ_a	$\gamma_{ab} + i(\nu_2-\omega_{ab})$
3	γ_b	$\gamma_{ab} + i(\nu_2-\omega_{ab})$
4	γ_b	$\gamma_{ab} + i(\omega_{ab}-\nu_2)$
5	γ_b	$\gamma_{bc} + i(\omega_{bc}-\nu_1)$
6	γ_b	$\gamma_{bc} + i(\nu_1-\omega_{bc})$
7	$\gamma_{ac} + i(\omega_{ac}-\nu_1-\nu_2)$	$\gamma_{ab} + i(\omega_{ab}-\nu_2)$
8	$\gamma_{ac} + i(\omega_{ac}-\nu_1-\nu_2)$	$\gamma_{bc} + i(\omega_{bc}-\nu_1)$
(b):		
ℓ = 1	γ_b	$\gamma_{bc} + i(\omega_{bc}-\nu_1)$
2	γ_b	$\gamma_{bc} + i(\nu_1-\omega_{bc})$
3	γ_c	$\gamma_{bc} + i(\nu_1-\omega_{bc})$
4	γ_c	$\gamma_{bc} + i(\omega_{bc}-\nu_1)$
5	γ_b	$\gamma_{ab} + i(\omega_{ab}-\nu_2)$
6	γ_b	$\gamma_{ab} + i(\nu_2-\omega_{ab})$
7	$\gamma_{ac} + i(\omega_{ac}-\nu_1-\nu_2)$	$\gamma_{ab} + i(\omega_{ab}-\nu_2)$
8	$\gamma_{ac} + i(\omega_{ac}-\nu_1-\nu_2)$	$\gamma_{bc} + i(\omega_{bc}-\nu_1)$

$\upsilon_{\ell 1} = \gamma_{ab} + i(\omega_{ab}-\nu_2)$ for the ab transition for all ℓ, and $\upsilon_{\ell 1} = \gamma_{bc} + i(\omega_{bc}-\nu_1)$ for the bc transition for all ℓ.

These coefficients explicitly together with the other constants and factors appearing in the amplitude-frequency determining equations (like linear net gain, etc.), for both cascade and competitive gas cases are given in Table 7 (p. 47). It is important to note that the strong Doppler limit is accurate enough for our purposes [11].

Competitive Case

In this section we solve the equations of motion for the competitive case to find the complex polarizations up to third order of integration and the coefficients of the frequency and amplitude determining equations. General discussions of Chapters 2 and 6 about the gas media apply here, also. The formal integrals for the off-diagonal terms are given by (59)-(61) with the v dependences included, and the new time variable of integration τ'. Similar to the homogeneous case $\rho_{ab}^{(1)}(t)$ is identical to the cascade case, Eq. (82) and $\rho_{ac}^{(1)} = \rho_{ab}^{(1)}$ with $b \to c$ and $\rho_{bc}^{(1)}(t) = 0$. In short from the equations of motion one can see that the competitive results can be obtained from the corresponding results of the cascade case by the following substitutions

1. $a \leftrightarrow b$
2. $\nu_2 \to -\nu_2$
3. $\bar{N}_{ab} \to -\bar{N}_{ab}$

and for the complex υ's we should take the complex conjugate of the cascade coefficients.

Tables 5 and 6 summarize the excitation parameters $N_{\ell w}$, and the complex frequencies $\upsilon_{\ell k}$ for the ab transition occurring in the third-order integrals $T_{\ell w}$, Eq. (105). For the ac transition the tables are the same with $b \leftrightarrow c$ and $1 \leftrightarrow 2$. As was mentioned in the previous section, the third-order saturation coefficients together with the other factors of the amplitude-frequency determining equations are tabulated in the third section of this chapter.

Table of Coefficients and Perturbation Tree Diagrams

This section, although in fact is a summarized form of the gas Laser three-level theory, does not contain more than what we introduced up to now. Figures 3 and 4 are perturbation tree diagrams for the ab transitions of the cascade and competitive cases respectively, yielding the $\rho_{ab}^{(3)}$ terms. The frequencies appearing in each term also correspond to Tables 4(a) and 6. Table 7 is the summary of coefficients for the gas cases corresponding to Table 1 for the homogeneous cases.

An easy way of evaluation (and also getting some insight into the different contributing terms) of the third order integrals for the off-diagonal (polarization) terms is by summation of the product of terms along the "limbs" of what we call the perturbation "tree," when the three time integrations are performed. For example Figure 3 is the "tree" for the gas cascade ab transition and Figure 4

Table 5. Definitions of the parameters $N_{\ell w}$ for the ab transition of the gas, competitive case.

$N_{\ell w}$	w = 1	2	3
ℓ = 1,2,3,4	$\bar{N}_{ab}$	$\bar{N}_{ab}$	$\bar{N}_{ab}$
5,6	$\bar{N}_{ac}$	$\bar{N}_{ac}$	0
7	0	$\bar{N}_{ab}$	$\bar{N}_{ab}$
8	$\bar{N}_{ac}$	0	$\bar{N}_{ac}$

For the ac transition the parameters are the same with b $\leftrightarrow$ c. The general definitions of other parameters are the same as in the footnote of Table 3.

Table 6. Definitions of the complex frequencies $\upsilon_{\ell k}$ appearing in the third-order integrals (105) for the ab transition of the gas competitive case.

$\upsilon_{\ell k}$	k = 2	k = 3
ℓ = 1	γ_a	$\gamma_{ab} + i(\omega_{ab}-\nu_2)$
2	γ_a	$\gamma_{ab} + i(\nu_2-\omega_{ab})$
3	γ_b	$\gamma_{ab} + i(\nu_2-\omega_{ab})$
4	γ_b	$\gamma_{ab} + i(\omega_{ab}-\nu_2)$
5	γ_a	$\gamma_{ac} + i(\omega_{ac}-\nu_1)$
6	γ_a	$\gamma_{ac} + i(\nu_1-\omega_{ac})$
7	$\gamma_{bc} - i(\omega_{bc}+\nu_2-\nu_1)$	$\gamma_{ab} + i(\omega_{ab}-\nu_2)$
8	$\gamma_{bc} - i(\omega_{bc}+\nu_2-\nu_1)$	$\gamma_{ac} + i(\nu_1-\omega_{ac})$

$\upsilon_{\ell 1} = \gamma_{ab} + i(\omega_{ab}-\nu_2)$ for all ℓ. For the ac transition parameters are the same with b $\leftrightarrow$ c, 1 $\leftrightarrow$ 2.

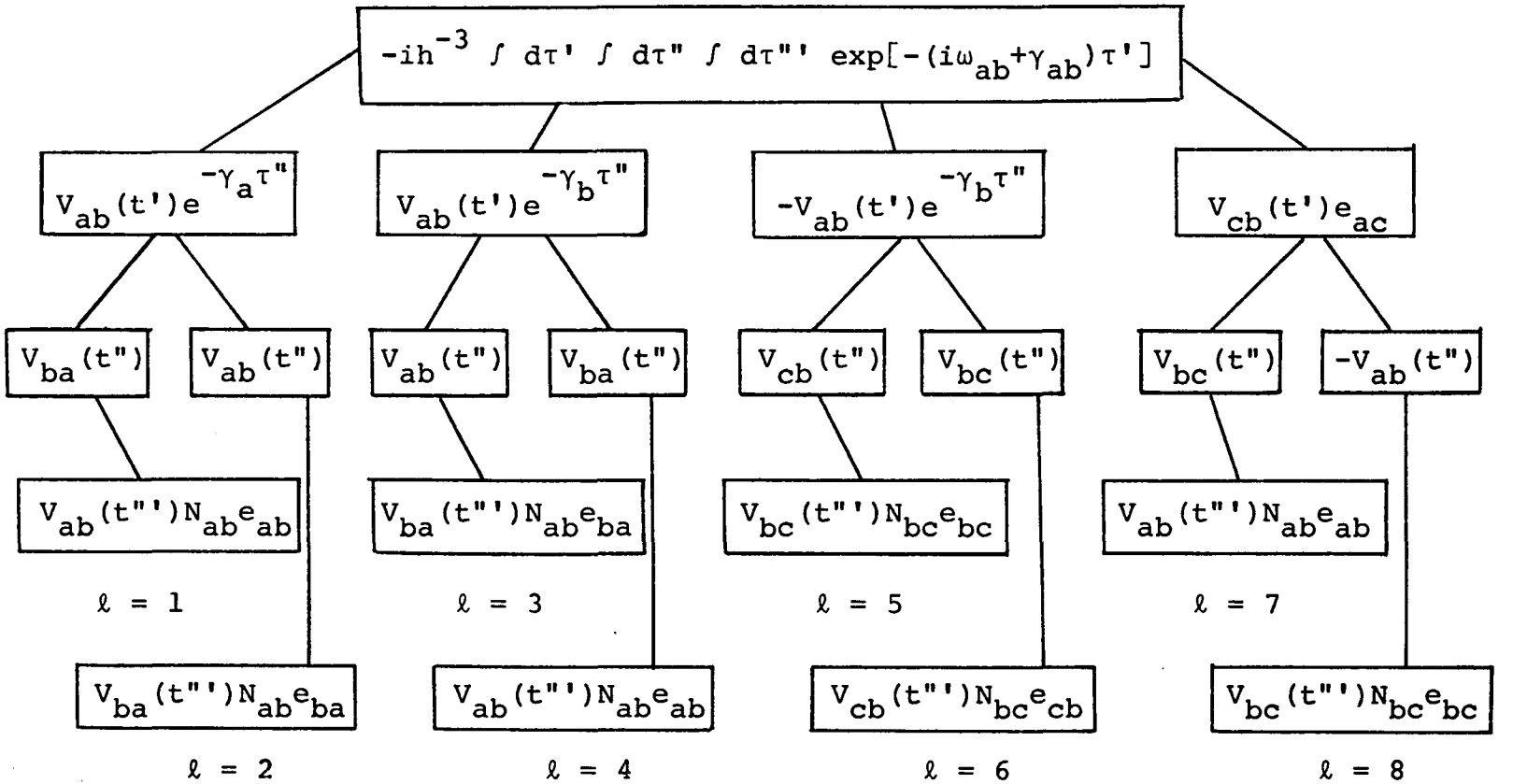

Figure 3. Perturbation tree yielding $\rho_{ab}^{(3)}$ for the inhomogeneous cascade case -- Terms like e_{ba} are defined as

$$e_{ba} = \exp[-(i\omega_{ba}+\gamma_{ab})\tau'''].$$

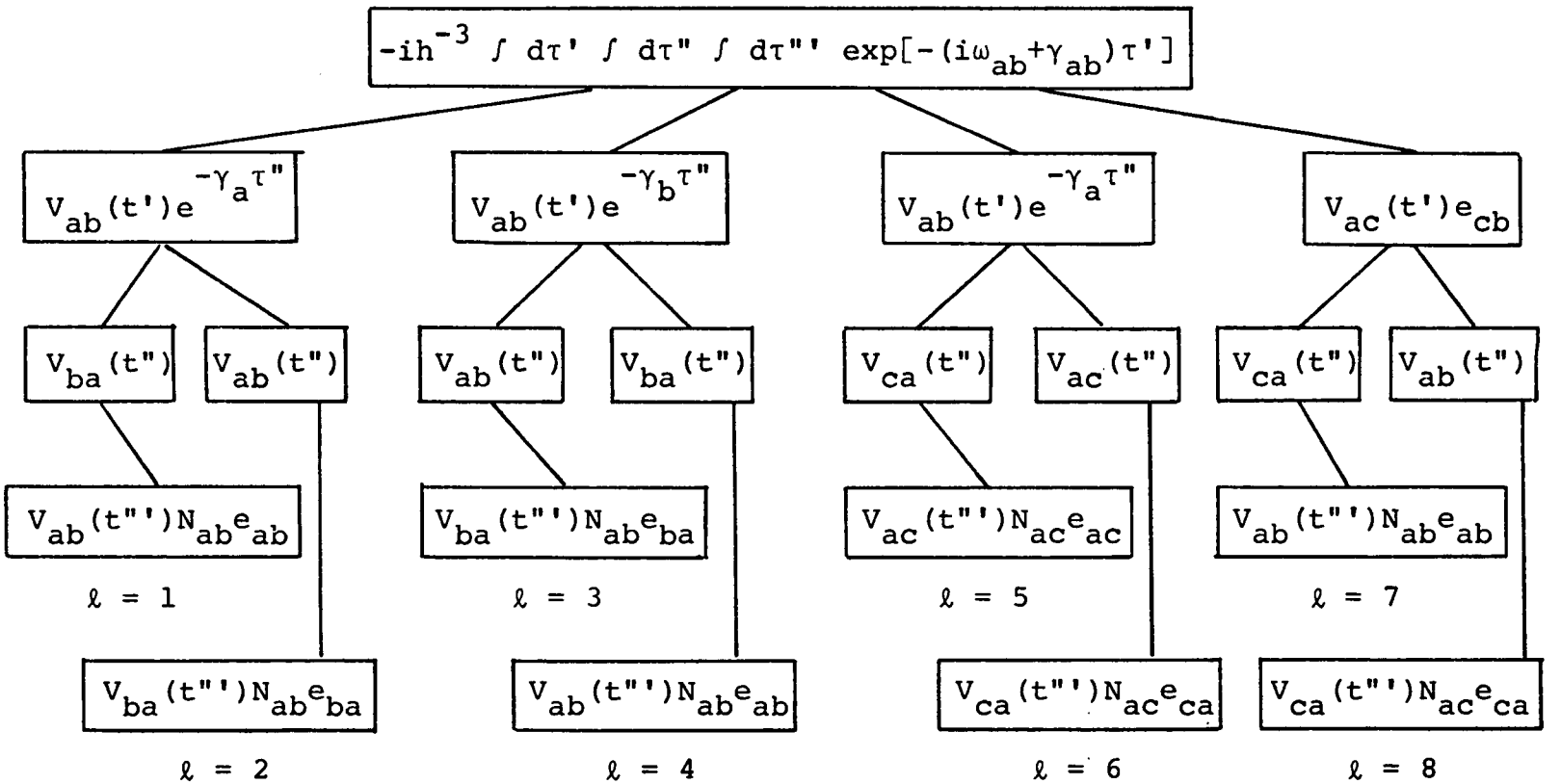

Figure 4. Perturbation tree for the ab transition of the inhomogeneous competitive case -- Terms like e_{ba} are defined in the figure caption of Figure 3.

Table 7. Coefficients appearing in the amplitude and frequency determining equations (70)-(73), for the Doppler limit for the ab transition.

Coefficient	Physical Interpretation
$\alpha_2 = -\frac{1}{2}\frac{\nu_2}{Q_2} + F_{ab}^{(1)} \exp[-(\omega_{ab}-\nu_2)^2/(Ku)^2]$	linear net gain
$\beta_2 = [1+L_{ab}(\omega_{ab}-\nu_2)]F_{ab}^{(3)}$	self saturation for n = 2
$F_{ab}^{(1)} = \frac{1}{2}\sqrt{\pi}\,\nu_2[\wp_{ab}^2/(\hbar\varepsilon_o Ku)]\,\bar{N}_{ab}$	first order factor
$F_{ab}^{(3)} = \frac{1}{4}(\frac{1}{2}\wp_{ab}/\hbar)^2(\gamma_a^{-1}+\gamma_b^{-1})\gamma_{ab}^{-1}F_{ab}^{(1)}$	third order factor
$\sigma_2 = \frac{1}{2}\frac{\nu_n}{\varepsilon_o}\wp_{ab}^2 (Ku\hbar)^{-1}\bar{N}_{ab}\,\mathrm{Re}Z[\gamma_{ab} + i(\omega_{ab}-\nu_2)]\Big\vert_{\text{in the Doppler limit}}$	linear mode pulling
$\rho_2 = [(\omega_{ab}-\nu_2)/\gamma_{ab}]L_{ab}(\omega_{ab}-\nu_2)F_{ab}^{(3)}$	self-pushing
$\upsilon_{2222} = i\gamma_{ab}F_{ab}^{(3)}[\frac{1}{\gamma_{ab}} + \mathcal{D}_{ab}(\omega_{ab}-\nu_2)]$	complex self-saturation
$\upsilon_{2211} = -\frac{i}{8}\frac{F_{bc}^{(1)}}{\gamma_b}(\wp_{ab}/\hbar)^2[\mathcal{D}_{ab+bc}(\omega_{ac}-\nu_1-\nu_2) + \mathcal{D}_{ab+bc}(\omega_{ab}-\omega_{bc}-\nu_2+\nu_1)]$	complex cross-saturation, hole burning part (cascade)

Table 7.--Continued

Coefficient	Physical Interpretation
$\upsilon_{2112} = -\frac{i}{8} F_{bc}^{(1)} (\wp_{ab}/\hbar)^2 \mathcal{D}_{ac}(\omega_{ac}-\nu_1-\nu_2)$ x $\mathcal{D}_{ab+bc}(\omega_{ac}-\nu_1-\nu_2)$	complex cross-saturation, quadrupole part (cascade)
$\upsilon_{2211} = \frac{i}{8} \frac{F_{ac}^{(1)}}{\gamma_a} (\wp_{ab}/\hbar)^2 [\mathcal{D}_{ab+ac}(\omega_{ab}+\omega_{ac}-\nu_1-\nu_2) + \mathcal{D}_{ab+ac}(\omega_{ab}-\omega_{ac}-\nu_2+\nu_1)]$	complex cross-saturation, hole burning part (competitive)
$\upsilon_{2112} = \frac{i}{8} F_{ac}^{(1)} (\wp_{ab}/\hbar)^2 \mathcal{D}_{bc}(\omega_{ab}-\omega_{ac}+\nu_1-\nu_2)$ x $\mathcal{D}_{ab+ac}(\omega_{ab}-\omega_{ac}+\nu_1-\nu_2)$	complex cross-saturation, quadrupole part (competitive)

For further explanation refer to the footnote of Table 1. $\mathcal{Z}(\upsilon)$ is given by Eq. (97).

represents the gas competitive ab transition. Note that the R.H.S. branches in each diagram are the contributions from the second order coherence terms ($\rho_{ac}^{(2)}$ in cascade case and $\rho_{bc}^{(2)}$ in competitive case). The corresponding diagrams for n = 1 modes are given by interchanging ab $\leftrightarrow$ bc and $\gamma_a \leftrightarrow \gamma_c$ for the cascade and ab $\leftrightarrow$ ac and $\gamma_b \leftrightarrow \gamma_c$ for the competitive. At this point, our theory is fairly complete, and in the next chapter we discuss the results obtained.

CHAPTER 6

NUMERICAL RESULTS AND CONCLUSIONS OF PART I

In this chapter we report computer analysis of the intensity equations (74) and (75) for both homogeneous and gas cases, yielding plots of mode intensities and the coupling constant C (76) versus cavity detuning. The intensities are given in units of $\frac{1}{2}(\wp/\hbar)^2(\gamma_a\gamma_b)^{-1}$ (replaced by the corresponding γ's for other transitions), which together with the relative excitation $\mathcal{N}$ (77) eliminate the dependence on the electric-dipole matrix elements $\wp$'s which are often not known accurately. All transitions are weakly coupled (Figures 7, 14, and 17). We discuss the homogeneous case first. For the competitive transitions, the coupling constant has a maximum of about .3 at resonance falling off by 10% at 100 MHZ off-resonance (Figure 7), and for the cascade transitions it is practically a constant about .068 (very weak). For relative excitations $\mathcal{N}_1 = \mathcal{N}_2 = 1.2$, the two modes oscillate almost independently of each other (Figures 5 and 6). We see that in the cascade case (Figure 5), the intensity of mode 1 oscillating alone is about 21% less than the two modes oscillating together, while in the competitive case (Figure 6) it is about 35% more than the two mode transitions. This illustrates the fact that

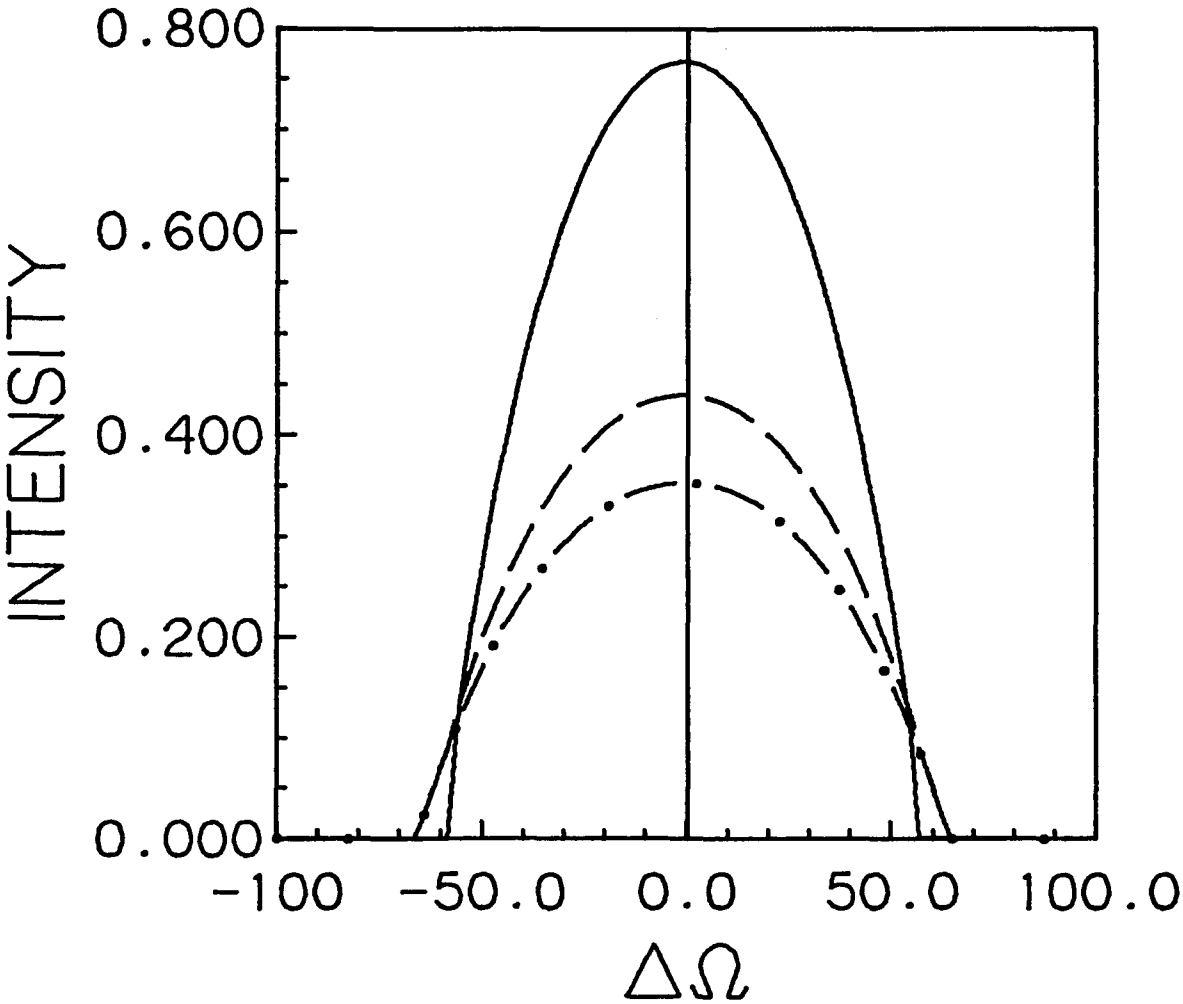

Figure 5. Graph of three-level cascade transitions versus cavity detuning (which is about the same for both modes), homogeneously broadened, stationary atoms -- Solid line and dashed lines correspond to ab and bc transitions of Figure 1(a), and the dashed-dotted line is the single-mode intensity of bc transition. Laser parameters used are γ_a= 15.5 MHz, γ_b = 41.0 MHz, γ_c = 51.0 MHz, γ_{ab} = 128.0 MHz, γ_{bc} = 146.0 MHz, γ_{ac} = 133.0 MHz, and $\mathcal{N}_1 = \mathcal{N}_2 = 1.2$ (Eq. (77)).

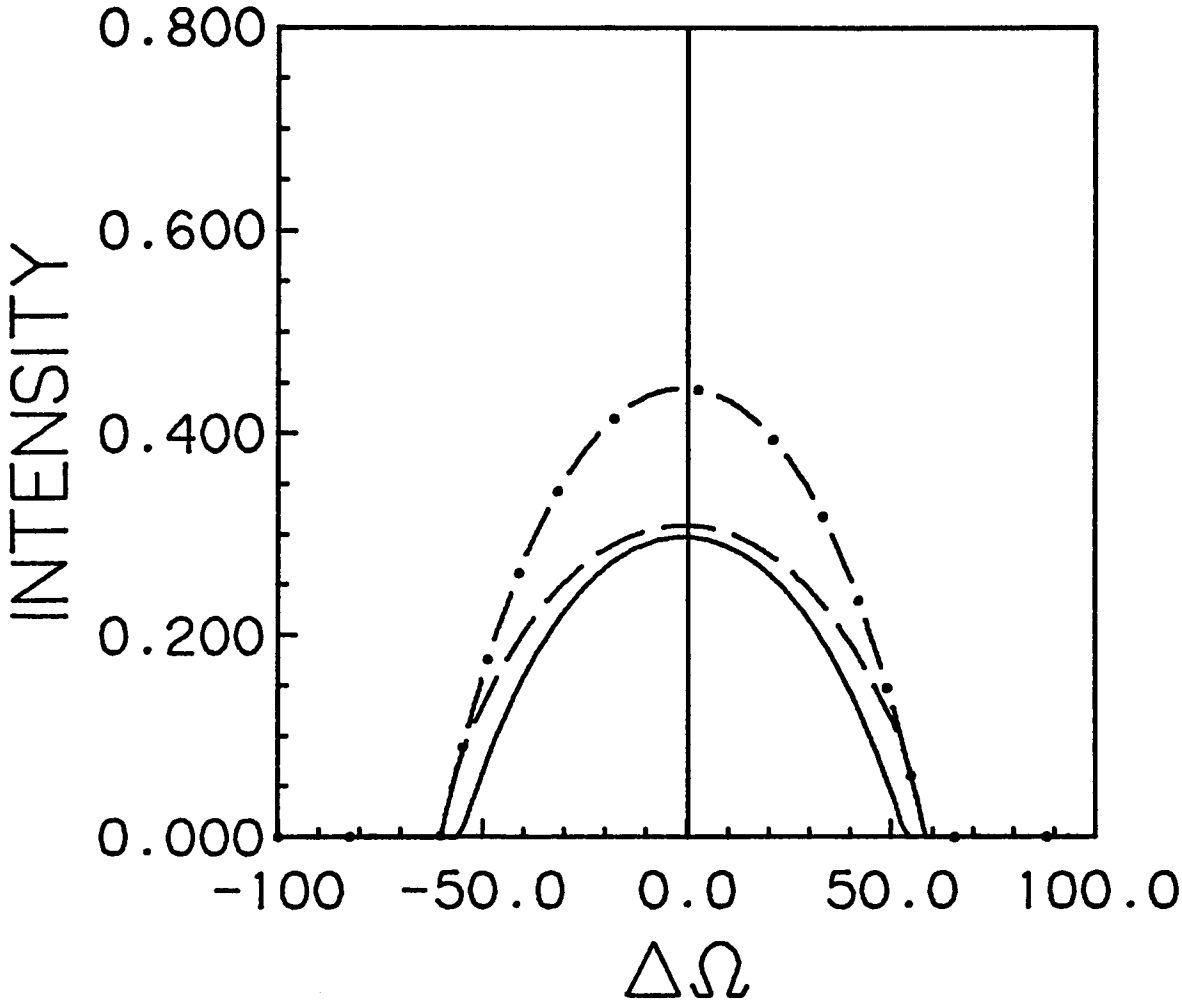

Figure 6. Graph of three-level competitive transitions versus cavity detuning (same for both modes) for homogeneously broadened stationary atoms -- Solid line and dashed line correspond to ab and ac transitions of Figure 1(b), and the dashed-dotted line is the single-mode intensity of ac transition. Laser parameters used are γ_c = 51.0 MHz, γ_{ab} = 128.0 MHz, γ_{ac} = 146.0 MHz, γ_{bc} = 133.0 MHz, and $\mathcal{N}_1 = \mathcal{N}_2 = 1.2$ (Eq. (77)).

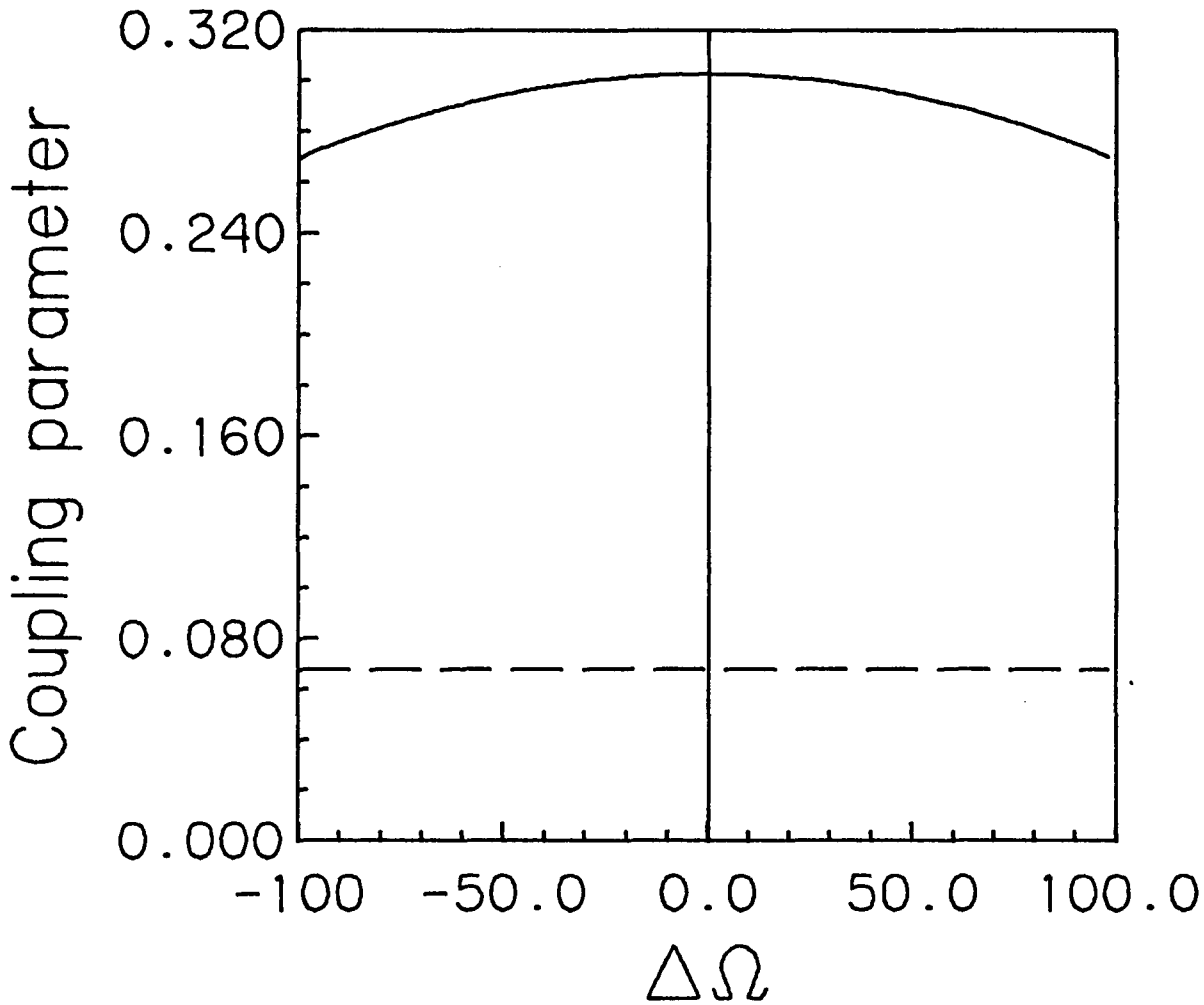

Figure 7. Graph of coupling parameters (Eq. (76)) versus cavity detuning (same for all transitions) for homogeneous case -- Solid like is the coupling parameter of the competitive transitions and the dashed line corresponds to cascade case. Laser parameters are the same as in Figures 5 and 6. Coupling is weak in both cases ($C < 1$).

cascade transitions help one another. Nevertheless, a relative excitation of .99 (less than threshold) for one mode and 1.2 for the other is not enough to bring the first mode above threshold. With excitation levels of 1.2 and 1.05, in the cascade case the second mode starts to oscillate close to resonance (Figure 8) (and of course with much less intensity), while in the competitive case the first mode suppresses the first one for all frequencies. However interesting enough, we found that when we detune the modes by about 50 MHZ, at this same excitation level, in the competitive case, the second mode starts to oscillate very weakly in the domain of frequencies, where the intensity of the first mode is falling off to zero (Figure 9). Thus even for the weak coupling ($C \simeq .3$), the effect of competition is quite pronounced. Now we turn to the gas cases.

Figures 10 and 11 show the corresponding transitions of the gas case to Figures 5 and 6 of the homogeneous case, plus that we see the Lamb dip explicitly. In the competitive transitions (Figure 11) we see a simple Lamp dip at resonance with the intensity of mode 1 by about 53% more while oscillating alone. In the cascade case (Figure 10), when the two modes are oscillating together, we see that the effect of the mutual aid at resonance is so strong that there are small peaks at the center of the Lamb dips. The intensity of the mode 1 oscillating alone is about 40% less

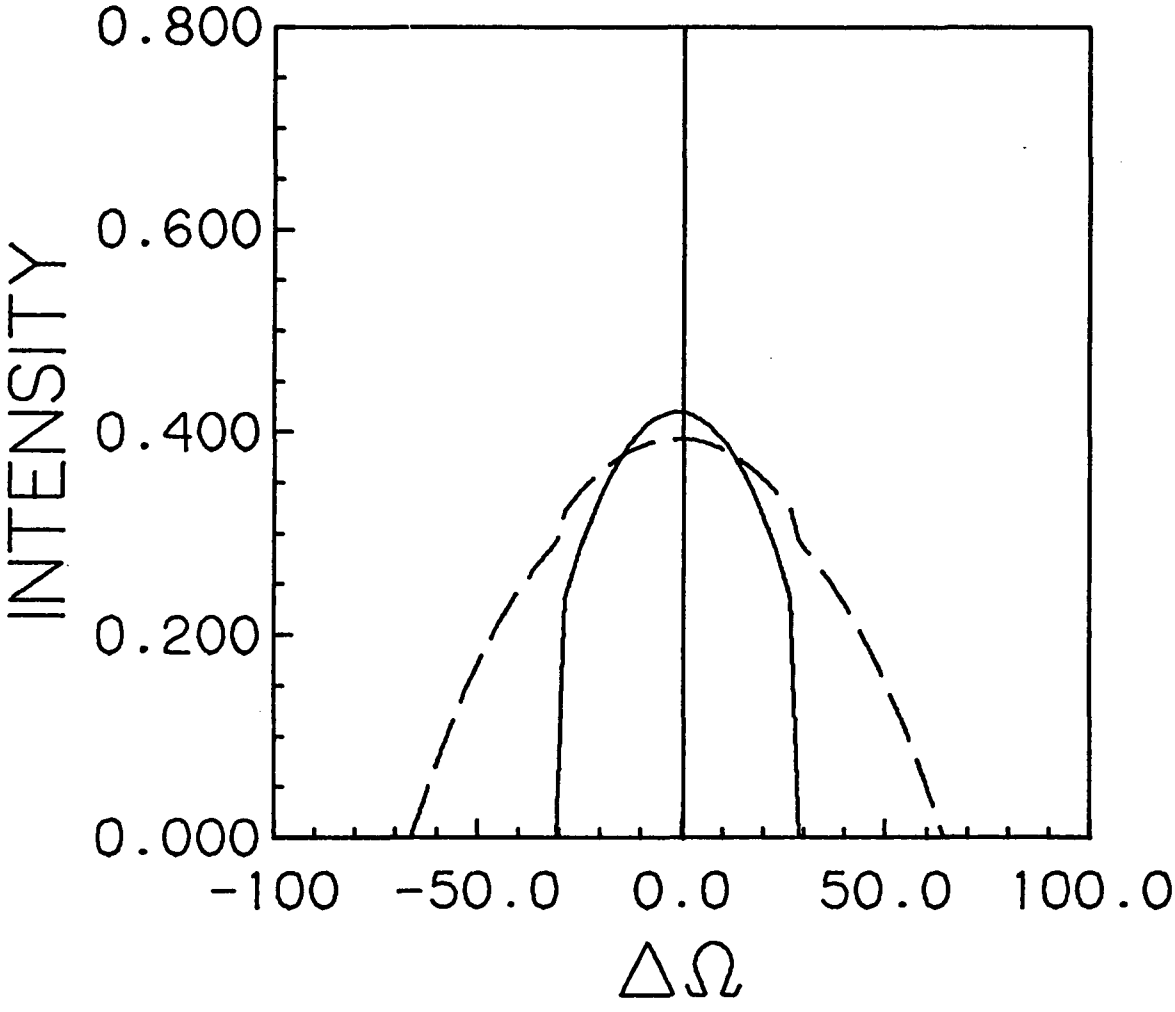

Figure 8. Graph of cascade transitions versus cavity detuning, homogeneous case, for n_2 = 1.05 -- All the rest of the parameters are the same as in Figure 5. This mode starts to oscillate only close to resonance. Its intensity is considerably reduced, while the intensity of mode 1 is not changed much, i.e., the modes oscillate almost independently (weakly coupled).

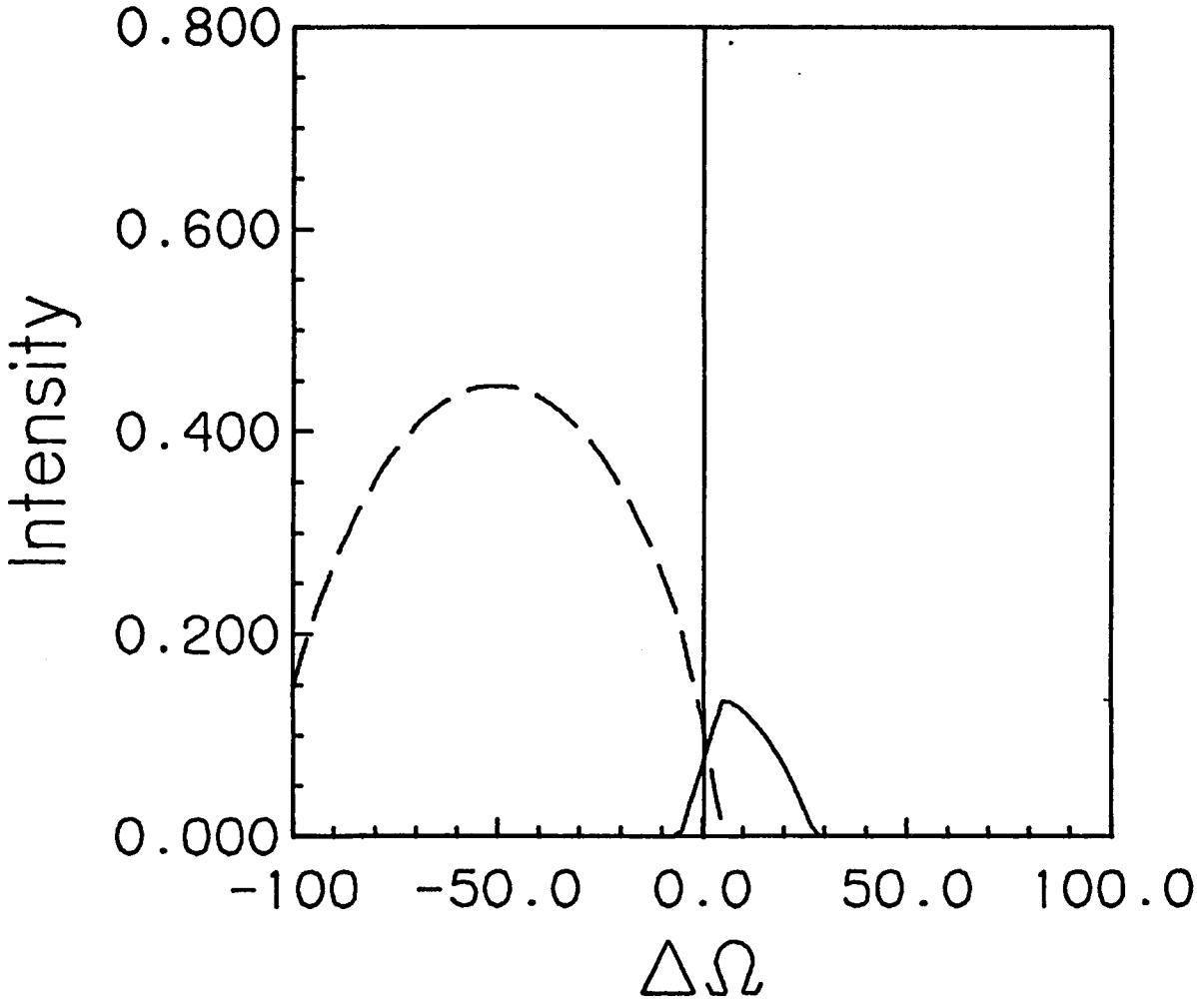

Figure 9. Graph of competitive transitions versus cavity detuning, homogeneous case, for n_2 = 1.05 and n_1 = 1.2 and the two transitions detuned from each other by 50 MHz -- All the rest of the parameters are the same as in Figure 5. Without the detuning mode 2 does not oscillate at n_2 = 1.05.

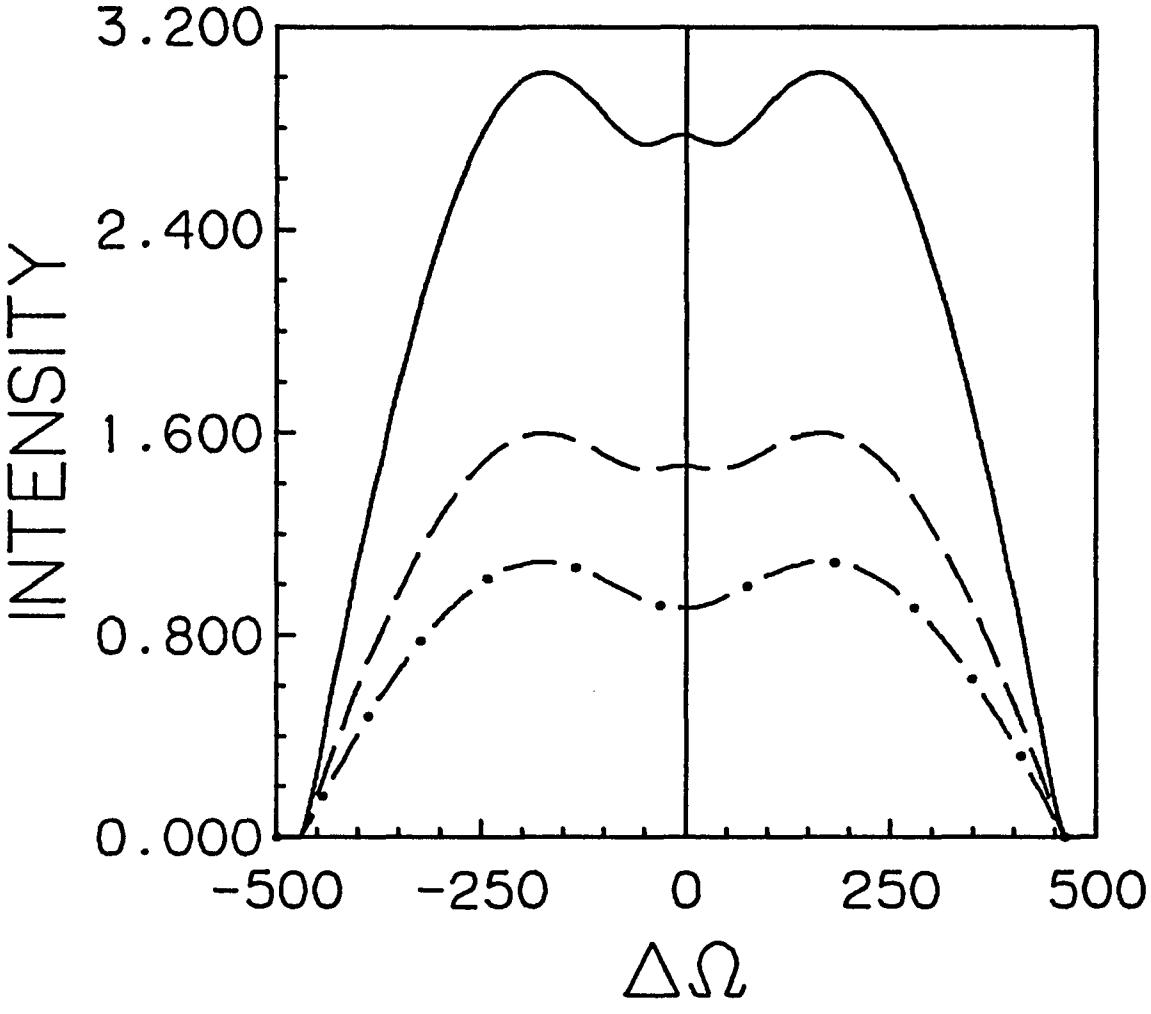

Figure 10. Graph of three-level cascade transitions versus cavity detuning (which is about the same for both modes), inhomogeneously broadened, stationary atoms -- Solid line and dashed lines correspord to ab and bc transitions of Figure 1(a), and the dashed-dotted line is the single-mode intensity of bc transition. Laser parameters used are same as in Figure 5, plus a Doppler broadening of Ku = 1010 MHz.

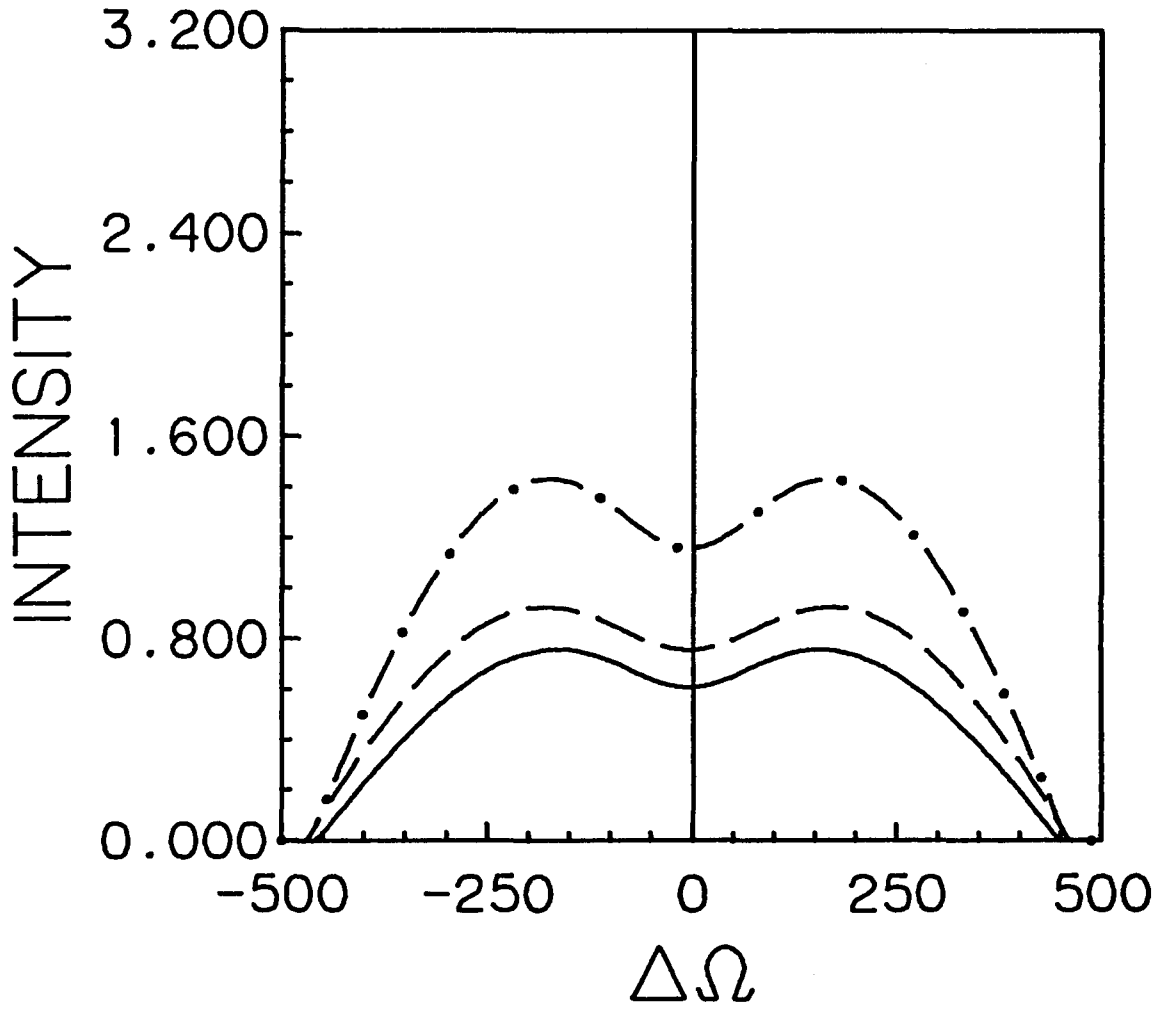

Figure 11. Graph of three-level competitive transitions versus cavity detuning (same for both modes) for inhomogeneously broadened stationary atoms -- Solid line and dashed line correspond to ab and ac transitions of Figure 1(b), and the dashed-dotted line is the single-mode intensity of ac transition. Laser parameters used are the same as in Figure 6, plus a Doppler broadening of Ku = 1010 MHz.

than its intensity oscillating together with the other mode. In fact the plot of coupling constant versus frequency for the cascade case (Figure 14, dashed line) shows that the coupling between the modes is stronger at resonance, which justifies the appearance of the small peaks in the center of the Lamb dips. This effect is more clearly observed with the excitation parameters of 1.2 and 1.05 (Figure 12). Mode 2 (with η_2 = 1.05, solid line) shows a tendency toward a dip at the center, while before it reaches there, mode 1 has helped it to get more intense and it shows even a peak rather than the dip at resonance. Despite the homogeneous case a relative excitation of 1.2 for mode 2 is enough to start the first mode pumped just to η_1 = .99 or 1.0 to lase. A plot for such a case (Figure 13) shows that mode 1 is oscillating weakly (η_1 = 1.0) with no Lamb dip [9] and mode 2 shows the Lamb dip with no peak at the center. Figures 15 and 16 are two-mode plots at excitation levels of 1.2 and detuned by 50 MHZ from each other. The cascade transitions start oscillating by about the same 50 MHZ apart, while the effect of competition prohibits the other competitive mode from oscillating till about 200 MHZ farther apart. Figure 17 shows the coupling parameters for the detuned gas cases versus cavity frequency. We see a slight increase in the coupling constant for competitive transitions close to resonance (about -50 MHZ), where the two modes have equal intensity and hence they compete more strongly (the

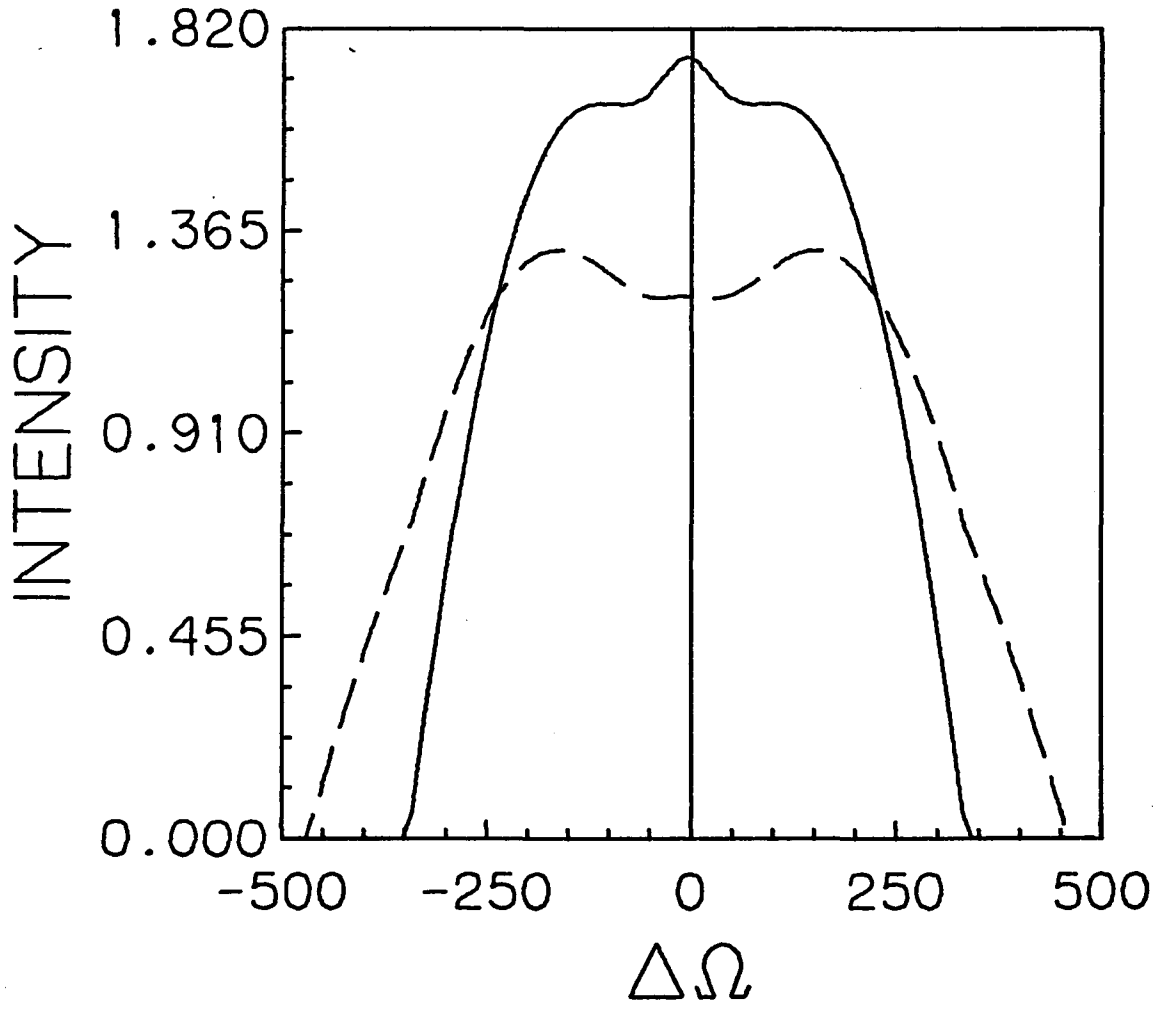

Figure 12. Graph of cascade transitions versus cavity detuning, inhomogeneous case, for π_2 = 1.05 (solid line) -- All the rest of the parameters are the same as in Figure 10.

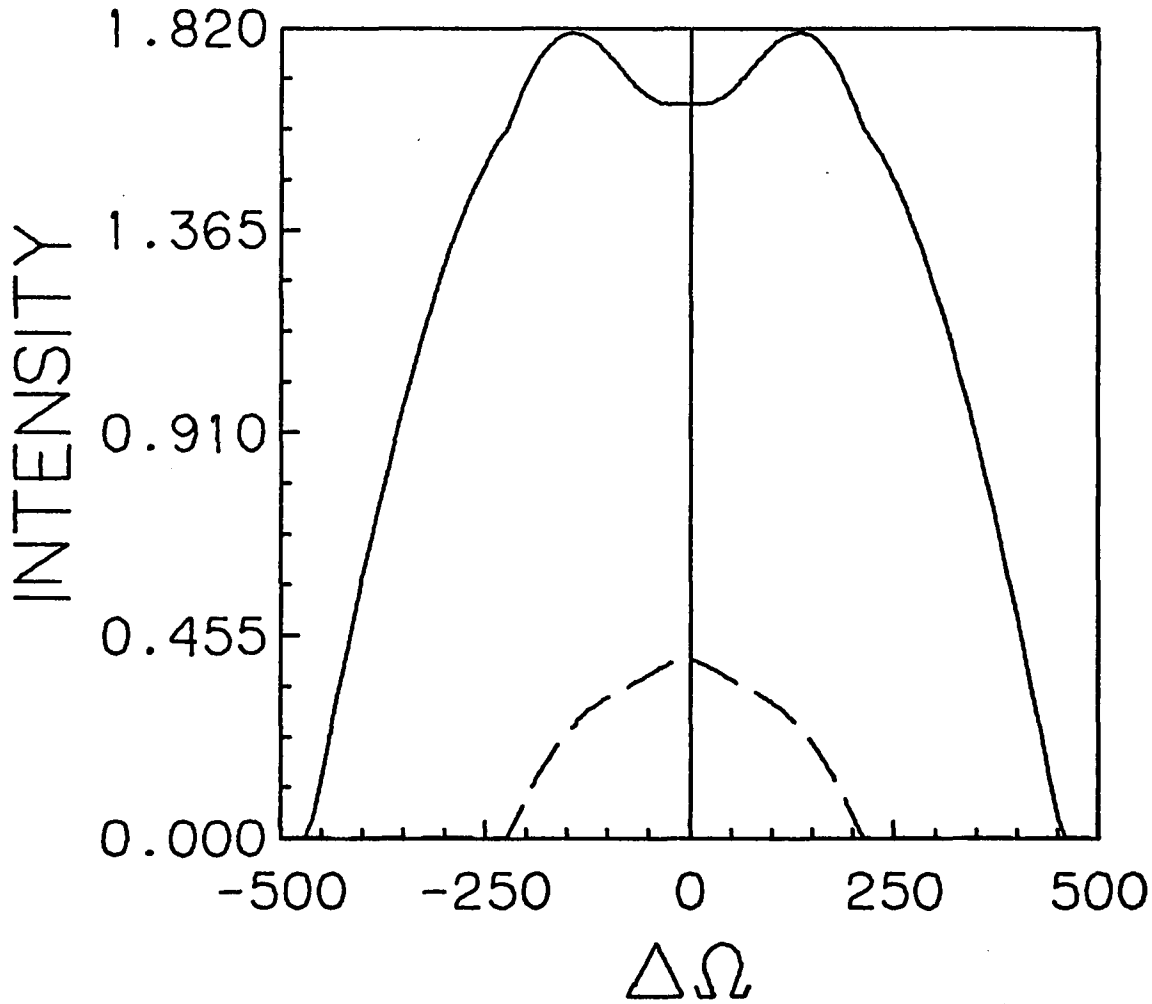

Figure 13. Graph of cascade transitions versus cavity detuning, inhomogeneous case, for n_2 = 1.2 (solid line) n_1 = 1.0 (dashed line) -- All the rest of the parameters are the same as in Figure 10.

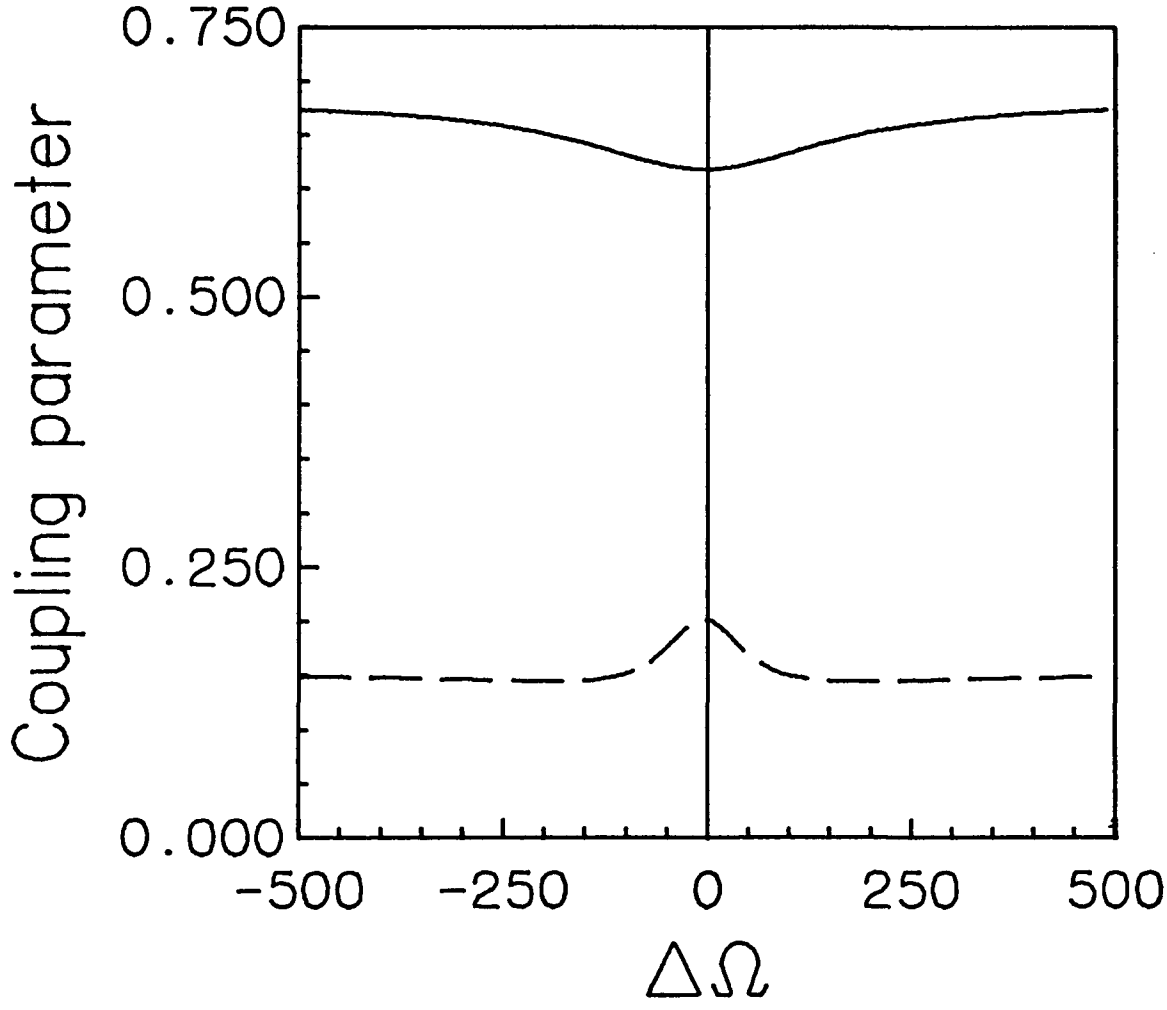

Figure 14. Graph of coupling parameters versus cavity detuning (same for all transitions) for inhomogeneous case -- Solid line is the coupling parameter of the competitive transitions and the dashed line corresponds to cascade case. Laser parameters are same as in Figures 5 and 6, plus a Doppler broadening of Ku = 1010 MHz.

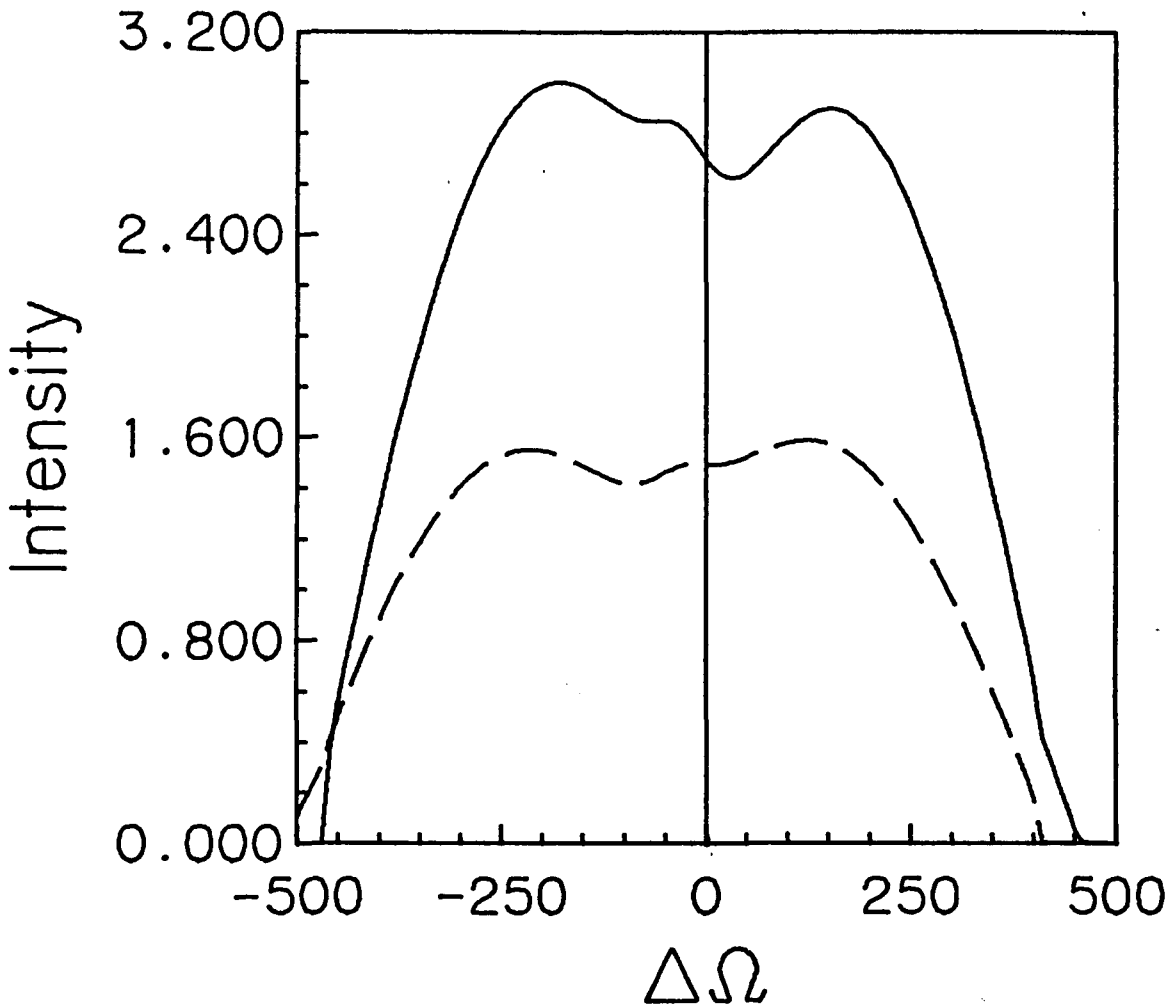

Figure 15. Graph of three-level cascade transitions versus cavity detuning for the gas case with the two transitions detuned from each other by 50 MHz -- Solid line and dashed lines correspond to ab and bc transitions of Figure 1(a). Laser parameters are same as in Figure 10.

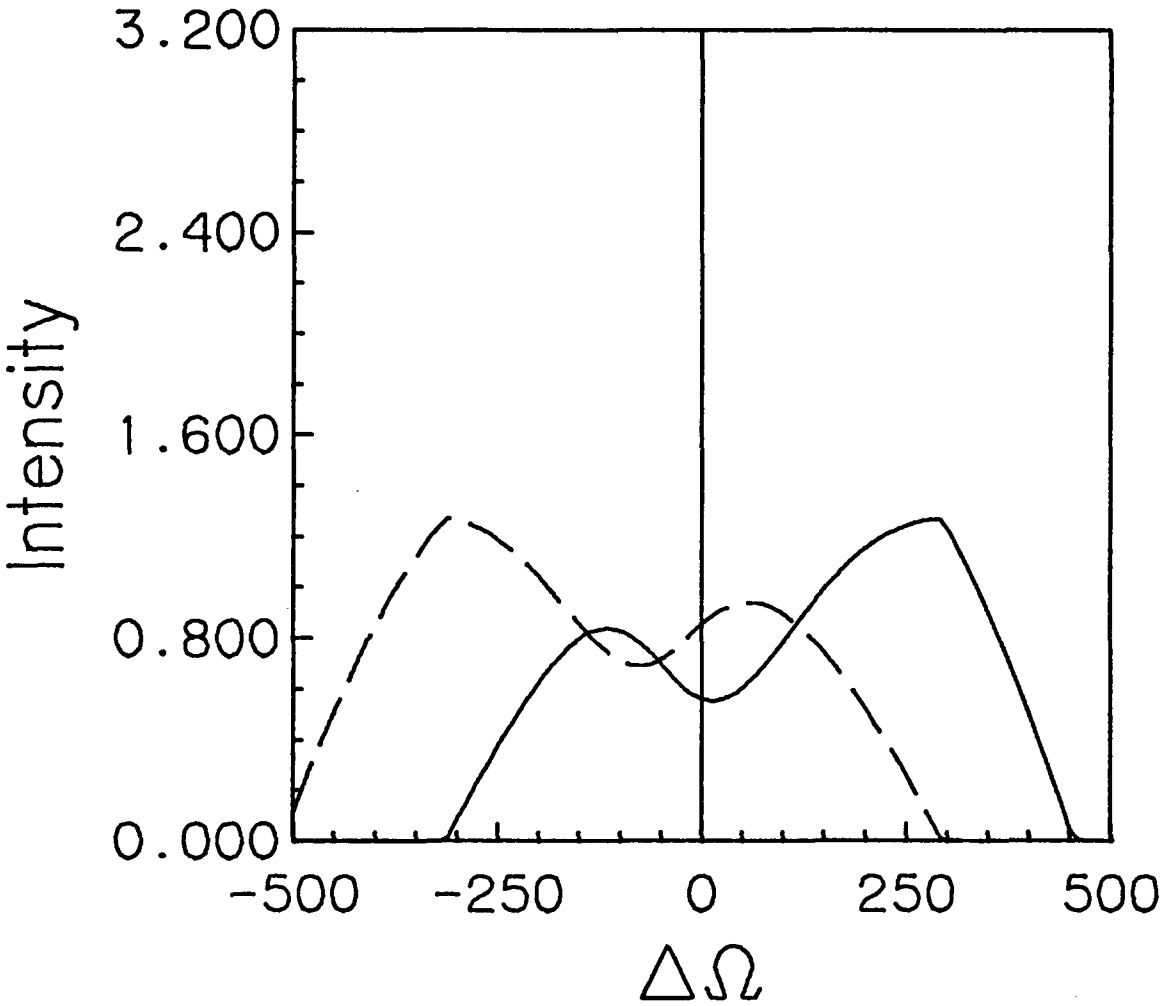

Figure 16. Graph of three-level competitive transitions versus cavity detuning for the gas case with the two transitions detuned from each other by 50 MHz -- Solid line and dashed lines correspond to ab and ac transitions of Figure 1(b). Laser parameters are same as in Figure 10.

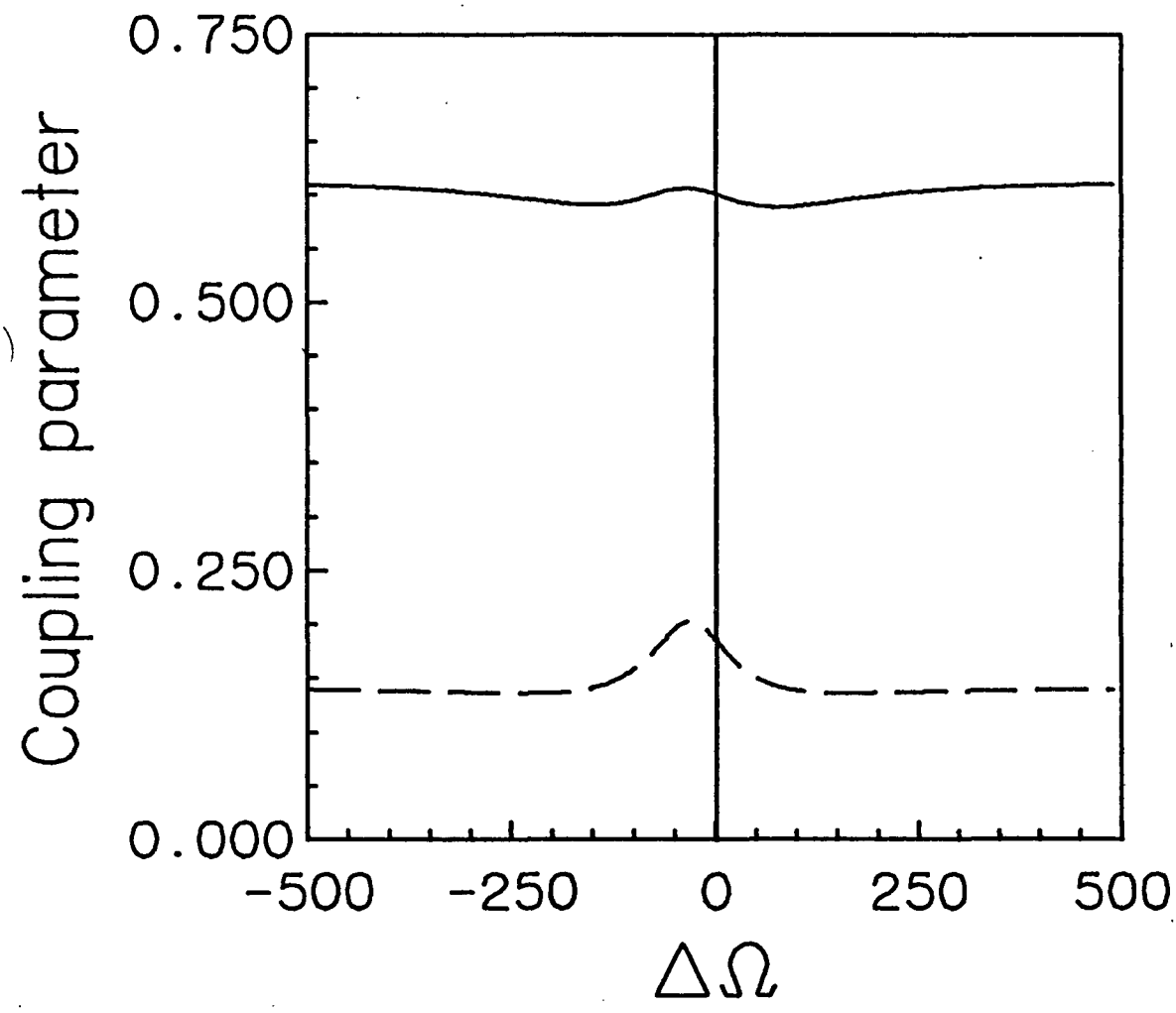

Figure 17. Graph of coupling parameters versus cavity, for the detuned inhomogeneous cases -- Solid line is the coupling parameter of the competitive transitions and the dashed line corresponds to the cascade case. Laser parameters are same as in Figures 15 and 16.

cross-saturation parameters showing relatively more increase than the self-saturations). A final interesting computer run showed us that in fact when we neglect the coherence terms (particularly in cascade case with same relative excitations for both modes) as is usually done by previous authors, the homogeneous transitions are not affected by a considerable amount, but we lose the small peak we had observed in the center of the Lamb dip before. Hence this interesting effect in the cascade case is solely due to the coherence term ρ_{ac}.

PART II

THEORY OF ANHARMONIC MULTILEVEL CASCADE LASER TRANSITIONS

CHAPTER 7

INTRODUCTION TO MULTILEVEL CASCADES

In Chapters 7 to 10 we consider a medium having a set of levels, such as those found in the anharmonic oscillator. We suppose that a single mode field is resonant between adjacent levels for a number of level pairs (see Figure 18). This multimode configuration is a generalization of the two-mode cascade problem of Chapter 3, and, in fact, the relevant laser coefficients can be obtained by inspection from the simpler values in Chapters 4 and 5. Unequal level spacing is necessary here, for otherwise a given mode could interact with more than one pair of levels.

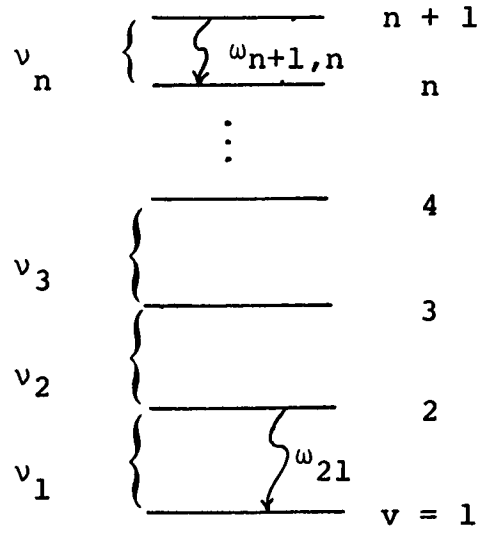

Figure 18. Energy level diagram for multimode cascade.

Our interest in this multilevel cascade problem has been stimulated by the extensive work done on the CO laser, and our analysis applies to some aspects of CO laser operation. Chapter 8 defines our model and outlines the extensions to the three-level cascade. Later chapters deal with numerical results and the deviation of the third-order theory from the exact results.

The first CO laser operation was reported by Patel and Kerl [12] in 1964. In his more complete report of 1966, Patel [13] showed several interesting characteristics of P-branch transitions including the normalized gain at different temperatures for different rotational sub-levels of each vibrational level and for different values of relative population inversions. His studies of the time-dependence of the population inversions was contradicted later by Hancock and Smith [14]. Specifically they showed that by adding vibrationally cold CO (or some other suitable gas), it is possible to maintain a total population inversion. Patel [13] showed that R branch rotational transitions for $300°K < T < 400°K$ never yield gain, thereby precluding laser oscillation on these branches. Different characteristics of CO lasers and other diatomic lasers have been studied extensively since then. Eppers, Osgood, and Greason [15]; Osgood, Nichols, Eppers, and Petty [16]; and Osgood, Eppers, and Nichols [17] reported high-power cw transitions in CO lasers (in different gas mixtures) with $\sim$9% efficiency.

With a rotating mirror Q-switch, they obtained powers of the order of 95W from 320 cm^3 active volume with 20% efficiency. Yardley [18, 19, 20] observed over 210 laser transitions with high resolution in a Q-switched CO-He laser through as high energy levels as v = 37 (lowest v = 4) and in his later paper [20], he discussed some of the inversion and energy transfer processes in CO lasers. One of the most recent and detailed papers on the characteristics of a CO laser is the work of Bhaumik, Lacina, and Mann [21] which includes discussion of kinetic processes together with some experimental observations.

One important feature of the CO lasers is the anharmonicity intrinsic in the molecule; that is, the vibrational levels get closer as the vibrational quantum number increases (see Figure 18). This anharmonicity is important because it causes V-V exchanges to favor high levels at the expense of lower levels; i.e., to create an inversion. This occurs due to the fact that as V = 19 → 18 transition must be accompanied by additional energy to cause a V = 1 → 2 transition, whereas the reverse exchange has the energy difference to spare (is exothermic). The basic concepts of the anharmonic oscillators are discussed by Herzberg [22]. A detailed study of dipole-moment function and vibration-rotation matrix elements for CO has been done by Young and Eachus [23] and some experimental workers [24, 25, 26, 27, 28, 29]. In our simplified model we use dipole moment

values that fit these models approximately. Caledonia and Center [30] and Center and Caledonia [31] developed a model for the steady-state vibrational distribution functions of anharmonic oscillators based on rate-equation type of solutions including the collisional exchange processes of vibration-vibration (V-V) and vibration-translation (V-T) and the radiative decay rates for different species of gas present in the system. Other theoretical models by Treanor, Rich, and Rehm [32] and Rich [33] are also based on the rate-equation approximation, and depict characteristics like small-signal gain versus v and vibrational populations versus v at different temperatures, pressures, and gas mixtures. None of these theories have been quite adequate for CO, or in general, as we are interested in, for a multilevel cascade laser. Jeffers and Kelley [34] have done calculations for the V-V transfer probabilities in CO-CO collisions and Jeffers and Wiswall [35, 36], Abraham and Fisher [37, 38], and Fisher [39, 40] have studied pulsed CO lasers; in particular Abraham and Fisher [37] have considered conditions for obtaining maximum gain in a pulsed CO/N_2 laser and have studied the time evolution of the maximum gain for different vibrational transitions. Short pulse ($\sim$1 nsec) energy extraction from CO amplifiers has been studied by Hopf [41]. The time evolution of CO vibrational distribution function in electrically pumped $CO-N_2$-He lasers has been studied by Rockwood et al. [42],

who solved the coupled time-dependent rate equations for the first 50 vibrational levels of CO considering V-V and V-T processes, spontaneous and stimulated emission, electron impact excitation and de-excitation, and kinetic heating of the lasing medium.

Next let us summarize our work given in the following chapters. In Chapter 8 we discuss our model for a multilevel cascade cw laser. Particular attention is paid to application to diatomic media, to pumping and relaxation mechanisms in CO lasers, and to the time-dependency of the pumping coefficients. Chapter 9 is mainly the mathematical formulation for the model which is, in fact, a straightforward generalization of our homogeneous three-level cascade laser. In Chapter 10 we discuss our numerical results. In Chapter 11 we postulate a more simplified hypothetical model for the equations of motion of the number density of the vibrational levels and the intensities of the transitions. We solved these equations numerically on a computer to get an estimate of the error of the third order theory versus the exact results. The results are shown in terms of the intensity plots versus the relative inversion densities. Although one might expect that the high intensity due to the cascading process may break the third-order theory very soon, we found that it is reasonably good enough for the relative excitations as high as $\Pi = 1.2$ or even more.

We found that errors from neglecting the higher orders in cross-saturation coefficients have opposite sign from those of self-saturation coefficients in cascade case and partially cancel one another out. Hence for a given excitation the third-order cascade treatment tends to be more accurate than the corresponding competitive case.

A fairly complete list of experimental work is given in the References [43-72].

CHAPTER 8

RELATIONSHIP BETWEEN CO LASERS AND OUR MODEL

The energy level diagram (Figure 18) defining part of the cascade model we use is considerably simpler than that for the CO molecule. (The diatomic molecules like CO have an anharmonic potential energy model known as the Morse potential [73]). The latter features a set of rotational levels for each vibrational level, whereas we consider a single level alone. In turn, the rotational levels have magnetic sublevels. We approximate the latter by the single level here as cases of nonzero atomic angular momenta. Furthermore, it is typically found that only one rotational level per vibrational level is involved in laser transitions. For example, a cascade could take place between the levels ($v = 10$, $J = 8$), ($v = 9$, $J = 9$), and ($v = 8$, $J = 10$). Here we have considered a P-branch set, inasmuch as the Q and R branches are not observed in laser oscillation [13]. The other rotational levels do interact with the laser transition indirectly through rapid collisions that repopulate the population distribution. We suppose that the Boltzmann distribution in the rotational levels corresponding to a single vibrational level is

maintained in time through the collisions. As such the level lifetimes are not affected by the collisions, but the induced dipole moments dephase accordingly (the T_2 time is reduced, here represented by dipole decay constants like γ_{21}). Hence we do not include any special factors in the atomic equations of motion to account for these processes.

Vibration-vibration (V-V) collisions lead to an effect that tends to pump an inversion [20]. Specifically, because the higher lying levels are more closely spaced than the lower levels, the collision process

$$CO(v-1) + CO(1) \rightarrow CO(v) + CO(0) + \Delta E \qquad (109)$$

releases energy (see Figure 19). The reverse process must absorb energy and is therefore less probable. Hence V-V collisions tend to pump the molecules up higher in vibrational quantum number.

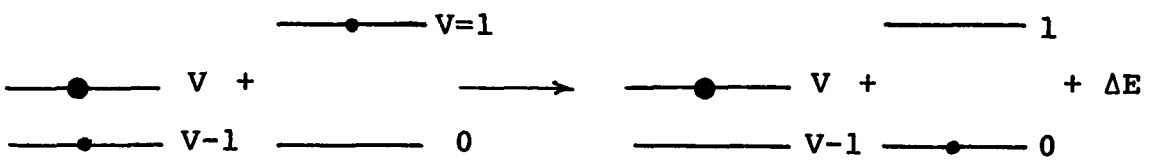

Figure 19. Pictorial representation of Eq. (109).

V-V rates decrease with increasing quantum number (as ΔE increases) and for sufficient high v ($v \sim 30$ [37]) radiative and V-T processes are the dominant factors in the relaxation rates. The V-V transition probabilities due to short-range forces decrease with lowering the temperature, but this is compensated by the long-range forces which increase the rate constants. Thus V-V exchange in upper levels ($v>8$ [14]) becomes the efficient process determining the level lifetimes (T_1) for the laser transitions. Hancock and Smith [14] also discuss the V-V and V-T energy transfer rates. They point out that Patel's [13] explanation, which involves complicated and time-dependent mechanisms, is wrong. Once a small portion of CO molecules is vibrationally excited into the higher levels, the excited molecules relax mainly by the V-V energy exchange process, and since the lower levels have a larger decay rate, the ratios of population densities in the adjacent levels increases thereby allowing the lasing process to occur. One might describe the lion's share of the time-dependence of pumping and relaxation processes by writing the equation of motion for the population density, N_k, of one of the levels (ignoring the small coherence terms) as

$$\dot{N}_k = - \sum_{\ell \neq k} W_{\ell k} N_\ell N_k + \sum_{\ell \neq k} W_{k\ell} N_{\ell+1} N_{k-1}$$

$$- \frac{i}{\hbar} [\text{the dipole interaction term}]_{kk} \qquad (110)$$

The kinetic terms also contain processes which take the molecule from k to k+1 level. These have been left out for reasons of simplicity. We suppose that, in steady-state cases, the decay "constant"

$$\gamma_k \equiv \sum_{\ell \neq k} W_{\ell k} N_\ell , \tag{111}$$

and pump rate

$$\lambda_k \equiv \sum_{\ell \neq k} W_{k\ell} N_{\ell+1} N_{k-1} , \tag{112}$$

are time and population independent.

As a further simplification, we consider cw operation as in the three-level cases and sufficiently low intensities that third-order perturbation theory is valid. As discussed in Chapter 11, the small intensity restriction is not as severe in the cascade case as in the competitive case due to the partial cancellation of neglected higher order terms. Our numerical results are concerned with homogeneously broadened media, although corresponding Doppler case coefficients follow equally readily from the three-level case according to the simple prescription given in Chapter 9.

CHAPTER 9

PERTURBATION SOLUTION FOR THE MULTILEVEL CASCADE

With the assumption that only one cavity mode is resonant with any given transition of the cascade chain (see Figure 18), the electric dipole perturbation potential is denoted by

$$V_{n,n-1} = -\frac{1}{2}\wp_n E_n(t)\exp[-i(\nu_n t+\phi_n)]U_n(z),$$

$$\nu_n \neq \nu_{n-1} \neq \nu_{n-2} \neq \cdots \tag{113}$$

where n refers to the upper level of the transition.

We can avoid doing the algebra by utilizing the three-level coefficients like the net gain α_n, self-saturation β_n, pulling (σ_n) and pushing (ρ_n) coefficients. The mode intensity equations of motion have the general form

$$\dot{I}_n = 2I_n\{\alpha_n-\beta_n I_n-\theta_{n,n+1}I_{n+1}-\theta_{n,n-1}I_{n-1}\}. \tag{114}$$

Here for N mode operation, the cross-saturation coefficients $\theta_{1,0}$ and $\theta_{N,N+1}$ vanish, truncating the equations for I_1 and I_N. The θ's can be determined by noting that $\theta_{n,n+1}$ represents the saturation of mode I_{n+1} on the adjacent lower mode I_n. This is like the process I_2 on I_1 in the three-level case, and the coefficient $\theta_{n,n+1}$ is, in fact,

given by θ_{12} with the subscript substitutions 1→n, 2→n+1, a→n+2, b→n+1, and c→n. Similarly, $\theta_{n,n-1}$ represents the saturation of mode I_{n-1} on the adjacent higher mode I_n and is given by θ_{21} with the substitutions 2→n, 1→n-1, a→n+1, b→n, and c→n-1. In the earlier chapters, we used the complex coefficients υ_{nnmm} and υ_{nmmn}, but the substitution schemes remain the same. For reference purposes, we write down the equations of motion and the first and third order polarizations. The intermediate steps of integration are along the lines of the three-level problem and are not presented. The equations of motion for the density matrix components have the general form

$$\dot{\rho}_{nn} = \lambda_n - \gamma_n\rho_{nn} - [\frac{i}{\hbar}\sum_p V_{np}\,\rho_{pn} + c.c.] \tag{115}$$

for the diagonal terms and

$$\begin{aligned}\dot{\rho}_{np} &= -(i\omega_{np}+\gamma_{np})\rho_{np} - \frac{i}{\hbar}[\sum_{k\neq n} V_{nk}\rho_{kp} - \sum_{k\neq p}\rho_{nk}V_{kp}] \\ &= -(i\omega_{np}+\gamma_{np})\rho_{np} + \frac{i}{\hbar}V_{np}(\rho_{nn}-\rho_{pp}) - \frac{i}{\hbar}[\sum_{\substack{k\neq p\\ k\neq n}} \\ &\quad \times V_{nk}\rho_{kp} - \sum_{\substack{k\neq n\\ k\neq p}}\rho_{nk}V_{kp}]\end{aligned} \tag{116}$$

for the off-diagonal terms, with the formal integral

$$\rho_{np} = \frac{i}{\hbar}\int_{-\infty}^{t} dt' \exp[-(i\omega_{np}+\gamma_{np})(t-t')]\{V_{np}(\rho_{nn}-\rho_{pp}) + \sum_{k\neq n,p}\rho_{nk}V_{kp} - \sum_{k\neq n,p}V_{nk}\rho_{kp}\}, \quad (117)$$

and the familiar initial conditions

$$\rho_{nn}^{(0)} = \lambda_n/\gamma_n, \ \rho_{np}^{(0)} = 0 \text{ for n and p = 1 to N+1.}$$

For the first order polarization term we get a very similar expression to the three level results, i.e.,

$$P_n^{(1)}(t) = -(\wp_n^2/\hbar)\bar{N}_{n,n-1}E_n(t)[\frac{(\omega_{n,n-1}-\nu_n) + i\gamma_{n,n-1}}{(\omega_{n,n-1}-\nu_n)^2 + \gamma_{n,n-1}^2}], \quad (118)$$

but the third order polarization has two extra terms for the middle levels proportional to $E_nE_{n+1}^2$ due to the cascading process from the upper levels. It is given by

$$P_n^{(3)}(t) = +i(\wp_n^2/\hbar)E_n\mathcal{D}_{n,n-1}(\omega_{n,n-1}-\nu_n)\{\frac{3}{8}(\frac{1}{\gamma_n} + \frac{1}{\gamma_{n-1}})$$

$$\times (\wp_n/\hbar)^2E_n^2\frac{N_{n,n-1}}{\gamma_{n,n-1}}L_{n,n-1}(\omega_{n,n-1}-\nu_n) - \frac{1}{4}\frac{1}{\gamma_n}$$

$$\times (\wp_{n+1}/\hbar)^2E_{n+1}^2\frac{N_{n+1,n}}{\gamma_{n+1,n}}L_{n+1,n}(\omega_{n+1,n}-\nu_{n+1})$$

$$- \frac{1}{4}\frac{1}{\gamma_{n-1}}(\wp_{n-1}/\hbar)^2E_{n-1}^2\frac{N_{n-1,n-2}}{\gamma_{n-1,n-2}}L_{n-1,n-2}(\omega_{n-1,n-2}$$

$$- \nu_{n-1}) + \tfrac{1}{8}(\wp_{n-1}/\hbar)^2 E_{n-1}^2 [N_{n,n-1} \mathcal{D}_{n,n-1}(\omega_{n,n-1} - \nu_n)$$

$$- N_{n-1,n-2} \mathcal{D}_{n-1,n-2}(\omega_{n-1,n-2} - \nu_{n-1})] \mathcal{D}_{n,n-2}(\omega_{n,n-2}$$

$$- \nu_n - \nu_{n-1}) - \tfrac{1}{8}(\wp_{n+1}/\hbar)^2 E_{n+1}^2 [N_{n+1,n} \mathcal{D}_{n+1,n}(\omega_{n+1,n}$$

$$- \nu_{n+1}) - N_{n,n-1} \mathcal{D}_{n,n-1}(\omega_{n,n-1} - \nu_n)] \mathcal{D}_{n+1,n-1}(\omega_{n+1,n-1}$$

$$- \nu_n - \nu_{n+1})\}. \tag{119}$$

The intensity determining equations are given by

$$\dot{I}_1 = 2I_1(\alpha_1 - \beta_1 I_1 - \theta_{12} I_2) \tag{120}$$

for the lowest level,

$$\dot{I}_m = 2I_m(\alpha_m - \beta_m I_m - \theta_{m,m-1} I_{m-1}) \tag{121}$$

for the uppermost level. Again we find the steady-state solutions by the same method as for the three-level case (also discussed in [11]).

CHAPTER 10

NUMERICAL RESULTS OF PART II

In this section we present intensity plots for a five mode cascade case. The intensities are again dimensionless and studies of the different pairs of adjacent transitions also showed that they are weakly coupled with a coupling constant of .108 for the data we used. Our studies also show for the data we chose for the decay rates and even with the maximum excitations of $r = 1.2$, the third-order theory still yields quite acceptable results for the intensities of the cascade transitions. Figures 20 through 24 show graphs of intensity versus the cavity detuning for the five modes, starting with the first mode oscillating alone with $r = 1.2$ and then together with other modes each pumped just to the threshold level; i.e., at $r_n = 1.0$. The mutual aid in cascading processes is again clear. Since we pump all the lower levels (other than the uppermost one) just to the threshold, the increase in the intensities due to the additional transitions is not strong. A slight increase in the intensity of the upper transition occurs whenever a new (lower) mode starts to oscillate. This effect was also observed (as expected) in the simpler three-level cases. This is the normal case in a multilevel cascade laser like

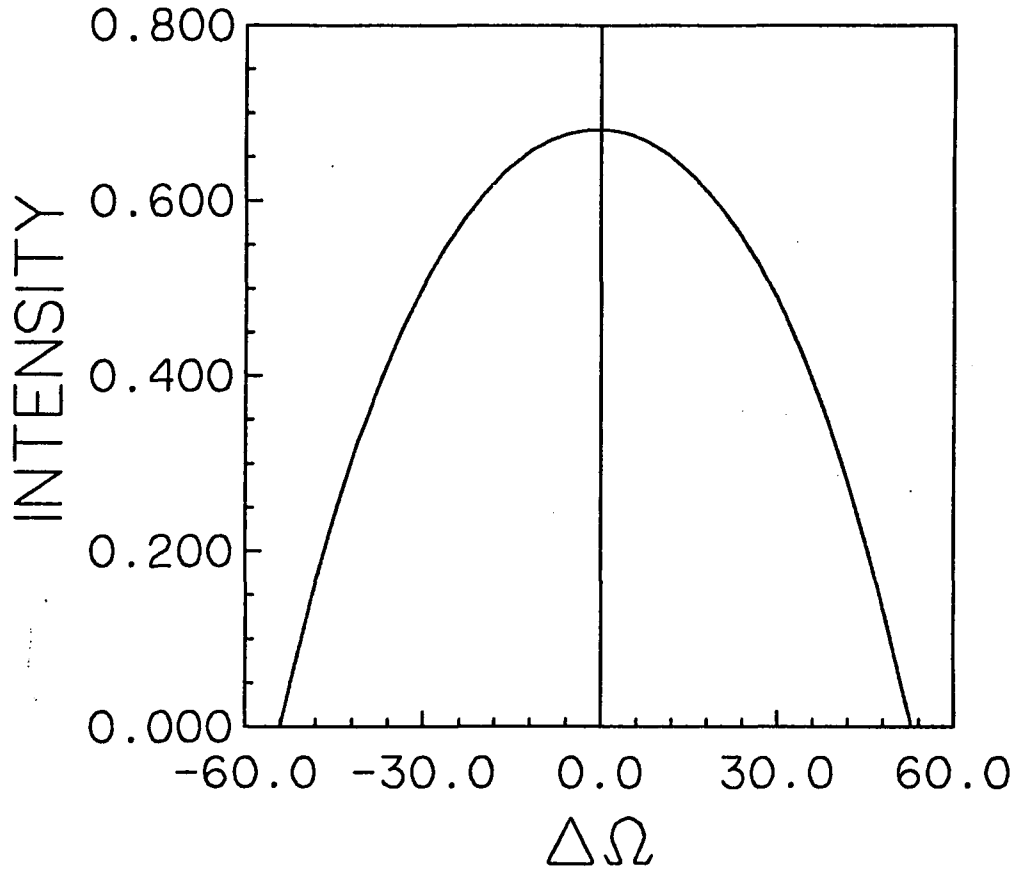

Figure 20. Graph of intensity of the uppermost transition of a six-level-anharmonic-cascade oscillating alone at $\mathcal{N}_5 = 1.2$ (Eq. (77)) -- Other parameters used are $\gamma_6 = 20.0$ MHz, $\gamma_5 = 19.0$ MHz, and $\varphi_5 = 1.40$.

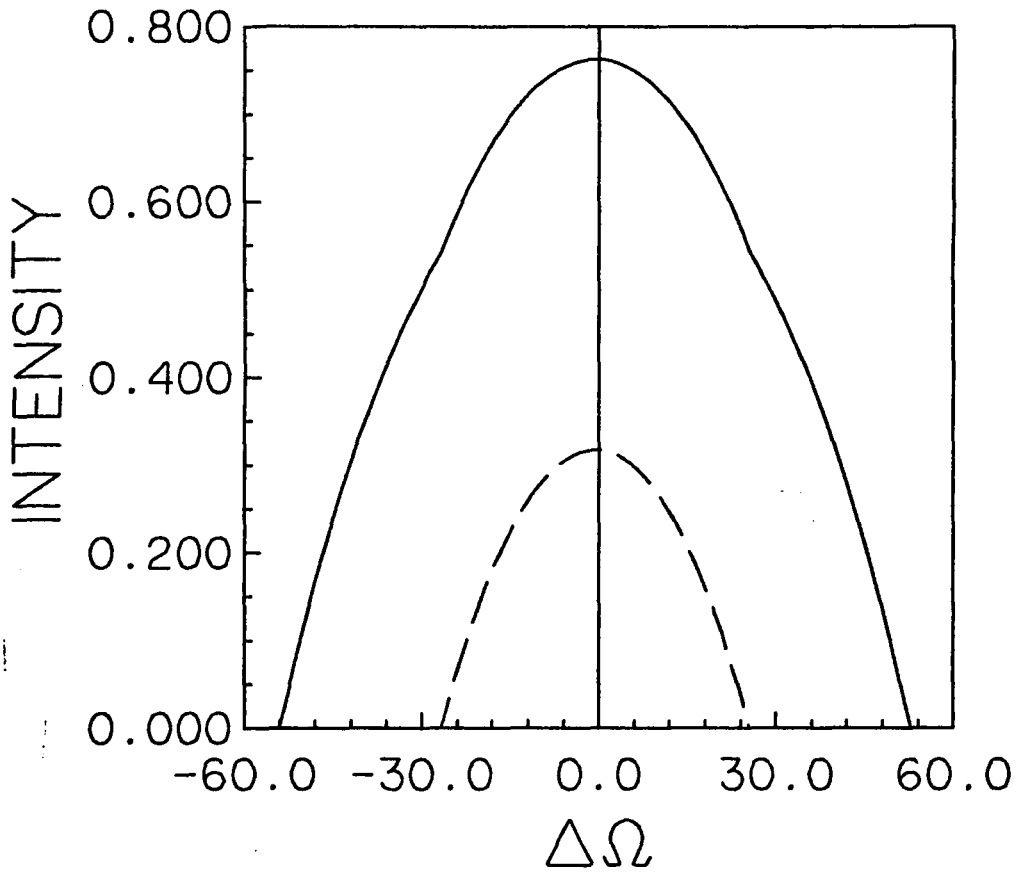

Figure 21. Graphs of intensities of the two upper modes oscillating together at π_5 = 1.2 and π_4 = 1.0 -- Parameters for the fourth mode are γ_4 = 17.0 MHz, and φ_4 = 1.35, and the rest are same as in Figure 20.

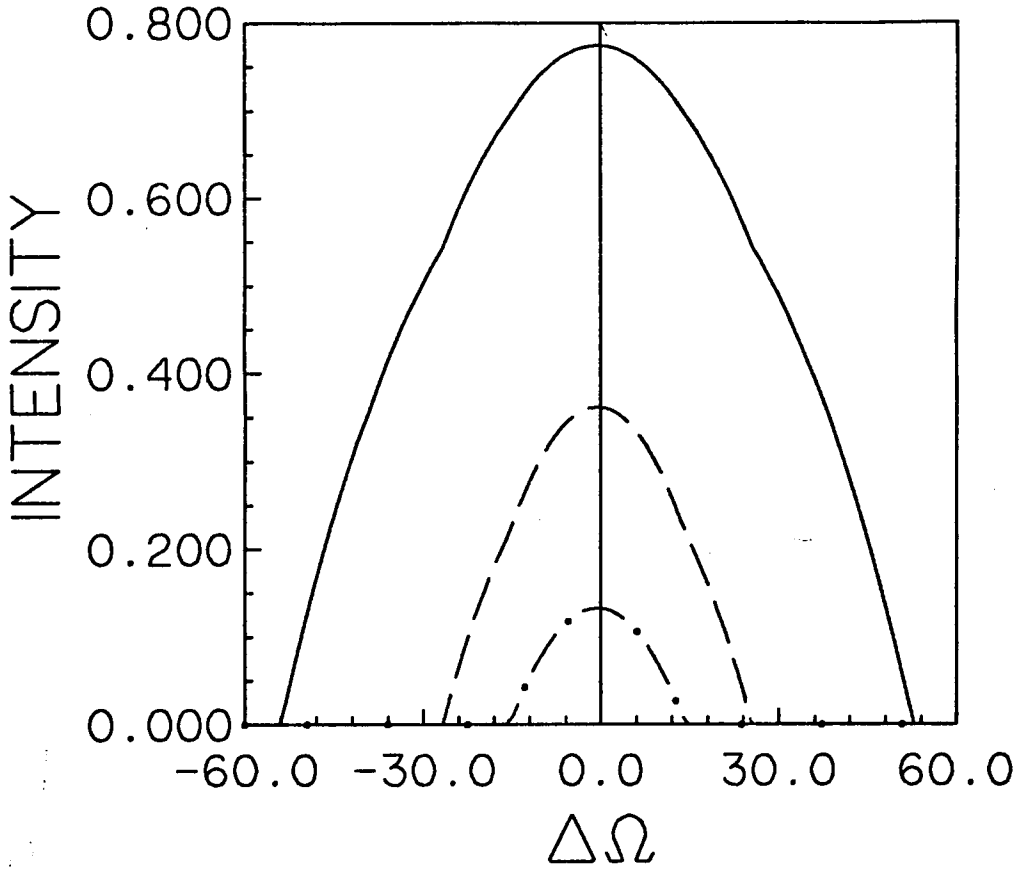

Figure 22. Graphs of intensities of the three upper modes oscillating together at $\kappa_5 = 1.2$ and $\kappa_4 = \kappa_3 = 1.0$ -- Parameters for the third mode are $\gamma_3 = 14.9$ MHz and $\varphi_3 = 1.30$. Other parameters are same as in Figures 20 and 21.

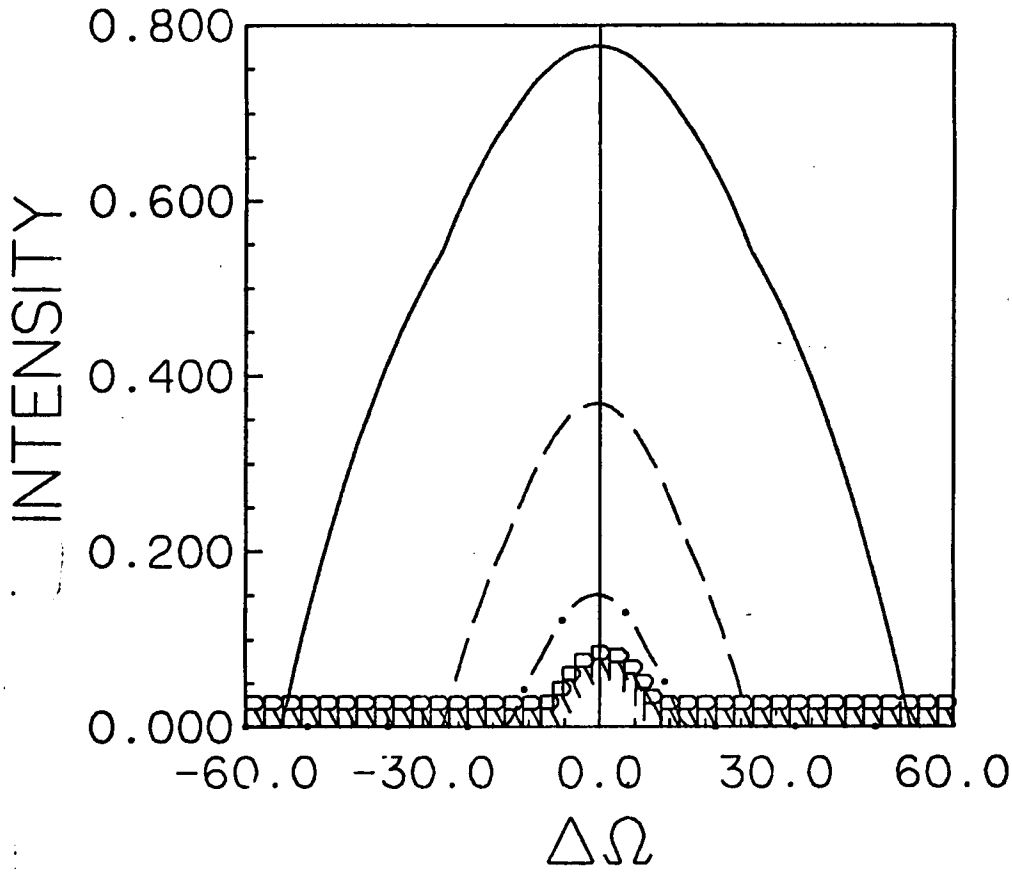

Figure 23. Graphs of intensities of the four upper modes oscillating together at $r_5 = 1.2$ and $r_4 = r_3 = r_2 = 1.0$ -- Parameters for the second mode are $\gamma_2 = 12.0$ MHz and $\beta_2 = 1.25$. Other parameters are given in the footnotes of Figures 20-22.

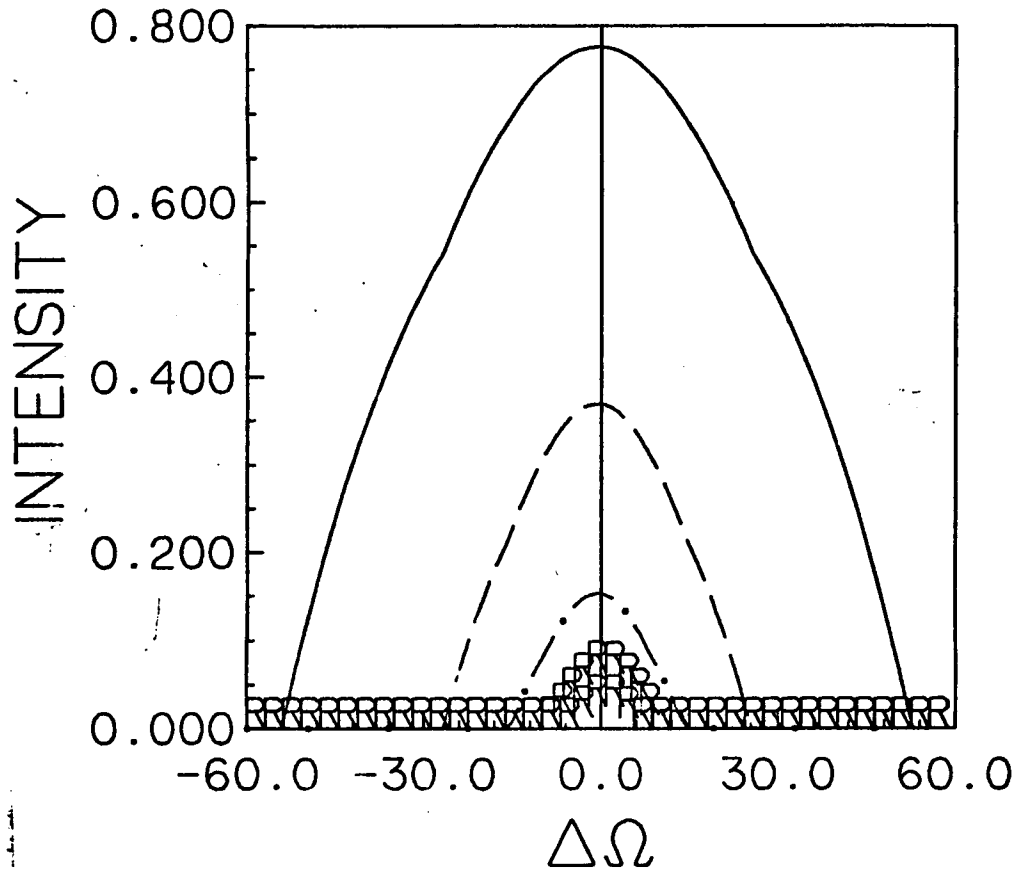

Figure 24. Graphs of intensities of all of the five modes oscillating together at $r_5 = 1.2$ and $r_4 = r_3 = r_2 = r_1 = 1.0$ -- Parameters for the lowest mode are $\gamma_1 = 9.0$ MHz and $\beta_1 = 1.2$. Other parameters are given in the footnotes of Figures 20-23.

CO. As a trial computer run we obtained intensity plots with pumping to the lower levels, too, and found that the intensities increase substantially by addition of an extra mode. However, this generally does not occur in experimental cases. Typically one is interested in extracting the most energy by pumping a single level. In our runs we also used slightly decreasing values for the electric dipole moments $\wp$ coming down the ladder, a choice corresponding to the case for anharmonic diatomic molecules. Solutions for three, four, and five mode cases with equal $\wp$'s yielded intensities slightly smaller than the previous corresponding cases. In another trial run we filtered out the middle transition to see whether the cascading process would go through, but obviously it introduces a huge loss to the cascade chain and the upper two modes and the lower two lased as two independent pairs (Figure 25). Yardley [20] mentions similar experimental results in which the absorption of transitions by atmospheric water vapor may break the chain of the cascade. He noted also that the use of a grating to select individual lines results in loss of intensity or even completely quenching the laser oscillation.

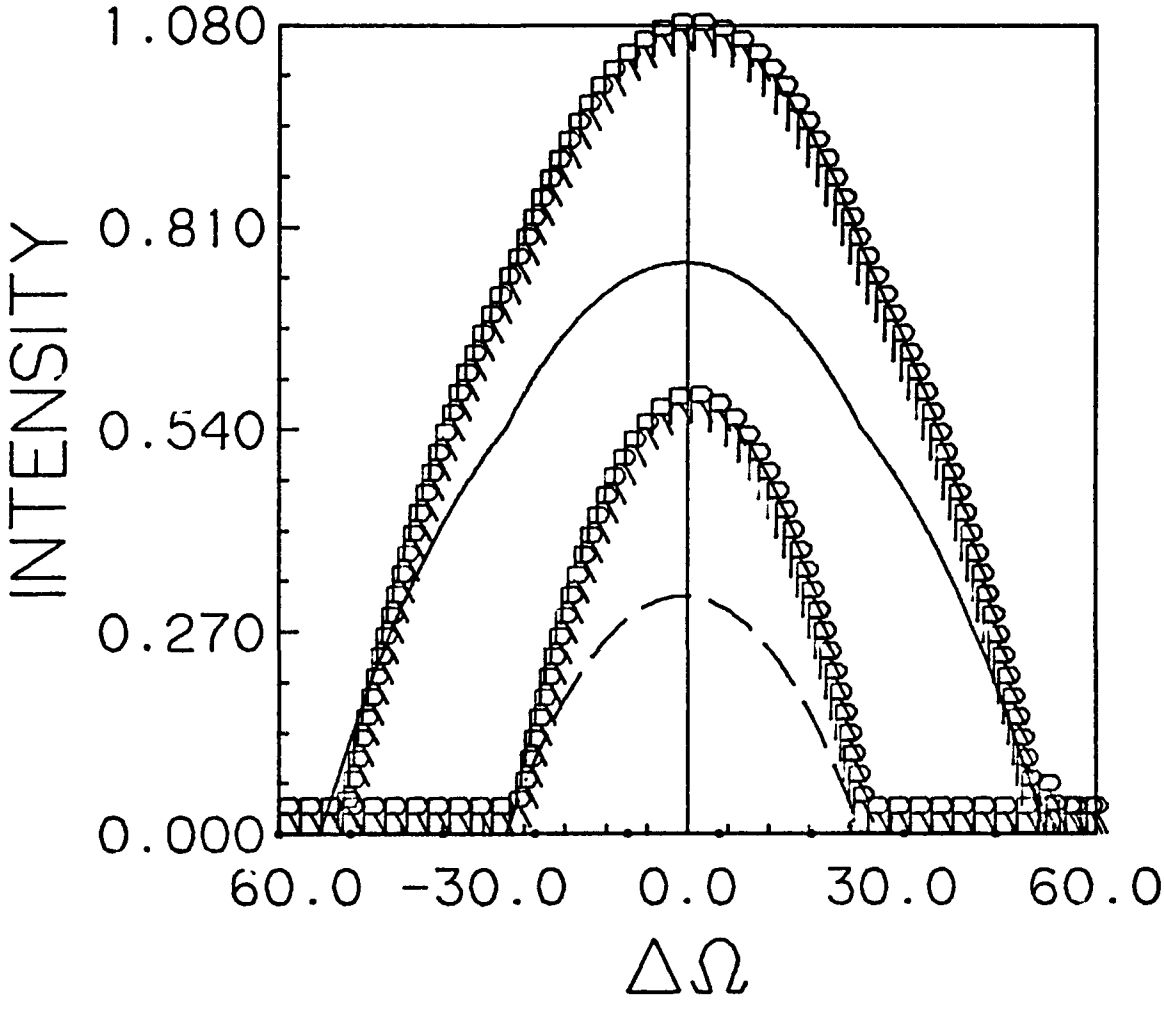

Figure 25. Graphs of intensities of the five modes oscillating together at $\mu_5 = 1.2$, $\mu_4 = 1.0$, $\mu_3 = 0.2$, $\mu_2 = 1.2$, and $\mu_1 = 1.0$ -- Laser parameters used are same as in Figures 20-24. As is seen in this graph, the third mode is not only filtered out, but it also breaks the cascade chain and the upper two modes and the lowest two oscillate as two independent pairs.

CHAPTER 11

AN ESTIMATE OF THE DEVIATION OF THE THIRD-ORDER THEORY FROM THE EXACT RESULTS

In this chapter we introduce a simplified rate equation model which ignores the coherence terms, and will give a rough estimate of the error involved in using the third-order theory. We ignore the mode functions for simplicity appropriate for unidirectional ring laser [9]. In a simple notation the third-order intensity

$$I_1 = \frac{g - \kappa}{g} I_s, \tag{122}$$

where g represents the gain (per unit length) and κ the loss, and I_s is the saturated intensity. The exact intensity is given by

$$I_2 = \frac{g - \kappa}{\kappa} I_s. \tag{123}$$

We see that in terms of the ratio $\frac{g}{\kappa} = A$ (a kind of relative excitation), they are given by

$$I_1 = \left(\frac{A - 1}{A}\right) I_s, \tag{124}$$

and

$$I_2 = (A - 1) I_s. \tag{125}$$

Thus the ratio of I_1/I_2 as a function of the relative

excitation is in fact what we are looking for as an estimate of the error. We write our rate equations for the homogeneous three-level model (Figure 26) as

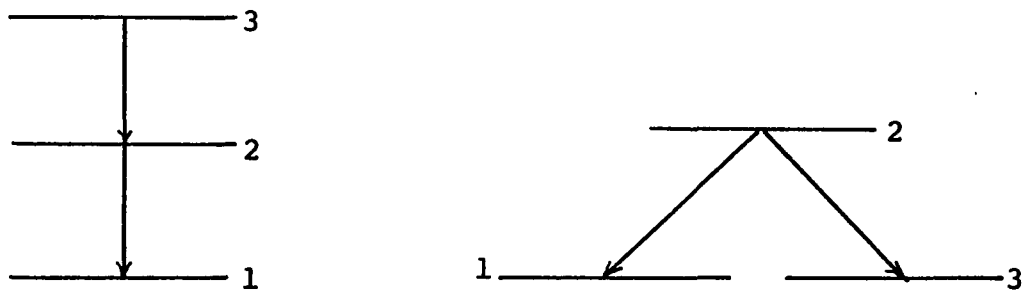

Figure 26. Three-level cascade and competitive configurations.

$$\dot{n}_1 = \lambda_1 - \gamma_1 n_1 + \frac{\sigma_1 I_1}{\hbar\nu_1} (n_2 - n_1), \tag{126}$$

$$\dot{n}_2 = \lambda_2 - \gamma_2 n_2 - \frac{\sigma_1 I_1}{\hbar\nu_1} (n_2 - n_1) + \frac{\sigma_2 I_2}{\hbar\nu_2} (n_3 - n_2), \tag{127}$$

$$\dot{n}_3 = \lambda_3 - \gamma_3 n_3 - \frac{\sigma_2 I_2}{\hbar\nu_2} (n_3 - n_2), \tag{128}$$

where the new term σ that we have introduced here is the optical cross-section of the corresponding transition. We can also write down the equation of the time-evolution of the intensities as

$$\frac{dI_1}{dt} = c\sigma_1 (n_2 - n_1) I_1 - \frac{\nu_1}{Q_1} I_1, \tag{129}$$

and

$$\frac{dI_2}{dt} = \pm c\sigma_2(n_3-n_2)I_2 - \frac{\nu_2}{Q_2} I_2, \tag{130}$$

where c is the velocity of light and Q is again the quality factor of the cavity. The plus sign in Eq. (130) is for the cascade, and the negative sign for the competitive case. We solve the equations (126)-(128) in the steady-state case and by substituting the values of the n's (as functions of I_1 and I_2) into Eqs. (129) and (130) we solve for the steady-state intensities in third-order and exact forms for both cascade and competitive configurations. In the steady-state case we let $\dot{n}_1 = 0$, $\dot{n}_2 = 0$, and $\dot{n}_3 = 0$. We also define the two combinations of the pumping and the decay rates as

$$N_{21} = (\lambda_2/\gamma_2) - (\lambda_1/\gamma_1) \tag{131}$$

$$N_{32} = (\lambda_3/\gamma_3) - (\lambda_2/\gamma_2) \tag{132}$$

(N_{23} for the competitive case is $-N_{32}$ of Eq. (132)), which are the relative excitation for each mode, but later we define dimensionless quantities for relative excitations and the intensities. Solving (126)-(128) yields

$$n_3-n_2 = \frac{N_{32}\left[1+\left(\frac{1}{\gamma_1}+\frac{1}{\gamma_2}\right)\frac{\sigma_1 I_1}{\hbar\nu_1}\right] + \frac{1}{\gamma_2}\frac{\sigma_1 I_1}{\hbar\nu_1} N_{21}}{\left[1+\left(\frac{1}{\gamma_1}+\frac{1}{\gamma_2}\right)\frac{\sigma_1 I_1}{\hbar\nu_1}\right]\left[1+\left(\frac{1}{\gamma_2}+\frac{1}{\gamma_3}\right)\frac{\sigma_2 I_2}{\hbar\nu_2}\right] - \frac{1}{\gamma_2^2}\frac{\sigma_1 I_1}{\hbar\nu_1}\frac{\sigma_2 I_2}{\hbar\nu_2}} \tag{133}$$

$$n_2-n_1 = \frac{N_{21}\left[1+\left(\frac{1}{\gamma_2}+\frac{1}{\gamma_3}\right)\frac{\sigma_2 I_2}{\hbar\nu_2}\right] + \frac{1}{\gamma_2}\frac{\sigma_2 I_2}{\hbar\nu_2} N_{32}}{\left[1+\left(\frac{1}{\gamma_1}+\frac{1}{\gamma_2}\right)\frac{\sigma_1 I_1}{\hbar\nu_1}\right]\left[1+\left(\frac{1}{\gamma_2}+\frac{1}{\gamma_3}\right)\frac{\sigma_2 I_2}{\hbar\nu_2}\right] - \frac{1}{\gamma_2^2}\frac{\sigma_1 I_1}{\hbar\nu_1}\frac{\sigma_2 I_2}{\hbar\nu_2}} \tag{134}$$

and to the third-order in intensities, they reduce to

$$n_3 - n_2 \cong N_{32} - N_{32}\left(\frac{1}{\gamma_2}+\frac{1}{\gamma_3}\right)\frac{\sigma_2 I_2}{\hbar\nu_2} + \frac{1}{\gamma_2}\frac{\sigma_1 I_1}{\hbar\nu_1} N_{21}, \tag{135}$$

and

$$n_2 - n_1 \cong N_{21} - N_{21}\left(\frac{1}{\gamma_1}+\frac{1}{\gamma_2}\right)\frac{\sigma_1 I_1}{\hbar\nu_1} + \frac{1}{\gamma_2}\frac{\sigma_2 I_2}{\hbar\nu_2} N_{32}. \tag{136}$$

By substituting Eqs. (133)-(136) into Eqs. (129) and (130) we find for the exact cascade case

$$\frac{dI_1}{dt} = c\sigma_1 I_1\left\{\frac{N_{21}\left[1+\left(\frac{1}{\gamma_2}+\frac{1}{\gamma_3}\right)\frac{\sigma_2 I_2}{\hbar\nu_2}\right] + \frac{1}{\gamma_2}\frac{\sigma_2 I_2}{\hbar\nu_2} N_{32}}{\left[1+\left(\frac{1}{\gamma_1}+\frac{1}{\gamma_2}\right)\frac{\sigma_1 I_1}{\hbar\nu_1}\right]\left[1+\left(\frac{1}{\gamma_2}+\frac{1}{\gamma_3}\right)\frac{\sigma_2 I_2}{\hbar\nu_2}\right] - \frac{1}{\gamma_2^2}\frac{\sigma_1 I_1}{\hbar\nu_1}\frac{\sigma_2 I_2}{\hbar\nu_2}}\right\}$$

$$- (\nu_1/Q_1) I_1, \tag{137}$$

and

$$\frac{dI_2}{dt} = c\sigma_2 I_2 \left\{ \frac{N_{32}\left[1+\left(\frac{1}{\gamma_1}+\frac{1}{\gamma_2}\right)\frac{\sigma_1 I_1}{\hbar\nu_1}\right] + \frac{1}{\gamma_2}\frac{\sigma_1 I_1}{\hbar\nu_1} N_{21}}{\left[1+\left(\frac{1}{\gamma_1}+\frac{1}{\gamma_2}\right)\frac{\sigma_1 I_1}{\hbar\nu_1}\right]\left[1+\left(\frac{1}{\gamma_2}+\frac{1}{\gamma_3}\right)\frac{\sigma_2 I_2}{\hbar\nu_2}\right] - \frac{1}{\gamma_2^2}\frac{\sigma_1 I_1}{\hbar\nu_1}\frac{\sigma_2 I_2}{\hbar\nu_2}} \right\}$$

$$- (\nu_2/Q_2) I_2, \tag{138}$$

and for the third-order (denoted by a superscript (3)) cascade

$$\frac{dI_1^{(3)}}{dt} = c\sigma_1 I_1^{(3)} \left[N_{21} - N_{21}\left(\frac{1}{\gamma_1}+\frac{1}{\gamma_2}\right)\frac{\sigma_1 I_1^{(3)}}{\hbar\nu_1} + \frac{1}{\gamma_2}\frac{\sigma_2 I_2^{(3)}}{\hbar\nu_2} N_{32}\right]$$

$$- (\nu_1/Q_1) I_1^{(3)}, \tag{139}$$

and

$$\frac{dI_2^{(3)}}{dt} = c\sigma_2 I_2^{(3)} \left[N_{32} - N_{32}\left(\frac{1}{\gamma_2}+\frac{1}{\gamma_3}\right)\frac{\sigma_2 I_2^{(3)}}{\hbar\nu_2} + \frac{1}{\gamma_2}\frac{\sigma_1 I_1^{(3)}}{\hbar\nu_1} N_{21}\right]$$

$$- (\nu_2/Q_2) I_2^{(3)} \tag{140}$$

Before going any further we can make a quick check on the value of the coupling constant we can find from Eqs. (139) and (140) (corresponding to Eqs. (74) and (75)) and compare it with the result we find from Table 1. From Eqs. (139) and (140), we find

$$\beta_1 = cN_{21} \frac{\sigma_1^2 I_1^{(3)}}{\hbar\nu_1} \left(\frac{1}{\gamma_1} + \frac{1}{\gamma_1}\right), \tag{141}$$

$$\beta_2 = cN_{32} \frac{\sigma_2^2 I_2^{(3)}}{\hbar\nu_2} \left(\frac{1}{\gamma_2} + \frac{1}{\gamma_3}\right), \tag{142}$$

$$\theta_{12} = c \frac{\sigma_1\sigma_2 I_2^{(3)}}{\gamma_2\hbar\nu_2} N_{32}, \tag{143}$$

and

$$\theta_{21} = c \frac{\sigma_2\sigma_1 I_1^{(3)}}{\gamma_2\hbar\nu_1} N_{21}. \tag{144}$$

The coupling constant of Eq. (76) is therefore

$$C = \frac{\theta_{12}\theta_{21}}{\beta_1\beta_2} = \frac{\gamma_1\gamma_3}{(\gamma_1+\gamma_2)(\gamma_2+\gamma_3)}, \tag{145}$$

which is always less than one and proves again that the coupling between the transitions is weak and the third-order theory should remain quite accurate. By ignoring the quadrupole parts, from Table 1 we get

$$C = \frac{4}{9} \frac{\gamma_a\gamma_c}{(\gamma_a+\gamma_b)(\gamma_b+\gamma_c)}, \tag{146}$$

which is still smaller than the value of (145) by a factor of $\frac{4}{9}$ which is due to neglecting the mode functions (no spatial dependence and integration). Now we see that we should find the estimate of the error of our theory by

varying both the relative excitation parameters and the ratio of the decay rates. We got the exact and third order plots of dimensionless intensities for three different values of the ratios of γ_2/γ_1 and γ_2/γ_3 (assuming that the two ratios are equal) and for fixed values of N_{32} and varying N_{21}. By choosing three values of 0.1, 1.0, and 10 for the ratio of $\gamma_2/\gamma_1 = \gamma_2/\gamma_3$ we think that we cover a range of all the possible cases that may occur. To define the dimensionless intensities I's, we divide all the intensities by the "saturation power"

$$I_1^s = [\frac{\sigma_1}{\hbar\nu_1} (\frac{1}{\gamma_1} + \frac{1}{\gamma_2})]^{-1}, \tag{147}$$

and the corresponding value of I_2^s. To define dimensionless variables N's for the relative excitations, we assume (as in our theory before) that the σ's and the loss factors ν/Q's are equal for both modes. We define the dimensionless N as

$$N = \frac{c\sigma N - \nu/Q}{\nu/Q} \tag{148}$$

which is like (gain-loss)/loss of the laser cavity. Again we must note a difference between this notation and our previous notation, where the threshold value for the relative excitation was equal to unity and here it would be zero. The exact equations for the cascade case reduce to

$$\frac{1}{I_1}\,\frac{1}{\nu/Q}\,\frac{dI_1}{dt} =$$

$$\frac{N_{21}+N_{21}I_2+N_{32}I_2\,\dfrac{1}{(1+\gamma_2/\gamma_3)} - I_1-I_1I_2 + \dfrac{I_2}{(1+\gamma_2/\gamma_3)}}{[1+I_1][1+I_2] - \dfrac{I_1I_2}{(1+\gamma_2/\gamma_3)(1+\gamma_2/\gamma_1)}}$$

$$+ \frac{\dfrac{I_1I_2}{(1+\gamma_2/\gamma_3)(1+\gamma_2/\gamma_1)}}{\cdots} \qquad (149)$$

and a similar equation for second mode by interchanging $I_1 \leftrightarrow I_2$, $N_{21} \leftrightarrow N_{32}$, and $(\gamma_2/\gamma_1) \leftrightarrow (\gamma_2/\gamma_3)$. The third order equation for I_1 for the cascade now is given by

$$\frac{1}{I_1^{(3)}}\,\frac{1}{\nu/Q}\,\frac{dI_1^{(3)}}{dt} = N_{21}-I_1^{(3)}(N_{21}+1) + \frac{I_2^{(3)}}{1+\gamma_2/\gamma_3}\,(N_{32}+1), \qquad (150)$$

and for $I_2^{(3)}$ by the same interchange relations. Corresponding to Eq. (149), for the competitive case we get

$$\frac{1}{I_1}\frac{1}{\nu/Q}\frac{dI_1}{dt} =$$

$$\frac{N_{21}+N_{21}I_2-N_{23}\dfrac{I_2}{(1+\gamma_2/\gamma_3)} - I_1-I_1I_2 - \dfrac{I_2}{(1+\gamma_2/\gamma_3)}}{[1+I_1][1+I_2] - \dfrac{I_1I_2}{(1+\gamma_2/\gamma_3)(1+\gamma_2/\gamma_1)}}$$

$$+ \frac{\dfrac{I_1I_2}{(1+\gamma_2/\gamma_3)(1+\gamma_2/\gamma_1)}}{\cdots}. \qquad (151)$$

We can get the equation for I_2 by the same interchange rules except for the minor difference $N_{21} \leftrightarrow N_{23}$. Corresponding to Eq. (150), for the competitive case we get

$$\frac{1}{I_1^{(3)}}\frac{1}{\nu/Q}\frac{dI_1^{(3)}}{dt} = N_{21}-I_1^{(3)}(N_{21}+1) - \frac{I_2^{(3)}}{1+\gamma_2/\gamma_3}(N_{23}+1). \qquad (152)$$

In steady-state cases, Eqs. (149)-(152) and the similar ones for I_2's are set equal to zero and solved on a computer. The value of $N_{32}(N_{23})$ is fixed at 0 (threshold) and the value of N_{21} is varying from 0 to 1.0 (which corresponds to a value of 2.0 for our previous relative excitations and we never exceeded the value of 1.2 to get our results). The computer plots for the values of $\gamma_2/\gamma_3 = \gamma_2/\gamma_1 = 1.0$ for the cascade case are reproduced in Figures 27 and 28. Up to $N_{21} = .2$ the exact and the third order results are almost identical. In fact, for the mode which is lasing just at threshold, we always get identical

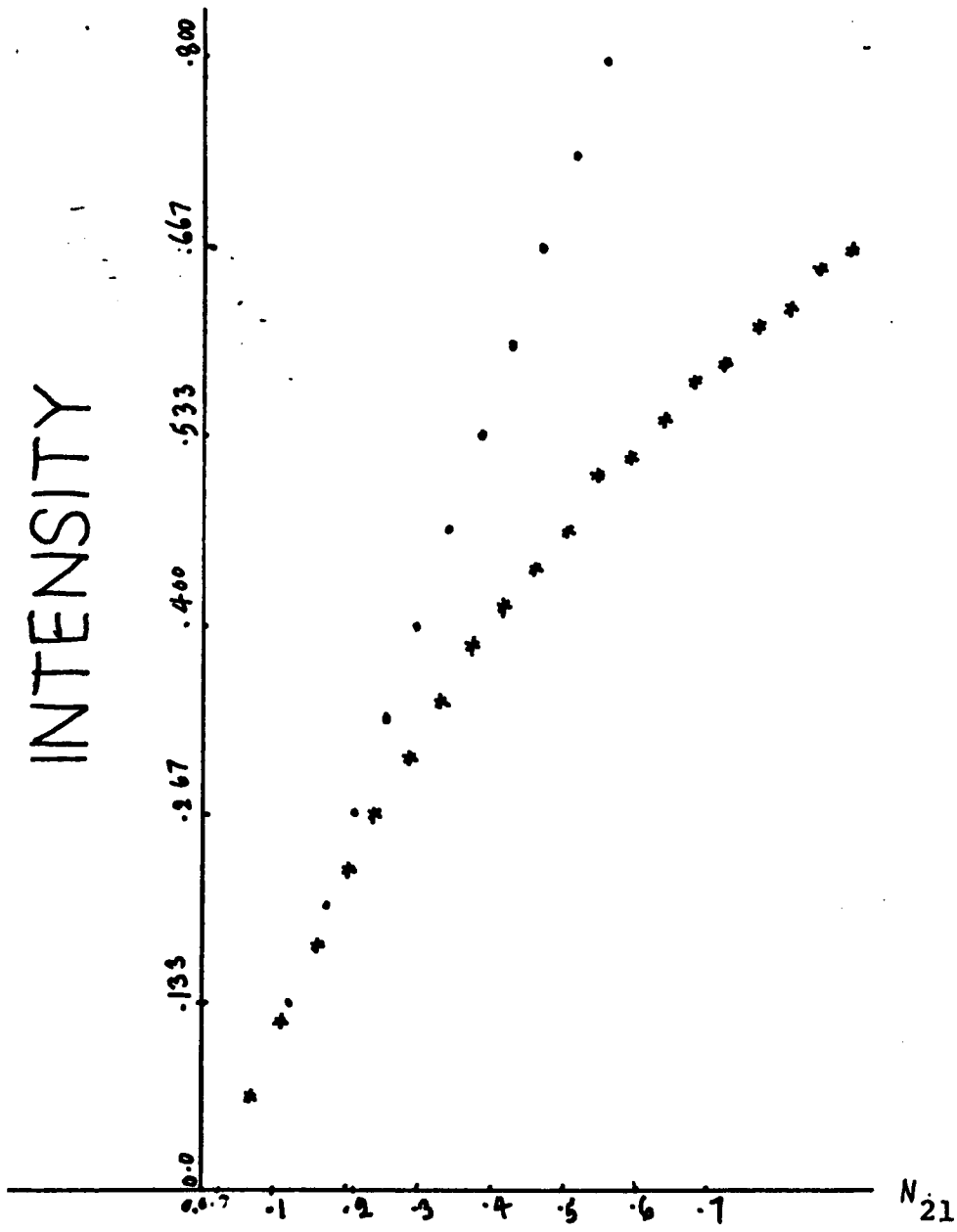

Figure 27. Graphs of intensities of the exact (dotted line) and the third-order (star points) cascade case for mode 1, versus N_{21} (Eq. (146)) -- N_{32} is fixed at 0.0 (threshold value) and $(\gamma_2/\gamma_3) = (\gamma_2/\gamma_1) = 1.0$.

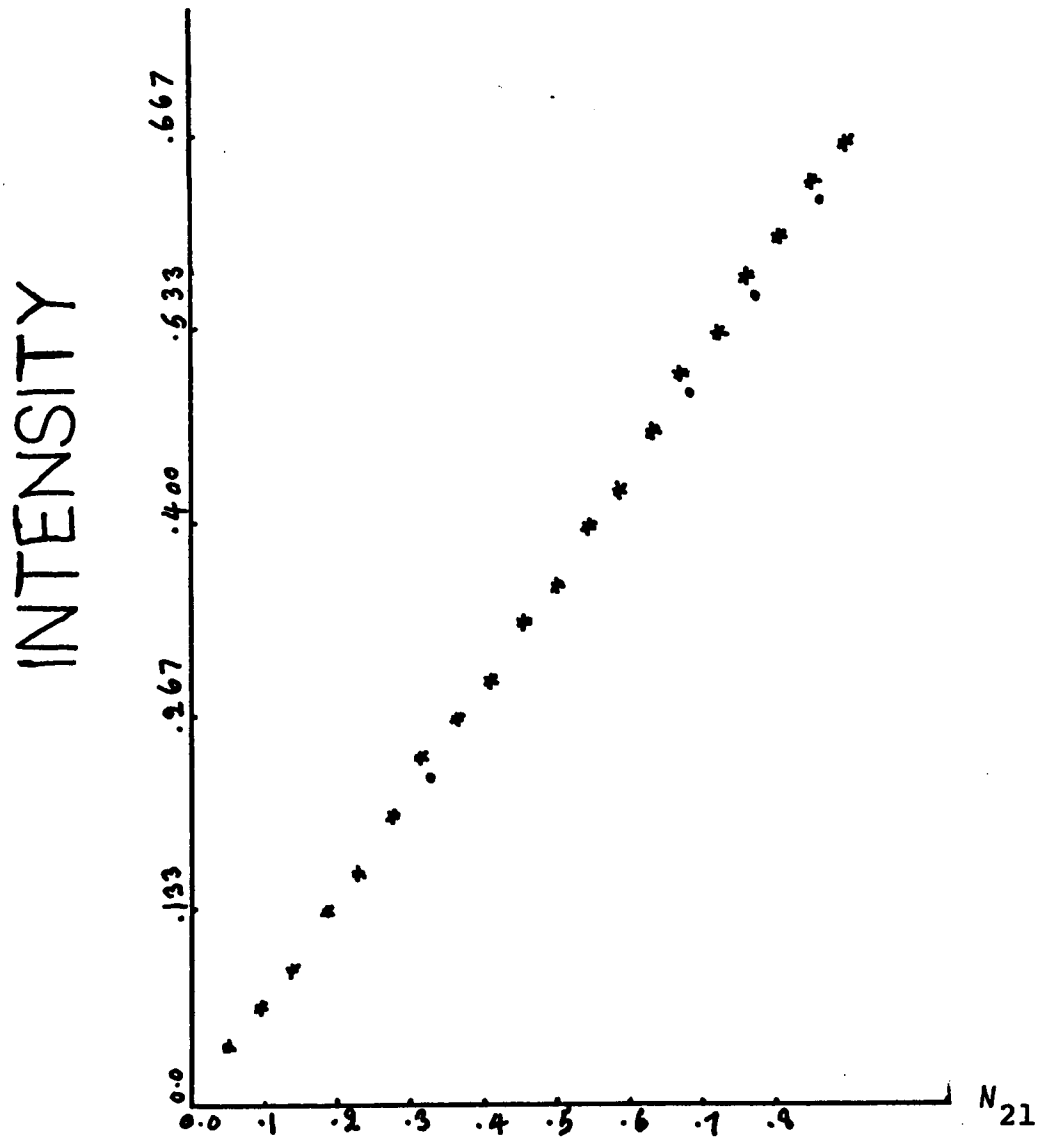

Figure 28. Graphs of intensities of the exact (dotted line) and the third-order (star points) cascade case for mode 2, versus N_{21} (Eq. (146)) -- N_{32} is fixed at 0.0 (threshold value) and $(\gamma_2/\gamma_3) = (\gamma_2/\gamma_1) = 1.0$. The two graphs are almost superimposed.

results from the exact and the third-order theory and for the first mode at $N_{21} = .4$, we get about 26% error in the third-order intensity versus the exact result. For the extreme cases of $\gamma_2/\gamma_1 = \gamma_2/\gamma_3 = 10$ and $\gamma_2/\gamma_1 = \gamma_2/\gamma_3 = .1$ (which are normally even beyond the practical cases), we get about 28% and 25% error (respectively) in the intensities. The .1 ratio of γ's also results in huge intensities further above threshold, but such ratio of decay rates does not exist in the laser systems up to now. We see that the third-order theory, in fact, underestimates the intensities for the cascade case due to the self-saturation of the modes.

The errors of the third-order theory for the cascade case are much smaller than those for the competitive case. As was mentioned before, cross-saturation terms for the cascade case have opposite signs to the self-saturation terms and the errors due to neglecting the higher order terms partially cancel each other. An error-estimate representation of strong-signal lasers is also given in Reference [10].

APPENDIX A

CONDITIONS FOR STABLE SOLUTIONS

As was mentioned in Chapter 4, stable physical solutions have non-negative intensities and satisfy the condition $\dot{I}_1 = \dot{I}_2 = 0$. Referring to Eqs. (74) and (75) we see when both linear net gains α_1 and α_2 are positive, laser oscillation can occur provided the "effective" net gains

$$\alpha_1' \equiv \alpha_1 - \theta_{12} I_2$$

$$\alpha_2' \equiv \alpha_2 - \theta_{21} I_1 \qquad \text{(A.1)}$$

are positive. Here, α_1' is the linear gain that mode 1 sees in the presence of mode 2 oscillating with $I_2^{(s)} = \frac{\alpha_2}{\beta_2}$. In the cascade case α_1' is greater than α_1, i.e., the two transitions help each other to lase. To see whether the solutions are stable we can do a small vibrations analysis, i.e., we expand the intensities about the stationary solutions $I_n^{(s)}$ in question

$$I_n(t) = I_n^{(s)} + \varepsilon_n(t), \qquad \text{(A.2)}$$

where $\varepsilon_n(t)$ is the small deviation. We substitute (A.2) into the intensity equations (74) and (75) and demand that

$\varepsilon_1 \to 0$, $\varepsilon_2 \to 0$ as $t \to \infty$ for stability. We complete the discussion here for the cascade case. The competitive case (θ's > 0) is given in Reference [9]. If one of the intensities is zero to start with, e.g., $I_1^{(s)} = 0$, then $I_2^{(s)} = \frac{\alpha_2}{\beta_2}$ and we get

$$\dot{\varepsilon}_1 = 2\varepsilon_1 \left[\alpha_1 - \theta_{12} \frac{\alpha_2}{\beta_2}\right] + 0(\varepsilon^2)$$

$$\dot{\varepsilon}_2 = -2 \left(\alpha_2/\beta_2\right)\left(\beta_2\varepsilon_2 + \theta_{21}\varepsilon_1\right) + 0(\varepsilon^2). \tag{A.3}$$

From the first equation we see $\varepsilon_1 \to 0$ in time provided

$$\alpha_1' = \alpha_1 - \theta_{12} \frac{\alpha_2}{\beta_2} < 0. \tag{A.4}$$

If $\alpha_1 < 0$ and $|\theta_{12}|$ is large enough, then α_1' can be positive and I_1 can build up. For this situation the solutions are unstable. Similar discussion applies to the solution $I_1^{(s)} = \frac{\alpha_1}{\beta_1}$ and $I_2^{(s)} = 0$. In general when both linear gains α_n are positive, there are the stationary two-mode solutions

$$I_1^{(s)} = \frac{\left(\frac{\alpha_1}{\beta_1}\right) - \left(\frac{\theta_{21}}{\beta_1}\right)\left(\frac{\alpha_2}{\beta_2}\right)}{1 - C} = \frac{\left(\frac{\alpha_1'}{\beta_1}\right)}{1 - C}$$

$$I_2^{(s)} = \frac{\left(\frac{\alpha_2}{\beta_2}\right) - \left(\frac{\theta_{12}}{\beta_2}\right)\left(\frac{\alpha_1}{\beta_1}\right)}{1 - C} = \frac{\left(\frac{\alpha_2'}{\beta_2}\right)}{1 - C}, \tag{A.5}$$

where the "coupling constant"

$$C = \frac{\theta_{12}\theta_{21}}{\beta_1\beta_2}. \tag{A.6}$$

If the coupling is small, $\alpha_1' \to \alpha_1$, and $\alpha_2' \to \alpha_2$, and the modes oscillate independently with single mode steady-state intensities α_1/β_1 and α_2/β_2.

The stability equations are

$$\dot{\varepsilon}_1 = -2\, I_1^{(s)}\ (\beta_1\varepsilon_1+\theta_{12}\varepsilon_2)$$

$$\dot{\varepsilon}_2 = -2\, I_2^{(s)}\ (\beta_2\varepsilon_2+\theta_{21}\varepsilon_1). \tag{A.7}$$

In matrix form this reads

$$\frac{d}{dt}\begin{pmatrix}\varepsilon_1\\ \\ \varepsilon_2\end{pmatrix} = \frac{-2}{1-C}\begin{pmatrix}\alpha_1' & \alpha_1'(\theta_{12}/\beta_1)\\ \\ \alpha_2'(\theta_{21}/\beta_2) & \alpha_2'\end{pmatrix}\begin{pmatrix}\varepsilon_1\\ \\ \varepsilon_2\end{pmatrix}$$

$$= \Theta\begin{pmatrix}\varepsilon_1\\ \\ \varepsilon_2\end{pmatrix}. \tag{A.8}$$

To determine the time development, we diagonalize the matrix Θ. The eigenvalues $\lambda_{1,2}$ are equal to

$$\lambda_{1,2} = -\frac{\alpha_1'+\alpha_2'}{1-C} \pm \sqrt{\left[\frac{\alpha_1'+\alpha_2'}{1-C}\right]^2 - 4\,\frac{\alpha_1'\alpha_2'}{1-C}}. \tag{A.9}$$

In diagonal form $\dot{\varepsilon}_1$ and $\dot{\varepsilon}_2$ equations become

$$\dot{\varepsilon}_1' = \lambda_1 \varepsilon_1'$$

$$\dot{\varepsilon}_2' = \lambda_2 \varepsilon_2'. \tag{A.10}$$

For positive λ's, ε's increase with time and the solutions are unstable.

For neutral coupling (C = 1), the stationary solutions of the intensity equations read

$$\beta_1 I_1^{(s)} + \theta_{12} I_2^{(s)} = \alpha_1$$

$$\beta_2 I_2^{(s)} + \theta_{21} I_1^{(s)} = \alpha_2 \tag{A.11}$$

with zero determinant. Hence I_1 and I_2 are not independent of each other, $\lambda_{1,2} = 0$ and they have neutral stability, i.e., any solution satisfying (A.11) is stable. If C > 1 and α_1', α_2' are both positive, one of λ's is positive and solutions are unstable. Since α_1', $\alpha_2' < 0$ implies the trivial solution $I_1 = I_2 = 0$, we see that unlike the competitive case, there is no two-mode strong coupled (C > 1) stable solutions. For $I_1^{(s)} = 0$ as discussed before $I_2^{(s)} = \frac{\alpha_2}{\beta_2}$, $\alpha_1' < 0$, $\alpha_2 > 0$ and coupling is weak. If C < 1 and α_1' and α_2' are both positive (for $I_1^{(s)}$, $I_2^{(s)}$ to be positive), then $\lambda_{1,2}$ are both negative, i.e., the two modes can oscillate and are stable and the coupling is weak. These conditions are summarized in Table 2.

REFERENCES

1. Javan, A., Phys. Rev. 107, 1579 (1957).

2. Lamb, W. E., Jr., Phys. Rev. 134, A 1429 (1964).

3. Haken, H., R. Der Agobian, and M. Pauthier, Phys. Rev. 140, A 437 (1965).

4. Feld, M. S., and A. Javan, Phys. Rev. 177, 540 (1969).

5. Feldman, B. J., and M. S. Feld, Phys. Rev. A 1, 1375 (1970).

6. Feldman, B. J., and M. S. Feld, Phys. Rev. A 5, 899 (1972).

7. Hänsch, Th., and P. Toschek, Z. Physik 236, 213 (1970).

8. Sargent, M., III, and M. O. Scully, "Physics of Laser Operation," Chap. A2 of Laser Handbook, edited by F. T. Arecchi and E. O. Schulz-Dubois (North-Holland, Amsterdam, 1972).

9. Sargent, M., III, M. O. Scully, and W. E. Lamb, Jr., "Laser Physics," Addison-Wesley Pub. Co., Reading, Mass. (1974).

10. Stenholm, S., and W. E. Lamb, Jr., Phys. Rev. 181, 618 (1969).

11. O'Bryan, C. L., III, and M. Sargent, III, Phys. Rev. A 8, 3071 (1973).

12. Patel, C. K. N., and R. J. Kerl, Appl. Phys. Letters 5, 81 (1964).

13. Patel, C. K. N., Phys. Rev. 141, 71 (1966).

14. Hancock, G., and J. W. M. Smith, Appl. Optics 10, 1827 (1971).

15. Eppers, W. C., Jr., R. M. Osgood, Jr., and P. R. Greason, IEEE J. Quantum Electron. 6, 4 (1970).

16. Osgood, R. M., Jr., E. R. Nichols, W. C. Eppers, Jr., and R. D. Petty, Appl. Phys. Letters 15, 69 (1969).

17. Osgood, R. M., Jr., W. C. Eppers, Jr., and E. R. Nichols, IEEE J. Quantum Electron. 6, 145 (1970).

18. Yardley, J. T., J. Chem. Phys. 52, 3983 (1970).

19. Yardley, J. T., J. Mol. Spectrosc. 35, 314 (1970).

20. Yardley, J. T., Appl. Optics 10, 1760 (1971).

21. Bhaumik, M. L., Lacina, W. B., and Mann, M. M., IEEE J. Quantum Electron. 8, 150 (1972).

22. Herzberg, G. "Molecular Spectra and Molecular Structure," Vol. I, Spectra of Diatomic Molecules, Van Nostrand Reinhold Co., New York (1950).

23. Young, L. E., and W. J. Eachus, J. Chem. Phys. 44, 4195 (1966).

24. Heaps, H. S., and G. Herzberg, Z. Physik 133, 48 (1952).

25. Herman, R. C., and K. E. Schuler, J. Chem. Phys. 22, 481 (1954).

26. Herman, R., and R. F. Wallis, J. Chem. Phys. 23, 637 (1955).

27. Herman, R., and R. J. Rubin, Astrophys. J. 121, 533 (1955).

28. Herman, R., R. W. Rathery, and R. J. Rubin, J. Mol. Spectry. 2, 369 (1958).

29. Cashion, K., J. Mol. Spectry. 10, 182 (1963).

30. Caledonia, G. E., and R. E. Center, J. Chem. Phys. 55, 552 (1971).

31. Center, R. E., and G. E. Caledonia, Appl. Optics 10, 1795 (1971).

32. Treanor, C. E., J. W. Rich, and R. G. Rehm, J. Chem. Phys. 48, 1798 (1968).

33. Rich, J. W., J. Appl. Phys. 42, 2719 (1971).

34. Jeffers, W. Q., and J. D. Kelley, J. Chem. Phys. 55, 4433 (1971).

35. Jeffers, W. Q., and C. E. Wiswall, IEEE J. Quantum Electron. 7, 407 (1971).

36. Jeffers, W. Q., and C. E. Wiswall, J. Appl. Phys. 42, 5059 (1971).

37. Abraham, G., and E. R. Fisher, Research Institute for Engineering Sciences Report 71-39, Wayne State University (October, 1971).

38. Abraham, G., and E. R. Fisher, J. Appl. Phys. 43, 4621 (1972).

39. Fisher, E. R., Research Institute for Engineering Sciences Report 72-48, Wayne State University (October, 1972).

40. Fisher, E. R., J. Appl. Phys. 44, 5031 (1973).

41. Hopf, F. A., Optics Comm. 9(1), 38 (1973).

42. Rockwood, S. D., J. E. Brau, W. A. Proctor, and G. H. Canavan, IEEE J. Quantum Electron. 9, 120 (1973).

43. Patel, C. K. N., Phys. Rev. Letters 12, 588 (1964); Phys. Rev. 136, 1187 (1964).

44. Hancock, G., and I. W. M. Smith, Chem. Phys. Lett. 3, 573 (1969); Chem. Phys. Lett. 8, 41 (1971).

45. Lacina, W. B., M. M. Mann, and G. L. McAllister, IEEE J. Quantum Electron. 9, 588 (1973).

46. Green, W. H., and J. K. Hancock, IEEE J. Quantum Electron. 9, 50 (1973).

47. Matthews, D. L., J. Chem. Phys. 34, 639 (1961).

48. Hooker, W. J., and R. C. Millikan, J. Chem. Phys. 38, 214 (1963).

49. Millikan, R. C., J. Chem. Phys. 38, 2855 (1963).

50. Millikan, R. C., and D. R. White, J. Chem. Phys. 39, 3209 (1963).

51. Millikan, R. C., J. Chem. Phys. 40, 2594 (1964).

52. Schulz, G. J., Phys. Rev. 135, A 988 (1964).

53. Sato, Y., and S. Tsuchiya, J. Chem. Phys. 50, 1911 (1969).

54. Miller, D. J., and R. C. Millikan, J. Chem. Phys. 53, 3384 (1970).

55. McFarlane, R. A., and J. A. Howe, Phys. Letters 19, 208 (1965).

56. Cheo, P. K., and H. G. Cooper, Appl. Phys. Lett. 5, 42 (1964).

57. Barrey, J. D., and W. E. Boney, IEEE J. Quantum Electron. 7, 101 (1971).

58. Brandelik, J. E., J. D. Barry, and W. E. Boney, Appl. Phys. Lett. 19, 141 (1971).

59. Graham, W. J., J. Kershenstein, J. T. Jensen, Jr., and K. Kershenstein, Appl. Phys. Lett. 17, 194 (1970).

60. Kan, T., J. A. Stregack, and W. S. Watt, Appl. Phys. Lett. 20, 137 (1972).

61. Rich, J. W., and H. M. Thompson, Appl. Phys. Lett. 19, 3 (1971).

62. Pilloff, H. S., S. K. Searles, and N. Djeu, Appl. Phys. Lett. 19, 9 (1971).

63. Corcoran, V. J., R. E. Cupp, W. T. Smith, and J. J. Gallagher, IEEE J. Quantum Electron. 7, 246 (1971).

64. Brechignac, P., and F. Legay, Appl. Phys. Lett. 18, 424 (1971).

65. Mann, M. M., M. L. Bhaumik, and W. B. Lucina, Appl. Phys. Lett. 16, 430 (1970).

66. Bhaumik, M. L., Appl. Phys. Lett. 17, 188 (1970).

67. Bhaumik, M. L., W. B. Lacina, and M. M. Mann, IEEE J. Quantum Electron. 6, 575 (1970).

68. Nighan, W. L., Appl. Phys. Lett. 20, 96 (1972).

69. Havey, M. E., and J. D. Barry, IEEE J. Quantum Electron. 7, 370 (1971).

70. Barry, J. C., W. E. Boney, and J. E. Brandelik, IEEE J. Quantum Electron. 7, 208 (1971).

71. Barry, J. D., W. E. Boney, and J. E. Brandelik, IEEE J. Quantum Electron. 7, 461 (1971).

72. Sackett, P. B., A. Hordvik, and H. Schlossberg, Appl. Phys. Lett., 22, 367 (1973).

73. Morse, P. M., Phys. Rev. 34, 57 (1929).